University of Pecs, Doctoral School of Earth Sciences

Ph.D. Thesis

A FULLY DISTRIBUTED INTEGRATED HYDROLOGIC MODEL FOR INTEGRATED WATER RESOURCES MANAGEMENT IN A HIGHLY REGULATED RIVER FLOODPLAIN

Submitted to University of Pecs in fulfilment of the requirements for the degree of

Doctor of Philosophy in Earth sciences

By

Ali Mohammed Mohammed Salem

Supervised by

Assistant Prof. Dr. Jozsef Dezső

2022

This Work Is Gratefully Dedicated To The Soul Of My Professor,

Dr. Mohamed El-Zeir.

To The Soul Of My Uncle,

Said Mansour and Mother-in-law Zenaat Barakat

And To My Family.

ACKNOWLEDGMENTS

First and foremost, I would like to thank **ALLAH** Almighty for giving me the ability, power, strength, knowledge and opportunity to undertake this research study and to persevere and complete it satisfactorily. Without his blessings, this achievement would not have been possible.

I express my heartful gratitude to my supervisor Dr. Jozsef Dezső for his untiring inspiration, laudable counseling and surpassing guidance who detailed and shaped the problem and provided the insightful lead with much care and affection throughout the study. I have been exceptionally lucky to have a supervisor who cared so much about my work, and who responded to my questions and queries so promptly.

Words fail us to express our ineffable gratitude to Prof. Dr. István Geresdi head of the doctoral school of earth sciences, for his valuable support and encouragement, for providing funds and facilities as well as guidelines at each and every step of my research. My sincere thanks to Prof. Dr Dénes Lóczy, for his constructive advice, valuable guidance insightful comments, valuable revision for each part of thesis, and hard questions that makes us perfect.

I am very much grateful Dr. Mostafa El-Rawy for his continuous motivation, critical reading and for offering me unlimited support and effort at every step of my research.

I thank Dr. Szigany szabolcs for his candid suggestions, help, encouragement they rendered me during the course of this endeavor.

Furthermore, it is a pleasure to thank Dr. Akos Halmai for his valuable suggestions, and support for GIS database preparation.

I gratefully acknowledge the South-Transdanubian Water Management Directorate for providing access to the valuable data that was needed in my research. I am very grateful to Dr. Marcin Słowik for conducting a Ground Penetrating Radar survey as a s part of a project 2016/23/B/ST10/01027 “Processes forming anabranching and meandering rivers: examples of selected rivers from Wielkopolska Lowland and Transdanubia”. I gratefully thank Mr. Richard Winston for his technical help in model development with the USGS software (MODFLOW, and ModelMuse) during the whole study period.

I would like to express my gratitude to the Egyptian Ministry of Higher Education (MoHE) and Tempus Public Foundation for providing me the Stipendium Hungaricum Scholarship and living funds for pursuing my research. Also, it was my great pleasure to be granted an academic leave of absence from my employer, the Head of Civil Engineering Department, Dean of the Faculty of Engineering, and president of Minia University, Egypt.

I would like to dedicate this thesis to the beautiful soul my wife, Sara Elhadad, for her love, patience, support, encouragement, and understanding. She allowed me to spend most of the time on this thesis.

Finally, I convey my deepest gratitude and appreciation to my family, collogues, especially, my friend Mahmoud Khaled, for their continuous patience and support. I express my heart-felt gratitude and love to my parents for all what they did to me during my entire life.

APPROVAL SHEET

This dissertation proposal entitled A Fully Distributed Integrated Hydrologic Model For Integrated Water Resources Management in A Highly Regulated River Floodplain submitted by Ali Mohamed Mohamed Salem for the degree DOCTOR OF PHILOSOPHY has been examined and approved for PROPOSAL HEARING.

Thesis Committee

_____

Advisor

_____

Head of the doctoral school

_____ _____

Member Member

_____ _____

Member Member

ABSTRACT

Growing awareness about the benefits of more sustainable management and allocation of water resources has highlighted the need to manage surface water and groundwater systems as a single integrated system. Hydrological models are a simplified representation of hydrological processes and can be applied for water and environment resources management and gain an integrated view of the status of Integrated Water Resources Management (IWRM). A reliable and accurate simulation of both land surface and groundwater hydrological processes represents the most essential step in IWRM. Coupling surface and groundwater models is the only way to achieve such a purpose. It has become imperative that surface and groundwater resources be managed as a holistic system. In this study, the land surface model (WetSpass-M) is coupled with the groundwater flow model (MODFLOW-NWT) to improve the long-term stressors simulation of the standalone model. The Drava floodplain region is highly affected by human activities and it suffers from water stress and intensification of drought hazards. WetSpass-M, a GIS-based spatially distributed water balance model, was implemented to assess monthly, seasonal, and annual averages of groundwater recharge, surface runoff, and actual evapotranspiration in the Drava basin, Hungary, for the period from 2000 till 2018. The long-term temporal and spatial average monthly precipitation (58 mm) is distributed as 29% (17 mm) for surface runoff, 27% (16 mm) for actual evapotranspiration, and 44% (25 mm) for groundwater recharge.

Understanding how changes in distinctive land use/land cover (LULC) types influence basin hydrology would greatly improve the predictability of the hydrological consequences of LULC dynamics for sustainable water resource management and promoting the region's economic growth. This study simulates the impacts of LULC changes from 1990 to 2018 on the hydrology of the Drava floodplain using the coupled surface water - groundwater model. A moderate expansion of built-up areas increased surface runoff, while the afforestation of arable land and meadows and the overgrowth of bare mudflats with willow shrubs increased evapotranspiration. As a consequence, the total annual groundwater recharge decreased by 5.3×10^7 m^3 in the floodplain. Moreover, an average groundwater level decline by 0.1 m is observed in the same period.

Declined groundwater recharge, increased runoff, and evapotranspiration exerted a negative effect on water resources in the Drava basin.

Integrated water resources management is necessary, particularly in a system where considerable interactions exist between surface and groundwater resources. The integrated study requires reliable estimation of the basin water budget and hydrologic fluctuations between surface and groundwater resources. For rehabilitation measures (focusing on water replenishment to oxbows) with the purpose of enhancing ecosystem services, the detailed hydrogeological study of alluvial deposits and soils is indispensable. Different fluvial sediment structures scenarios were investigated using a three-dimensional groundwater model MODFLOW-2005 via ModelMuse as a user graphical interface to assess the exchange between surface flow (from the Drava river and the Cún-Szaporca oxbow lake) and aquifer. The results show that the application of a multilayered structure provided the most realistic result. Two scenarios for the replenishment of the lake were analyzed.

This study explores the hydrological feasibility of alternative water management, i.e. the restoration of natural reservoirs (abandoned paleochannels) to mitigate water shortage problems. The consequences of applying a natural reservoir in augmenting surface water storage are investigated under variable management scenarios of recharging or feeding the reservoir. The assessment of such reservoir/groundwater interactions according to different scenarios of reservoir recharge is a precondition to establishing new water governance in the region, which can, in turn, be the basis for exploiting economic opportunities. Sustainable ecotourism and related development would ensure a safe livelihood for the local population. Different management scenarios for two natural reservoirs were simulated with different filling rates. In both instances, a natural reservoir with a feeding rate of 1 $m^3 s^{-1}$ is found to be the best scenario. In this case, 14 days of filling are required to reach the possible maximum reservoir stage of +2 m. The first-meter rise increases the saturation of soil pores and the second creates an open surface water body. Two filling periods per year, each lasting for around 180 days, are required. Such an integrated management scheme is applicable for floodplain rehabilitation in other regions with similar hydromorphological conditions and hazards, too.

The research approach of the integrated models can generally be applied to any catchment and inspired by the need of considering all aspects related to hydrological models for IWRM to bridge the gap between stakeholder involvement and natural hydrological processes in building and applying integrated models to ensure acceptability and application in decision-making for IWRM.

Table of Contents

LIST OF FIGURES

LIST OF TABLES

NOMENCLATURE

PET	Potential evapotranspiration
R_n	Net radiation
Δ	Slope of the saturation vapor pressure function
G	Soil heat flux density
U_2	Wind speed at 2 m height
T	Daily average air temperature
e_s	Saturation vapor pressure
e_a	Actual vapor pressure
γ	Psychometric constant
E_{ow}	Daily open-surface water evaporation
E_w	Average daily wind speed
ET_{raster}	Total evapotranspiration of a grid cell
S_{raster}	Total surface runoff of a grid cell
R_{raster}	Total groundwater recharge of a grid cell
v	Vegetated
s	Bare-soil
o	Open-water
i	Impervious area
a_v	Fraction areas of vegetated areas
a_s	Fraction areas of bare-soil areas
a_o	Fraction areas of open-water areas
a_i	Fraction areas of impervious areas
P_m	Monthly precipitation
SR_m	Monthly surface runoff
ET_m	Monthly evapotranspiration
R_m	monthly groundwater recharge

I_m	Monthly interception
C_{sr}	Actual surface runoff coefficient
C_h	A coefficient that describes the moisture condition of soil
I_R	Interception ratio
Sy	Specific yield
R_{nj}	Δh is the change in water table height with time
Q	Fow
K	Hydraulic conductivity averaged over the height of the aquifer
A	Area
$h_1 - h_2$	Difference in hydraulic head
L	the distance along the flow path between the points where h_1 and h_2 are measured
h	Hydraulic head in the porous mediumrespectively
Kx	Anisotropic hydraulic conductivity for the porous medium in x direction
Ky	Anisotropic hydraulic conductivity for the porous medium in y direction
Kz	Anisotropic hydraulic conductivity for the porous medium in z direction
W	Volumetric flux per unit volume at sources or sinks of the porous medium
Q_{RIV}	Flow between the river and the aquifer
C_{RIV}	Hydraulic conductance of the riverbed
H_{RIV}	River stage
h_a	Head in the aquifer beneath the riverbed
h_{rivbot}	Level of the river bottom
d	Thickness of the streambed deposits
q	Seepage rate
h_1^n	Lake stages during the present time step,
h_1^{n-1}	Lake stages during the previous time step,
W	Withdrawal rate from the lake
SP	Net rate of seepage between the lake and the aquifer
Qin	Stream inflows

Qout	Stream outflows
A_s	Surface area of the lake at the beginning of the time step.
Δt	Time step length
GHBin	Lateral groundwater inflow by GHB boundaries
GHBout	Lateral groundwater outflow by the GHB boundaries
ΔS	Total change of storage
QLAKin	Inflow from stream to the lake
QLAKout	Outflow from stream to the lake
LAKin	Discharge from the aquifer to the lake
LAKout	Aquifer recharge from the lake
Elak	Lake evaporation
QGWin	Groundwater recharge from streams
QGWout	Discharge from groundwater to streams
Ssat	Change in saturated zone storage
h_m	Observed groundwater level
h_s	Simulated groundwater level
$\bar{h}_m$	Mean observed groundwater level
ME	Mean error
MAE	Mean absolute error

LIST OF PUBLICATIONS

Journal Papers

1) **Salem, A.,** Dezső, J., El-Rawy, M.: Assessment of Groundwater Recharge, Evaporation, and Runoff in the Drava Basin in Hungary with the WetSpass Model. Hydrology, 6, 23, (2019).
2) **Salem, A.;** Dezső, J.; El-Rawy, M.; Lóczy, D. Hydrological Modeling to Assess the Efficiency of Groundwater Replenishment through Natural Reservoirs in the Hungarian Drava River Floodplain. Water 2020, 12, 250
3) **Salem, A.;** Dezső, J.; Lóczy, D. Integrated assessment of the impact of land use changes on groundwater recharge and groundwater level in the Drava floodplain, Hungary. Scientific Reports 2022, under review.
4) Lóczy, D.; Tóth, G.; Hermann, T.; Rezsek, M.; Nagy, G.; Dezső, J.; **Salem, A.;** Gyenizse, P.; Gobin, A.; Vacca, A.; et al. Perspectives of land evaluation of floodplains under conditions of aridification based on the assessment of ecosystem services. Hung. Geogr. Bull. 2020, 69, 227–243.
5) El-Rawy, M.; Batelaan, O.; Buis, K.; Anibas, C.; Mohammed, G.; Zijl, W.; **Salem, A.** Analytical and Numerical Groundwater Flow Solutions for the FEMME-Modeling Environment. Hydrology 2020, 7, 27
6) Aslam, M.; **Salem, A.;** Singh, V.P.; Arshad, M. Estimation of Spatial and Temporal Groundwater Balance Components in Khadir Canal Sub-Division, Chaj Doab, Pakistan. Hydrology 2021, 8, 178.
7) Amiri, M.; **Salem, A.**; Ghzal, M. Spatial-Temporal Water Balance Components Estimation Using Integrated GIS-Based Wetspass-M Model in Moulouya Basin, Morocco. ISPRS Int. J. Geo-Inf. 2022, 11, 139. https://doi.org/10.3390/ijgi11020139

Book chapter

1) Dezso″, J.; Lóczy, D.; **Salem, A.M.;** Nagy, G. Floodplain connectivity. In The Drava River: Environmental Problems and Solutions; Lóczy, D., Ed.; Springer Science + Media: Cham, Switzerland, 2018; pp. 215–230.

Conference Papers and Proceedings

1) Dezso″, J.; **Salem, A.;** Lóczy, D.; Marcin, S.; Dávid, P. Randomly layered fluvial sediments influenced groundwater-surface water interaction. In Proceedings of the 17th International Multidisciplinary Scientific GeoConference SGEM 2017, SGEM2017 Vienna GREEN Conference Proceedings, Vienna, Austria, 27–29 November 2017; Volume 17, pp. 331–338, ISBN 978-619-7408-27-0.
2) **Salem, A.;** Dezso″, J.; Lóczy, D.; El-Rawy, M.; Słowik, M. Modeling surface water-groundwater interaction in an oxbow of the Drava floodplain. In Proceedings of the 13th International Conference on Hydroinformatics (HIC 2018), Palermo, Italy, 1–6 July 2018; Volume 3, pp. 1832–1840.
3) **Salem, A.;** Dezső, J.; El-Rawy, M.; Lóczy, D. Water Management and Retention Opportunities Along the Hungarian Section of the Drava River. In Recent Advances in Environmental Science from the Euro-Mediterranean and Surrounding Regions, Proceedings of the EMCEI 2019 2nd Euro-Mediterranean Conference for Environmental Integration (EMCEI-2), Sousse, Tunisia, 10–13 October 2019, 2nd ed.; Environmental Science and Engineering; Springer: Cham, Switzerland; pp. 1697–1702.
4) **Salem, A.;** Dezső, J.; El-Rawy, M.; Lóczy, D. Statistical analysis of precipitation trend for Drava flood plain region in Hungary. In Proceedings of the GSRD International Conferenc, 579th International conferences on Engineering and Natural Science (ICENS); Istanbul, Turkey, 2019; pp. 43–47
5) **Salem, A.;** Dezső, J.; Elrawy, M.; loczy, D.; Halmai, Á. Estimation of groundwater recharge distribution using Gis based WetSpass model in the Cun-Szaporca oxbow, Hungary. In Proceedings of the 19th International Multidisciplinary Scientific GeoConference SGEM 2019; Albena, Bulgaria, 2019; Vol. 19, pp. 169–176.

Conference abstract and Proceedings

1) **Salem, A.;** Dezső, J.; El-Rawy, M Hydrological modelling for the interaction between grondwater and surface water along the Drava floodplain, Hungary In Proceedings of the 14th Miklos Iványi international PhD & DLA Sumposium. 29-30 October, 2018 Pécs, Hungary.
2) **Salem, A.;** Dezső, J.; El-Rawy, M.; Lóczy, D. Conjunctive Management of Groundwater and Surface Water Resources Using MODFLOW in Drava Basin, Hungary. In Proceedings of the chapman conferensce for Quest for Sustainability of Heavily Stressed Aquifers at Regional to Global Scales; Valencia, Spain, 21-24 October 2019
3) **Salem, A.;** Dezső, J.; El-Rawy, M.; Lóczy, D. Assessment the water replenishment of the Drava Floodplain oxbow In Proceedings of the 15th Miklos Iványi international PhD & DLA Sumposium. 28-29 October, 2019 Pécs, Hungary.
4) **Salem, A.;** Mihoub, M., Lóczy, D..Comparison of water balance of North Algeria and South-Western Hungary. In Proceedings of the 16th Miklos Iványi international Ph.D. & DLA Sumposium. 26-27 October 2020 Pécs, Hungary
5) **Salem, A.;** Dezso″, J.; Lóczy, D.; Integrated hydrolgocial modelling for integrated water resources management in Drava River floodplain" In Proceedings of the International Conference on the Status and Future of the World's Large Rivers, held in Moscow, Russia // Online from 3 to 6 August 2021

CHAPTER One

1. INTRODUCTION

1.1 General

Groundwater is a vital source of freshwater across the world for drinking, agricultural irrigation, and maintaining ecosystem services (IPCC, 2001). Incessant human interventions alter, at an increasing rate, the hydrological process and, consequently, reduce the availability of water in the floodplain. Moreover, a growing global population combined with climate change, pollution, and insufficient groundwater recharge results in dropping groundwater levels. A better understanding of the special and temporal distributions of water balance components, especially groundwater recharge, becomes essential for successful management of water resources and modeling subsurface fluid and contaminant transport (Arefaine et al., 2012), especially now where these resources become the primary source for drinking water (National Research Council, 2008).

The water resources are under serious pressure because of population growth, climate change, and industrialization, which make these resources more vulnerable (Heo et al., 2015). They can influence sustainable development and ecosystem services by influencing the socio-economical structure of the society (Yin et al., 2017). Moreover, land-use/land-cover (LULC) changes are among the major factors altering regional hydrological processes of river basins (Yang et al., 2019), such as streamflow (de Paulo et al., 2018), evapotranspiration (Deng et al., 2015), surface runoff (Rodriguez-Lloveras

et al., 2015), base flow (Wang et al., 2006), infiltration, interception, (Ghimire et al., 2014), and flood regime (Jodar-Abellan et al., 2019) of the catchment. In addition, human interventions have fundamentally altered the water availability of floodplain landscapes (De Vries, 2013), led to lower groundwater tables and deteriorated the balance of natural systems (Hu et al., 2002). The spatial distribution of groundwater quant ty and quality is highly influenced by human activities (Gehrels et al., 2001). Without accurate estimation, the effects of LULC changes on hydrologic components may be understated or exaggerated or even misinterpreted. There are still research questions as how concurrent changes in several LULC classes, and changes in the individual LULC classes influence changes of each hydrological component. The answers to these questions will improve the predictability of hydrological consequences of LULC changes and, thus, are crucial and urgent for efficient water resources management, ecological restoration (Tang et al., 2005), and sustainable development.

Channel/floodplain connectivity is a decisive factor of water supply to oxbow lakes and, thus, a main ecological requirement for floodplain restoration (Wren et al., 2008). The sedimentological sequences along the lower sections of rivers have been created by the alluviation of meandering rivers in historical times. For the rehabilitation measures with the purpose of enhancing ecosystem services, the detailed hydrogeological study of alluvial deposits and soils is indispensable. Hydrologists warn that subsurface and surface water have to be regarded as actively communicating components of a single system (Winter et al., 1999). The multi-layered sediments are of crucial importance as geological background to subsurface water dynamics. Obviously, the randomly layered geological units cause anisotropy. Their position and extension modifies the velocity of subsurface flow. Oxbow lakes and abandoned channels, the most common landforms of floodplains, are regarded particularly sensitive to human pressures (Hulisz et al., 2015; Jason et al., 2008). Major streams, like the Drava River, and their hyporheic zones maintain a hydraulic balance with groundwater. Among groundwater bodies and aquifers, the unconfined aquifer reacts most rapidly to rainfall events. Alluvial sediments indicate an extreme degree of heterogeneity in the hydraulic properties of sediments. Exchange between the alluvial aquifer system and surface water will be affected by the degree of the subsurface heterogeneity (Woessner, 2000). Although many studies

address the interaction between the groundwater and surface water (Rudnick et al., 2015), the degree of subsurface heterogeneity for aquifer was rarely addressed.

International examples show that the integrated (conjunctive) use of surface water and groundwater within a proper management system increases the efficiency of water utilization (Cheng et al., 2009), provides sufficient irrigation water for agriculture (Seo et al., 2018), and improves the environmental conditions of irrigated lands (Liu et al., 2013). The management of a sustainable river basin requires a better understanding of water resources systems and their relationships and types (e.g. groundwater, surface water, quantity and quality, upstream, downstream interactions, and biotic components). Computer models are widely available when it comes to applications in water resources and hydrological analyses. A surface water model is responsible for the surface water hydrology, such as actual interception, transpiration, evapotranspiration, surface runoff, soil water, and groundwater recharge, while a groundwater model covers all processes associated with groundwater, including saturated flow and groundwater discharge into rivers. Coupling the surface water and groundwater models eliminates the limitations inherent in each model to yield a solution that is more in line with real-world hydro(geo)logy. Integrated models in IWRM have gradually gained in significance as the problem of IWRM becomes more and more complex requiring more detailed, refined, and dynamic solutions in more challenging situations.

1.2 Problem Statement

The understanding and effective management of drought and flood issues within catchments are critical to the sustainability of these systems and the environments they support. Surface water and groundwater systems within catchments present significant feedbacks and consequently must be considered as a single system. Holistic consideration of these systems in catchment hydrology requires the understanding and quantification of both surface and subsurface flow processes and their interactions. Whilst there has been a significant contribution to the knowledge and understanding of hydrogeological research of surface water-groundwater interactions in the past few decades, there are still specific knowledge gaps on how different types of systems (i.e.

connected gaining and losing, and losing disconnected) function and interact at different spatial and temporal scales and in different hydrogeological environments. Consequently, a need has arisen for fully integrated surface-subsurface flow models which have become an essential tool in understanding and quantifying these interactions/processes. This body of research addresses some of the complexities of surface water-groundwater interactions in highly regulated river basins, at different spatial and temporal scales, and investigates a number of the dominant controls (e.g. sediment sequences and LULC changes) that influence the exchange processes and dynamics between surface water and groundwater.

Over the last centuries, half of European wetlands and more than 95% of riverine floodplains were converted to agricultural and urban lands (Gumiero et al., 2013). Human interventions have fundamentally altered the water availability of floodplain landscapes (EC, 2000). Changes in the water regimes of rivers are predicted to be damaging to these ecosystems under extensive human pressure, resources exploitation, and pollution. Abandoned channels and oxbow lakes, the most common landforms of floodplains, are regarded particularly sensitive to such pressures. They are highly sensitive to human activities. Recently, the Hungarian Drava floodplain was influenced by large-scale landscape degradation. Global climate change, on one hand, and human interventions, on the other hand, substantially alter and disturb the ecological regime and balanced water budget of floodplains (Bonacci and Oskoruš, 2019). River channelization and widespread agricultural utilization induced gradual desiccation in the Drava floodplain, loss of wetlands and reduced landscape diversity (Pinto et al., 2013). In response to specific regional influences, droughts tend to occur with a frequency equal to that of floods (Lóczy et al., 2014). The previously satisfactory water availability in the Drava floodplain, disconnected from the river channel, was replaced by the alternation of flood and drought periods – occasionally even within a single year (Lóczy et al., 2014). With groundwater tables dropping by 1.5 to 2.5 m, the entrenchment of the river leads to intensified drought hazard and water stress in the floodplain (Dezső et al., 2017; Lóczy et al., 2014). Increasing drought hazard is recognized as a key factor contributing to the loss of ecosystem services, including biodiversity and agricultural productivity, in the floodplain (Lóczy et al., 2020, 2014). Water shortages, particularly

manifested in decreased river discharge and wetlands desiccation, are aggravated by the acidification trend induced by global climate change. As a consequence, the ecological functioning of the natural systems and physical habitats have deteriorated.

Moreover, water shortages have adverse effects on agricultural productivity, related socio-economic conditions, and the life quality of the local population. The optimal design of groundwater table in the floodplain is a complex task because of the conflicts between agriculture, forestry, flood control, and natural conservation demands (Lóczy et al., 2014). The conditions for agriculture, the main source of subsistence for the population, became critical. Recently, a competition between water users represented a serious issue in the Drava floodplain (Bonacci and Oskoruš, 2019) and it is predicted to radically aggravate in the next few years. Water resources are limited and any shortage in them threatens the sustainable development of different sectors (e.g., industry, agriculture, municipal, and tourism) in the Drava basin. Protecting groundwater resources in the Drava basin is especially important for the provision of ecosystem services, landscape management, nature conservation, and economic development though improving agricultural productivity. Therefore, it is required to investigate and manage alternative water resources.

1.3 Motivation and Objectives

IWRM is a complex process and requires integration at a different level. It is crucial to study hydrological and groundwater flow models and all processes which influence this model to assess the availability of water and investigate the LULC change effects on water resources. This study aims to present a comparative analysis of the use of an Integrated Surface Water-Groundwater Hydrologic Modelling to capture hydrologic responses and to integrate water resources management for the highly-regulated river basin. Most studies focused only on one or two aspects of modeling for water resources management where a systematic approach is required. Therefore, the main aims of this thesis are:

- To assess the interactions between groundwater and surface water at a critical part of this system: between a protected oxbow (which is fed by water according to the ODP) and the main river (Drava).
- To assess groundwater potential, long-term spatial distribution of monthly, seasonal, and annual components of the water budget in the Drava basin.
- To assess the potential effects of LULC change on the total water budget and average groundwater level of the Drava floodplain
- To recommend suitable management strategies for restoration of the surface and groundwater resources under the water replenishment scenarios through natural reservoirs.

The Specific objectives are:

- To assess the effect of sedimentological sequences along the lower sections of rivers on surface water –groundwater interaction
- To analyze the exchange of water fluxes between the lake and aquifers and the changes in groundwater levels under each scenario of oxbow lake(s) replenishment
- To evaluate the feasibility of water replenishment through natural reservoirs under different management scenarios
- To quantify the water budget and water retention, under different management scenarios in the lower parts of the floodplain

One of the objectives of this thesis is to support the Government in their decision-making by providing access to improved (processed) data and to provide planners with tools to assess the effects of LULC changes on ecosystem services and explore the hydrological feasibility of alternative water management, i.e., the restoration of natural reservoirs (abandoned paleochannels) to mitigate water shortage problems. One of the challenges for the study is to feed their knowledge into regional and national planning systems to manage the Drava River basin now and in the future. The outcome of this study may serve as a contribution to their objectives, by providing an improved understanding of the special and temporal distributions of water balance components, the spatial extent and variation of groundwater levels, the effects of LULC change on

hydrology, and the dynamic interactions between groundwater and surface water within the Drava River basin, especially water balance between the lake and groundwater. This was done to achieve the goal of further understanding of the use of WetSpass–MODFLOW as a planning tool to predict the effect of natural and anthropogenic influences on the floodplain.

1.4 Research Question

- What is the impact of the replenishment of the Cún-Szaporca oxbow lake system on the hydrologic system adjacent to the lake area?
- What is the long-term spatial distribution of monthly, seasonal, and annual water balance components?
- How can coupled models (coupling WetSpass-Modflow) be applied to improve long-term stressor simulation?
- What are the potential effects of different LULC changes on groundwater recharge in the Drava River Basin and how can these effects be explained?
- What is the hydrological feasibility of applying natural reservoirs as an alternative water resource management?

Specific questions

- How can randomly layered fluvial sediments influence groundwater-surface water interaction?
- What is the effect of model discretization?
- What is the impact of the lake level variations on the temporal variability of groundwater heads and on the spatial extent of that influence?
- How are water balance components influenced by land use types?
- How are water balance components are influenced by soil types?
- How is the sensitivity of groundwater recharge to LULC changes spatially distributed within the Drava River Basin and how can this be explained?
- What are the recommended management strategies for water retention in the Drava basin?

To achieve the study's aims, the research strategy has been designed as follows:

- Set up Aa quasi-distributed hydrological model (WetSpass-M) for a highly-regulated river basin, the Drava River basin in the Hungary involving validation using the water table fluctuation method. The linear regression method is applied to perform a statistical analysis by identifying the trend of precipitation data.
- Build a three-dimensional groundwater flow model, calibrate it with observed groundwater levels and lake stages and conduct the sensitivity analysis for the groundwater flow model using computer code for universal sensitivity analysis, calibration, and uncertainty evaluation (UCODE-2005) with the help of ModelMate.
- Integrate framework model which couples the calibrated hydrological model (WetSpass-M) with the calibrated groundwater flow model (MODFLOW-NWT) to improve the simulation of a long term stressor.
- Perform a holistic investigation of sediment sequences by satellite image processing (SIP), Ground Penetration Radar (GPR) record, particle size distribution (PSD) of sediments measured in situ and determining hydraulic conductivity from each auguring.
- Reconstruct the stratification and layer variability of alluvial sediment formations where the subsurface flow is crucial.
- Create various modeling scenarios for different degree of aquifer heterogeneity to assess losses from the lake and water retention in the system.
- Simulate different management scenarios in augmenting surface water storage by applying two natural reservoirs and feed them into the coupled model to explore the hydrological feasibility of alternative water management.

1.5 Structure of the Thesis

This thesis consists of nine chapters including the introduction in Chapter 1 and conclusions in Chapter 9.

Chapter (1) Introduction: Includes problem statement, research objectives and scope of thesis.

Chapter (2) Literature Review: is a review of literature on the physical background of groundwater recharge and various methods of recharge estimation, modeling support for integrated water resources management, impact of land use change on groundwater, surface water-groundwater interactions, and modeling lake-groundwater interactions.

Chapter (3) Description of the study area: a short description of the study areas is provided in terms of location, hydromorphology, climate, geological and geomorphological settings, soil, land cover and surface and groundwater in the environment of the oxbow system.

Chapter (4) Hydrological Modelling of a Highly-regulated River Basin: is about building a hydrological modeling using the WetSpass-M model of the complex highly regulated basin, the Drava River in Hungary. It involves model description, structure, required input data and parameters, and validation with the water table fluctuation method. A summary of the limitations follows the detailed discussion of the model set up.

Chapter (5) Groundwater flow model: treats the developing of a groundwater model (MODFLOW-NWT) with ModelMuse as a graphical interface for the Drava Basin. It includes conceptualization, boundary conditions, sensitivity analysis using computer code, calibration, and uncertainty evaluation (UCODE-2005). The model is calibrated with an eight-year data series of observed groundwater levels and water budget.

Chapter (6) Integrated assessment of the impact of Land-use/land-cover changes on hydrology: studies the coupling of the land surface process model (WetSpass-M) with a physically based fully distributed groundwater flow model (MODFLOW) to improve simulation of the long term stressor. It is applied to assess the impacts of LULC changes from 1990 to 2018 on water balance components and groundwater levels of the Drava floodplain.

Chapter (7) Randomly layered fluvial sediments influenced groundwater-surface water interaction/ assessment of water replenishment to a floodplain lake: investigates

the sedimentology of the Cún-Szaporca oxbow of the Drava floodplain, evaluating the interactions between a protected oxbow and the main river (Drava) under different fluvial sediment structures scenarios using 3-D groundwater flow model. The model was applied to analyze two scenarios for the replenishment of the lake.

Chapter (8) Integrated water resources management: is concerned with the elaboration of different management scenarios for two natural reservoirs with filling rates ranging from 0.5 m^3 s^{-1} to 1.5 m^3 s^{-1} using the calibrated integrated model (WetSpass-M/ MODFLOW-NWT). It includes the assessment of lake–aquifer exchange fluxes and the Spatio-temporal extent of reservoir impact for each scenario.

Chapter (9) Conclusions and Recommendations for future studies

References: Have been shown at the end of the thesis.

Appendices: Appendix (A&B) contains the data entry.

CHAPTER Two

2. LITERATURE REVIEW

Computer models play an essential role in Integrated Water Resources Management (IWRM) providing a range of support to the assessment of water resources management and decision making. This chapter offers a review of Integrated Water Resources Management, the concept and methods of groundwater recharge, and models of groundwater hydrology. Moreover, surface water groundwater interaction, assessment of lake- groundwater interaction, and modeling techniques of lake/reservoir and aquifer system interactions are presented.

2.1 Integrated Water Resources Management

IWRM is an approach to utilizing, formulating, and implementing planning and management strategies for sustainably and ecologically developing water resources by considering the spatial and temporal interconnections with human, natural resources and environmental aspects among water users. Currently, it has been considered as a global paradigm for water resources management and has been broadly applied for practical water resources management problems (Gain et al., 2012). The water resources systems should be fully considered and dealt with as part of the broader environment including socio-economic demands under the impacts of the cultural and political situations.

The IWRM practice depends heavily on the use of computer-based models because both allocating and assessing water resources are non-trivial processes (Salem et al., 2021). In the beginning, the use of computer models in water resources management is naturally required to obtain quantitative knowledge of water resources at a given place and then to allocate resources in an efficient and optimized manner under specific constraints. The set of computer models used in the past differed slightly from those that

have been used to study natural processes in the water cycle, such as hydrological models. IWRM community tends to use more generic names, such as simulation models, to highlight their pioneering role in IWRM, i.e., simulate the natural process of producing resources with different initial and boundary conditions and to form the basis for 'what-if' analysis further.

The computer models in the latter group are mathematically similar to the process of solving optimization problems with the primary goal being defined as efficient use of water under different constraints. Since the water use represented by models in this category is often referred to as allocations to a different portion of water resources, these models are also called allocation models, although appropriation, strictly speaking, is only a small part of their purposes while nowadays more complex models focus on supporting overall decision making. Sheer (1981) presented the earliest attempt of using computer models in IWRM where the Potomac Reservoir and River Simulation Model (PRRISM) was applied from the late 1960s to the early 1970s, to simulate the water use from the reservoirs during the drought season in the Potomac River Basin, Metropolitan area Washington, USA.

Over the last two decades, the need for detailed models has increased dramatically with the use of several, such as PDM (Moore, 2007) and MODFLOW (Niswonger et al., 2011). While this step, in general, helps practitioners to improve individual paradigms and improve governance in return, it has fragmented the idea of integration. Consequently, researchers have increasingly recognized the problem of using highly specialized, fragmenting models in IWRM. Research on model integration in the context of IWRM has appeared in many of the research agendas, with some promising results, e.g. in WetSpass-Modflow. Their overall results demonstrate that the model can represent the results of integrated watershed modeling that includes surface hydrological and groundwater hydrological components. Besides, the results improve understanding regarding spatial patterns of groundwater influence on sewer flow, which can aid floodplain management schemes for the conjunctive use of ground surface water.

2.2 Groundwater Resources

Groundwater is a major source of freshwater across the world for drinking, water supply of food production, and agricultural irrigation and plays an important role in maintaining ecosystem services (IPCC, 2001; UN/WWAP, 2006). About 2 billion people worldwide rely on groundwater supplies (WWAP, 2015). Groundwater is a vital natural water resource globally due to its better protection from surface pollution and its low impact by seasonal fluctuations with regard to surface water (Zektser and Everett, 2004). Moreover, groundwater plays an essential role in sustaining rivers, wetlands, and lakes during dry periods. The groundwater is the stored water at the subsurface/underground of the earth, which exists in pores between sedimentary particles and in fissures and aquifers of solid rocks. Groundwater served as the largest reservoir of drinkable water and it is less contaminated by wastes as it can be stored in the saturated zone of the soil. Groundwater resources are indirectly affected by variations in precipitation, temperature, and evaporation and generally with a time delay while climate variability affects surface water resources more directly (Jyrkama and Sykes, 2007). The sustainability of groundwater resources relies on groundwater recharge, i.e. downward water flow to the water table and groundwater storage (Healy and Scanlon, 2010).

2.3 Groundwater Recharge

Groundwater recharge is a hydrological process by which water percolates down the soil and reaches the water table either by natural and artificial methods to replenish the aquifer with water from the land surface (Healy and Scanlon, 2010). Groundwater recharge can be defined as the entry of water into the saturated zone and until it reaches the water table surface (Freeze, 1969). This process is connected to the other water balance components since precipitation is partitioned into evapotranspiration, surface runoff, interception, and infiltration. In general, the amount of percolation into the groundwater system depends on various factors such as climate, vegetation cover, soil composition, geological formation, soil moisture content, land slope, land use/land

cover, topography, the presence or absence of enclosing beds, and depth to the water table. Recharge is encouraged by natural vegetation cover, flat topography, soil permeability, and depth of water table and unconfining beds (Al Kuisi and El-Naqa, 2013; Obuobie, 2008). Consideration of these characteristics is a prerequisite to the estimation of groundwater recharge. There are various sources of recharge to a groundwater system, including both natural and human-induced sources. Natural sources are represented by recharge from precipitation, rivers, lakes, ponds, and other aquifers. While irrigation losses from both fields and canals and, leaking water mains, septic tanks sewers, and over-irrigation of gardens, parks, and other public amenities present human-induced sources. There are three principal mechanisms of recharge according to Hendrickx (1992):

Direct (diffuse) recharge: water added to the groundwater reservoir in excess to soil moisture and evapotranspiration deficits by direct vertical infiltration from precipitation or irrigation.

Indirect recharge: Infiltration to the water table following runoff and localization in joints. Two principal categories of indirect recharge are apparent: that related to surface watercourses, and a localized recharge resulting from the horizontal surface concentration of water in the absence of well-defined channels, such as recharge through small depressions, sloughs, joints, and potholes.

2.3.1 Factors Affecting Recharge

Groundwater recharge is influenced by complex processes and several parameters which themselves are affected by many factors. Climate, vegetation characteristics, and Soil types can vary significantly over small regions. Therefore, lumped or point-based models do not present a complete look and accurate estimation of groundwater recharge. The impact of temporal and spatial variability on groundwater recharge is also becoming more widely appreciated.

2.3.1.1 Climate Variability

Climate variability is influencing groundwater recharge and level owing to changes in evaporation loss and precipitation (Waikar and Somwanshi, 2014). In most applications of groundwater flow modeling, the precipitation rate is often regarded as spatially constant or averaged over time in steady-state analyses. However, precipitation varies significantly even over short distances, and consequently, the result of the spatial variation of precipitation should not be neglected, especially in studies of large-scale modeling (Jyrkama and Sykes, 2007). Rainfall is considered one of the most important supplies of water in any region. The amount of water that is used for different purposes in a specific region depends on the amount of rainfall. Excess water means a waste of water which is so precious in any region. Moreover, it can raise the groundwater table that resulted in unsatisfactory saturation of the root zone. On the other hand, an extensive period with the absence of rainfall during the growing season leads to the wilting of plants. The availability of freshwater resources becomes a limiting factor for crop growth worldwide (Gat, 2004).

In the groundwater recharge process, precipitation is considered as the most important parameter. It provides the water that will recharge the groundwater system and represents the dynamic force in the hydrologic cycle. Precipitation is influenced by metrological factors such as temperature and wind resulting in dynamic and complex distribution while the spatial distribution and intensity of precipitation affect the amount of groundwater recharge. Storm events could be largely different in duration, intensity, and velocity, while lower temperatures can lead to mixed precipitation (Jyrkama and Sykes, 2007). The impact of rainfall and evapotranspiration on the groundwater basin is generalized. According to Karimi, et al. (2015), actual evapotranspiration represents the water amount that is subtracted from the soil through transpiration and evaporation. It changes with the accessibility of moisture and temperature throughout the year (Bakundukize et al., 2011). In the rainy season, when effective precipitation is larger than the potential evapotranspiration and the soil is at field capacity, the actual evapotranspiration will be at its maximum value and equal to PET which enables the aquifer to be recharged. The aquifer is no longer recharged when PET is larger than

precipitation. The used water for ET is taken from soil moisture storage and precipitation until it is depleted (Van Landtschoote, 2017). Thus, potential evapotranspiration (ETo or PET) is an important parameter of the water budget with high temporal and spatial variability. The climatic variability will influence ET and alters basin water yield (Lu et al., 2005; Shao et al., 2012).

2.3.1.2 Land use/land cover

LULC type has a substantial effect on groundwater recharge or infiltration (Dost et al., 2013; Walker et al., 2002). LULC is one of the most important controlling factor in basin hydrology (Fetter, 2001). Vegetation affects recharge through transpiration and interception. Large-scale vegetation controls the amount of infiltration rate, deep drainage, net rainfall, and the storage capacity of the aquifer. The stored water that could be removed by vegetation relies mainly on rooting depth. Shallow-rooted grasses remove less water than deeper-rooted trees and shrubs (Jyrkama and Sykes, 2007). Urban regions can also have an obvious effect on groundwater recharge by increasing impervious areas which alter their natural state (Hendrickx, 1992). However, the argumentative impact of urbanization is often on the quality of recharge, rather than on its quantity (Foster, 2001). The LULC is also useful to estimate the vegetative parameters' values such as evaporative zone depth and leaf area index (LAI). The LAI parameter is used for controlling both surface evaporation and transpiration (Ala-aho et al., 2015).

2.3.1.3 Soil Properties

Soil texture is the key point to understand all required information for the hydrological investigation of any region (Berhanu et al., 2013). Soil represents the main physical characteristics that control runoff and recharge and generation. The soil infiltration capacity relies on soil permeability, which controls its storage capacity and influences the hostility of the flowing water into deep layers. Since the soil texture has a significant impact on the soil infiltration capacity, sandy soil has the highest infiltration

rates while heavy clay and loamy soil show lower infiltration rates and higher surface runoff (SMEC, 2007).

The water saturation degree of the root zone controls the hydraulic conductivity distribution and consequently the infiltration to the groundwater table. Also, it affects the uptake water by roots and as the result the actual evapotranspiration (Berendrecht, 2004). Therefore, the groundwater recharge process is not only affected by temporal and spatial variability in the major metrological variables, but also relies on the spatial distribution of land surface characteristics, hydraulic conductivity, and depth properties of underlying soils.

2.3.2 Estimation of Groundwater Recharge

The evaluation of water balance components is critical for sustainable and effective management of surface water and groundwater resources such as estimation of water availability, quantification of sustainable amount of groundwater depletion, or prevention of desertification and land degradation. Estimation of groundwater recharge is a challenging and complex process as groundwater recharge depends on several parameters such as topography, land use, soil texture, groundwater depth, meteorological conditions, and other hydrologic characteristics (Batelaan and De Smedt, 2007). Measuring the groundwater recharge for a large area in situ is unmanageable; it is usually quantified by indirect techniques (Bakker et al., 2013; Scanlon et al., 2006). The selection of an appropriate technique to evaluate the groundwater recharge remains a difficult step. Moreover, several factors may attribute to the choice of the most reliable technique, such as the scale of space and time and the range and validity of the recharge estimates (Hendrickx, 1992; Scanlon et al., 2002). Quantifying groundwater recharge requires modeling the interaction between important processes in the hydrological cycle such as evapotranspiration, surface runoff, infiltration, and variations of groundwater levels (Jyrkama and Sykes, 2007). Scanlon et al. (2002) categorized groundwater recharge techniques based on hydrological zones from which the recharge data is obtained, namely unsaturated zone, saturated zone, and surface water. The different zones provide estimates of groundwater recharge over varying scales of space and time

The estimation techniques of groundwater recharge are further classified as follows: tracers methods, physical techniques, and numerical modeling approaches within each hydrologic zones.

2.3.2.1 Groundwater recharge estimation methods

Numerous techniques are used to estimate groundwater recharge including experimental methods, chloride ion mass balance method, Hydrological Budget (HB), empirical methods, distributed Double Hydrological budget (DHB), statistical approaches such as Water Table Fluctuation (WTF), recession curve displacement method (Rorabaugh Method) and numerical methods like water balance simulation (Anuraga et al., 2006; Batelaan et al., 2003; Carrera-Hernández and Gaskin, 2008; Salem et al., 2020b). Wang et al. (2008) used experimental methods through isotope tracers, and to estimate groundwater recharge. Lysimeter tools enable to present the actual drained water from the soil column. This allow to explore an explicit relationship between groundwater recharge and other water balance components. They are not appropriate in many developing contexts, however, their installation is costly. Moreover, the obtained groundwater recharge with lysimeters as an unsaturated-zone technique, is better to consider as point estimates (Scanlon et al., 2002), because of the heterogeneity of vegetation and soil.

The water table fluctuation method (WTF) has been applied in several studies to relate water levels in wells to groundwater recharge, via specific yield (Meinzer and Stearns, 1929; Rasmussen and Andreasen, 1959). Seasonal or annual estimates could be performed based on the periodic measurements of water levels of wells, but this method is intended for estimating the short-term in water table fluctuations in response to rainfall events. The spatial validity of this method ranges from a lower estimation of several square meters according to Healy and Cook (2002), to an upper limit of one thousand square meters according to Scanlon et al. (2002). Ideally, to achieve reliable estimates, numerous wells should be observed. In developing contexts, such observations may rarely be undertaken, however, again limiting the use of this approach. WTF is applied by evaluating the specific yield for an area of groundwater level fluctuation (Healy and

Scanlon, 2010). Moon et al. (2004) evaluated groundwater recharge using modified WTF and groundwater hydrographs for the basin of a river in South Korea. They concluded that the average groundwater recharge ratio was grouped based on their groundwater hydrographs and varied from 4 to 15%. Healy and Cook (2002) reviewed the applicability of the WTF method to evaluate groundwater recharge and demonstrated its limitations. Martin (2005) utilized WTF to quantify the annual average of groundwater recharge in Atankwidi, West Africa. He reported that the recharge varies from 13 mm to 143 mm. Salem et al. (2018b) used empirical methods based on precipitation depths and WTF to evaluate groundwater recharge in the Cún-Szaporca oxbow of the Drava floodplain, Hungary. Rasoulzadeh and Moosavi (2008) used an inverse approach and considering the WTF model as a forward model evaluated the WTF parameters and groundwater recharge for the vicinity of Tashk Lake in Iran. Theis (1937) reported that the recharge rate could be calculated by multiplying the specific yield by the annual rate of water table decline during periods of no recharge, assuming that the annual basin inflow equals the annual outflow over the long term. Similarly, the recharge rate is determined by multiplying the specific yield by the rate of water level rise multiplied by during recharge periods. Bear (1979) conducted the relationship between recharge and precipitation at different times.

The Rorabaugh method is applied when a series of groundwater recharge events take place during one runoff season. This method can be used when the recession curve is moved upward by a recharge event. The extent of the upward shift of the recession curve is used to estimate groundwater recharge (Rorabaugh, 1964; Rorabaugh and Simons, 1966). Winter et al. (2000) used principal component analysis (PCA) to categorize groundwater hydrographs of small lake watersheds to understand the features of recharge and the impacts of geology on water-table fluctuations. Manghi et al. (2009) applied (HB) method to evaluate groundwater recharge in Hemet sub basin, United States. They found that annual long-term average recharge was 12.5 million cubic meters, from 1997 to 2005. El-Rawy et al. (2016) applied DHB approach to quantify the distribution of recharge rate over the Zarqa River Basin, Jordan. Hendrickx (1992) highlighted five main techniques of evaluating direct groundwater recharge from precipitation, empirical methods, direct measurement, tracers, water budget methods,

and Darcian approaches. Commonly, groundwater recharge is estimated to a large extent as an imbalance between evaporative demand and precipitation at the land surface (Gebreryfael, 2008). Currently, with the advantage of Geographic Information Systems (GIS), physical-based hydrologic modeling has become essential in contemporary hydrology for evaluating these factors as well as the effect of climate change and human intervention on water resources and basin hydrology (Alemaw and Chaoka, 2003).

2.4 Models Used in Groundwater Hydrology

Groundwater models are conducted for numerous hydrologic investigation purposes such as water quantity estimations, remedial designs, and vulnerability assessments (Ella et al., 2002). The hydrological models were classified into three major classes. Those are:

- Empirical models (data-based models)
- Conceptual models (parametric models)
- Physically-based model (mechanistic models).

2. 4.1 Empirical models

An empirical model is based on investigation and observation, they are utilized to construct a relationship between rainfall and runoff to predict runoff in different regions (Chen et al., 2013). Physical transformation function to relate input to output is not considered in the empirical method. These models are often used in ungauged (unreachable) regions, where only little data or information are available on the region involved. An empirical model could be a clarification of a true system with the exploitation of experimental knowledge, mathematical justification, while not attempting to illustrate general physical laws. This type of model is developed by nature sometimes from analysis on easy knowledge sets. Several hydrological models are empirical and have an important function in developing the science of hydrologic

models. In these models, it is assumed that the climate boundary is absolute and the structure is static (IHMS, 2006).

2.4.2 Conceptual models

In the conceptual model the physical processes are taken into account which are acting upon the variables input to produce output variables. The conceptual method attempted to add physical importance to used constraints and variables in the mathematical function which present the connections between all processes that influence the system. Darcy formula (law of porous media flow) represents an example of a simple conceptual model. Conceptual models are widely employed as they are easy to use, can always be calibrated, and use limited input data.

2.4.3 Physically based models

Physically-based models are founded on the understanding of the behavior of involved processes and describe the system by involved equations grounded on the laws of conservation of mass, energy, and momentum. The physically-based model parameters are identical regarding the respective prototype physical characteristics (Ella et al., 2002). Physically-based models often use dispersed and deterministic input data. These models are distributed based which can explicitly represent the spatial distribution of the mainland surface characteristics such as soil, climatic variables, and topographic elevation (Wijesekara et al., 2012). Physically-based models have numerous worldwide applications. The estimated or measured hydrologic stresses and model parameters e.g. differences in natural groundwater recharge, human impacts such as groundwater extractions) could be adjusted in the input data file, so that the model is climatically and geographically transferable to any other region. Therefore, recent studies in hydrogeology mostly use physically based models (Cunderlik, 2003). WetSpass model is an example of physically distributed models.

2.5 Groundwater Flow Modeling

Numerical models enable detailed assessment of the impacts of hydraulic properties of the vadoze zone and their spatial variabilities on groundwater recharge. These models are depending on soil profile subdivided with a number of homogeneous layers with their hydraulic properties. They simulate the transformation of precipitation into flow considering all intermediate processes such as interception, evapotranspiration, runoff, and infiltration. Thus, they are able to evaluate groundwater recharge at several points and at many times. Initial conditions and boundary conditions, vegetation properties, and soil properties must be imposed in the models to estimate groundwater recharge. Groundwater flow modeling provides several advantages for the estimation of groundwater recharge. Three-dimension full distributed numerical groundwater flow models such as MODFLOW are applied to evaluate groundwater recharge by adjusting the input groundwater recharge until simulated groundwater level by model match the measured one. One issue in this approach that any changes in aquifer variables such as aquifer storage and hydraulic conductivity influence the simulated groundwater level. The uncertainty associated with transmissivity is often greater than that associated with groundwater recharge. Consequently, the accuracy of the estimated groundwater recharge could be low. The ability of groundwater flow modeling programs such as GMS MODFLOW to gather a wide variety of data into a consistent model is a tremendous advantage. However, without flow values, multiple possible solutions could be provided without a sense of which is the best fit, leading to the non-uniqueness issue of modeling systems. Moreover, head values should be continually observed to establish the variation in the system, which could be a concern in developing contexts in the case such information is limited. Where parameters such as rainfall are not integrated directly, it could be difficult to obtain an explicit relationship between recharge and rainfall. Once the relevant factors such as hydraulic conductivity and recharge are established, investigations of alternative scenarios through change factor values are straightforward and result in multiple outcomes. For example, Markstrom et al. (2008) developed the GSFLOW model through coupling watershed with the groundwater flow model, which links MODFLOW-2005 (Harbaugh, 2005) with PRMS (Leavesley et al., 1983) to

simulate surface water and groundwater resources. Conceptually, GSFLOW subdivided the coupled system into three compartments. The first compartment includes plant canopy, soil zone, impervious storage, and snowpack and it is simulated by PRMS. The second presents lakes and streams, while the third compartment is simulated by MODFLOW-2005 and includes unsaturated and saturated zones. Another example is the (Batelaan and De Smedt, 2007) coupled WetSpass model which calculates the long-term average of water-balance components to a regional groundwater flow model. Regional groundwater models are often quasi-steady state applied for evaluating the groundwater system (discharge-infiltration relations) and thus require long-term average recharge input. Therefore, WetSpass, considers the spatial distribution of land use, soil texture, slope, and climatological conditions in estimating groundwater recharge. WetSpass can be iteratively linked to a groundwater flow model, which provides the water table level, while WetSpass returns estimated groundwater recharge accordingly.

2.6 Hydrological Models

Hydrological models are simplified systems to estimate the hydrological cycle processes in an entire or parts of the river basin. They are dependent on a set of interrelated equations that try to transfer the physical laws, which control extremely complex natural phenomena. Also, different varieties of models can be applied, based on the input variables, the existing database, required analysis, and considered output, rainfall-runoff models described the representation of physical processes, they could either be based on a simple mathematical connection between the variables of input and output of the basin or involve the description of basic processes that participate in the runoff generation. In the past decades, numerous models have been developed in different parts of the world. These models could be generally categorized based on process description as data-driven models, conceptual models, and physically-based distributed models (Beven, 2012). Hydrologic models can be classified as distributed, undistributed conceptual, or stochastic etc. based on their physical parameterization and model structure.

Klemes (1983) proposed two types of modeling approach: a top-down and a bottom-up approach. Physically-based distributed models represent a bottom-up modeling approach (Savenije, 2001; Sivapalan, 2003). Physically-based distributed models were developed starting from the 1980s at the same time with the development of Geographical Information System Tools and Remote Sensing Techniques and can provide the highest accuracy in the modeling of precipitation-runoff processes (Xu, 2002). These models are based on the principles of physical processes depending on continuity and the conservation of mass, energy, and momentum. In this approach, hydrological processes are modeled by presenting a large number of model parameters that are presumed to be measurable at a micro or plot-catchment scale, representing the different heterogeneities in the catchment. In top-down modeling approaches, the equations applied to describe the physical processes often have (indirect) physical meaning but calibration is used to obtain the parameters. The modeling procedure in a top-down modeling approach usually starts with a simple model and progressively increased complexity through the step-wise inclusion of process descriptions (Montanari et al., 2006; Sivapalan, 2003).

In recent time, advances have been conducted in the hydrological process through understanding and modeling using topography-driven, conceptual, flexible, semi-distributed model structures (Gao et al., 2014; Gharari et al., 2014). Data-driven models are dependent on extracting information that is contained in hydrological data. These models include mathematical equations that do not depend on realistic principles such as energy, momentum, or mass balance equations (Solomatine and Wagener, 2011). The applications of such models are based on a proper analysis of the input/output time series (Bowden et al., 2005). Numerous hydrological models are available today for estimating groundwater recharge. Physically distributed models, such as MIKE SHE (System Hydrological European), are proper for ungauged basins (Zhang et al., 2015). TOPMODEL (Topographic Hydrologic Model) have performed well in assessing the areas of runoff in mountainous areas (Gumindoga et al., 2014), along with DREAM (Manfreda et al., 2005), and WetSpa (Wang et al., 1996). The ZOODRM model (Hughes et al., 2008) combines the temporal and spatial constraints on the inputs, such as the length of the daily rainfall time series, the spatial distribution of rainfall, and the number

of rain gauge stations. Hemmings et al. (2015) used the ZOODRM model to assess three precipitation distribution scenarios to incorporate the spatial relationships of rainfall with elevation and latitude, to estimate the spatial and temporal recharge rates of Montserrat Island. Sophocleous (1991) developed a simple modeling approach to estimate groundwater recharge from rainfall records, water-table fluctuations in wells, and vadose zone water balance analysis.

The Soil and Water Assessment Tool (SWAT) was applied widely to evaluate the effects of different soil textures, vegetation cover and land use, on water production, non-point source pollution, and sediment yield, which requires complicated and large parameters. The unsaturated zone physically-based numerical models such as SWAP simulate the water flow equation of the unsaturated zone, i.e. the Richard equation for porous media. Parametric models, like EARTH, use analytical or numerical relations between precipitation and groundwater recharge. These models deal with conceptual groundwater recharge that could not be included by existing numerical models such as groundwater recharge through a hard rock formation. Gehrels (2001) applied both the EARTH and SWAP models to predict groundwater recharge fluctuations in the porous media of the Veluwe region. Both models performed well to evaluate deep groundwater level fluctuation. Therefore, the parametric models could be applied in porous and hard rock formations. Lee and Chung (2007) reported that water balance components can be evaluated using the soil moisture budget method and base-flow model. This model uses the separating baseflow from the total streamflow discharge and obtains groundwater recharge (Lee and Chung, 2007).

Kendy et al. (2003) developed a multi-layer soil water balance model which operated daily to quantify groundwater recharge in an agricultural region in northern China. The data requirements of the model are relatively high. The subsurface is subdivided into layers according to soil horizons, each with properties of saturated hydraulic conductivity, saturation, and field capacity that control flow from one layer to another. Once one layer is saturated with infiltrating water, the excess water is transferred automatically downward to the next layer. The presented water below saturation flows down based on an exponential relationship between moisture content and hydraulic conductivity. The model was applied to the top two meters of the

subsurface, but theoretically could be extended for the entire vadose zone, to better control the dynamics of soil moisture storage and groundwater recharge. This approach calculated groundwater recharge at several discrete locations in the study area. The study of Kendy et al. (2003) neglected runoff, but the model could be modified easily to involve runoff calculation. Estimation of groundwater recharge is often confounded by high spatial variability.

In most water balance models, groundwater recharge is determined as the residual term of the water balance equation and a significant uncertainty could be associated with estimating groundwater recharge (Chen et al., 2005; Kendy et al., 2003). As evapotranspiration contributes to the largest term of the water balance in arid/semiarid regions and as several methods exist for determining evapotranspiration, it attributes significantly to this uncertainty. Improving the estimation of all other parameters in the soil water balance equation is the only way to decrease this uncertainty by increasing the temporal resolution of the accounting procedure. Thus, groundwater recharge is commonly used as a calibrating parameter in groundwater flow modeling (Ghiglieri et al., 2014).

2.7 WetSpass Model

WetSpass is an acronym for water and energy transfer between soil, plants, and atmosphere under a quasi-steady-state that was built upon the foundations of the time-dependent spatially distributed water balance model (Batelaan and De Smedt, 2007; Batelaan and Smedt, 2001). The model simulated the long-term average spatial distribution of water balance components surface runoff, actual evapotranspiration, and groundwater recharge at seasonal and annual scales using hydrometeorological data, topography, soil mapping, and land cover. WetSpass-M (Abdollahi et al., 2017) is a downscaled model from the seasonal temporal resolution to a monthly scale. In the WetSpass model, the total water balance for a raster cell grid is split into independent water balances for the bare soil, vegetated, bare soil, open-water, and impervious parts areas, and open-water of each cell. This accounts for the non-uniformity of the land use per cell grid, which is dependent based on the raster cell resolution of the raster cell. The

processes in each part of a cell are set in a cascading way. This means that an order of occurrence of the processes, after the precipitation event, is assumed. Defining such an order is a prerequisite for the seasonal timescale with which the processes will be quantified.

A mixture of empirical and physical relationships is applied to describe the processes. The quantity determined for each process is consequently limited by a number of constraints (Batelaan and De Smedt, 2007; Batelaan and Smedt, 2001). WetSpass is developed as to regional groundwater flow models are quasi-steady-state used applied to simulate infiltration–discharge - infiltration relations based upon on long-term average groundwater recharge input data. Thus, the estimated recharge through WetSpass can be applied as an input for regional steady-state and transient groundwater models and, hence, increase the confidence in the evaluation of groundwater recharge (Rwanga and Ndambuki, 2017). Baseflow, surface runoff and total discharge were applied to calibrate the WetSpass water balance components.

2.7.1 Application of the WetSpass model

Recently, energy and water transfer among plants, soil, and atmosphere (WetSpass) model (Batelaan and Smedt, 2001), under a quasi-steady state, has been used widely for groundwater recharge assessment. Abu-Saleem (2010) adjusted WetSpass model parameters for Jordanian conditions by developing a modified WetSpass model WetSpass-Jor. Abu-Saleem et al. (2010) used a WetSpass model to simulate the water balance components in the Hasa basin, Jordan. They concluded that 83.96% of the precipitation accounted for actual evapotranspiration while groundwater recharge and surface runoff and are represented by 0.64% and 15.4% of the precipitation, respectively. Arefaine et al. (2012) evaluated the water budget components in Northern Ethiopia using the WetSpass model. The results show that around 81% of precipitation is attributed to the actual evapotranspiration while the remaining 72% and 12% of the total precipitation are accounted to surface runoff and recharge. Abdollahi et al. (2012) developed the WetSpass-M model by downscaling the seasonal resolution to a monthly scale. Al-Kuisi and El-Naqa (2013) used the WetSpass model to quantify the water balance components

in the Jaf basin in. The model findings present that the major portion of the rainfall (94.6%) attributes to actual evapotranspiration, 4.9% accounts to surface runoff and 0.5% recharges the aquifer system.

Gebreyohannes et al. (2013) used the WetSpass model to assess the availability of surface and groundwater resources in the Geba basin, Ethiopia. The main findings show that 6% of precipitation recharges the groundwater system, 18% is accounted to surface runoff and 76% of rainfall is released through evapotranspiration. Aish (2014) evaluated the water budget components using the WetSpass model in the Gaza Strip. Annual mean rainfall of 53.5 mm is distributed as 77% of evapotranspiration, 11% of surface runoff, and 12% of groundwater recharge.

Armanuos et al. (2016) applied a Wetspass model to determine the spatial distribution of groundwater recharge in the Nile Delta aquifer, Egypt. The simulated results reveal that such a WetSpass model works well in estimating water balance parameters in the Nile Aquifer. Zarei et al. (2016) an estimated groundwater recharge, actual evapotranspiration, and surface runoff for different land-use in the Mashhad basin, Iran, using the WetSpass-M model. WetSpass-M reveals that 57% of rainfall contributes to actual evapotranspiration, 29% accounts for groundwater recharge, and the remaining14% became surface runoff. Ghouili et al. (2017) applied the WetSpass model to evaluate the groundwater recharge in Takelsa multilayer aquifer, Tunisia. The results show that the mean annual actual evapotranspiration, surface runoff, groundwater recharge, and are 461 mm, 92 mm, and 22 mm, respectively. 89% of the annual rainfall is lost by evapotranspiration while 17.8% and 4.3% are attributed to surface runoff and groundwater recharge respectively. Gebremeskel and Kebede (2017) assessed seasonal and annual average groundwater evapotranspiration, surface runoff, and recharge in the Werii watershed, Ethiopia, using the WetSpass model. Outputs of the study show that the total long-term temporal and spatial average rainfall (717 mm) is distributed as 90.7% (650.16 mm) for evapotranspiration, 6% (44.06 mm) for runoff, and 4.2% (30.06 mm) for recharge. The model was also applied to assess the groundwater recharge potential for proper management and planning of the water resource for the Birki watershed (Meresa and Taye, 2018). Accordingly, to the results of WetSpass, 85.5% of the precipitation is lost by evapotranspiration, 7.4% and 7.1% of the precipitation

becomes groundwater recharge and surface runoff, respectively. Aslam et al (2021) applied Wetspass-M to assess water balance components in the Khadir canal sub-division, Pakistan. Amiri et al (2022) integrated the GIS-Based Wetspass-M Model to assess spatial-Temporal Water Balance Components in Moulouya Basin, Morocco.

2.8 Impact of Land Use Change on Groundwater

LULC changes are complex and dynamic and have direct impacts on the subsurface and groundwater hydrology of the catchment area e.g. (Bhaduri et al., 2000; Fohrer et al., 2001; Tang et al., 2005) on soil, water, and the atmosphere (Mayer and Turner, 1994). The effect of LULC changes on the regional water balance is considered to be one of the most important research topics in global hydrology, and numerous studies show that large-scale LULC changes are the important factors leading to the hydrological cycle and regional climate changes (Hutjes et al., 1998; Zhang et al., 2001). Thus, the International Human Dimensions Programme on Global Environmental Change (IHDP), the Geosphere-Biosphere Programme (IGBP), an international program of biodiversity science (DIVERSITAS), the World Climate Research Programme (WCRP), etc. take the relationship between land use and land cover changes and Biosphere Aspects of the Hydrological Cycle (BAHC), as well as its climate frangibility (Hoff, 2002; Lambin et al., 2002). Also, in the established LUCC of IGBP and IHDP, one core problem is to understand the effect of the regional LULC changes on hydrological processes and water resources (Suzanne, 2001). Such research indicates that LULC changes remarkably affect the regional vegetation ecosystem and the regional hydrological cycle (Zhang et al., 2001). Thus, the mechanism of LULC changes in the region influencing the hydrological process become vigorous fields in the development of hydrology (Hoff, 2002).

Hydrological models play a significant role in the quantitative evaluation of the combined impact of LULC changes on hydrological processes (Pechlivanidis et al., 2013). In the last few decades, numerous hydrological models have been developed to assess the effect of LULC changes on the water balance components (Carrera-Hernández and Gaskin, 2008; Gumindoga et al., 2014; Niehoff et al., 2002; Singh and Saraswat,

2016; Zhang et al., 2015). Spatially distributed hydrologic models could provide the spatial patterns of the hydrological effect of LULC (Wang et al., 2013; Wang et al., 2013). In this method, the model domain is subdivided into grid cells, and each cell is classified with a land use category. Ghazavi and Ebrahimi (2016) assessed the effect of land use change on groundwater dynamics according to water balance modeling using MODFLOW, Remote Sensing (RS), and GIS. They concluded that increasing agricultural areas resulted in an increase in annual discharge and annual recharge from irrigation water. Singh and Saraswat (2016) evaluated the effects of soil texture and LULC on water balance components using the soil and water assessment tool (SWAT). Carrera-Hernández and Gaskin (2008) developed a simple daily soil-water balance (SWB) to estimate Spatio-temporal of aquifer recharge and to assess the impacts of urban growth in the Basin of Mexico. They found that urban growth in the alluvial plain had diminished groundwater recharge. Jat et al. (2009) also reported that the decrease in groundwater recharge has resulted from the increase in impervious areas in Ajmer, India. Hydrological models coupled with l and use models have also been developed but their application is limited to surface runoff and flood prediction (Lin et al., 2007; McColl and Aggett, 2007; Niehoff et al., 2002; Tong and Liu, 2006). The water and energy transfer between soil, plants, and atmosphere, the quasi-steady-state water balance (WetSpass-M) model performs well regionally (Abdollahi et al., 2017) and it is also applicable worldwide (Al Kuisi and El-Naqa, 2013; Armanuos et al., 2016; Gebremeskel and Kebede, 2017; Salem et al., 2019d, 2019a).

As land use data are usually derived from remote sensing images, the issue of a mixed pixel could increase inaccuracy and uncertainty if the grid cell is treated as a single land use type. The WetSpass model determines the water balance components of a grid cell while taking into account the fractions of bare soil, vegetation, impervious area, and open water; thus, the WetSpass model provides a good choice for evaluating the long-term average spatial patterns of groundwater recharge (Batelaan and De Smedt, 2007; Batelaan and Smedt, 2001). It considers many influencing factors, such as precipitation, temperature, wind speed and terrain, and land-use type, can assess the long-term impacts of land use changes on the water regime. It has been widely used to evaluate the effects of LULC change on the hydrological cycle (Dams et al., 2013, 2008;

Poelmans et al., 2010; Zomlot et al., 2017). Poelmans et al. (2010) coupled WetSpass with an urban model to identify the impact of urbanization on groundwater systems for the period 1976–2050 in Flanders, Belgium. Results predict a decrease in groundwater recharge with an increase in the built-up area in Flanders. Pan et al. (2011) evaluated the impacts of land use types on the hydrological processes and groundwater recharge in the Chinese basin of River Guishui using WetSpass model. They concluded that the reduction in farmland and urban expansion has decreased the groundwater recharge by 4×106 m^3 for the period between 1980–2005. Moreover, they concluded that decreases in the order of grassland, cropland, forest land cover types, and urban land. Zomlot et al (2017) quantified the impacts of LULC change on groundwater recharge in Flanders, Belgium. WetSpass, coupled with remote sensing, is applied to assess the hydrological dynamics under changes of the impervious surface area.

2.9 Application of ArcGIS in groundwater hydrology

The GIS has gained an extreme position in studying hydrogeology over the conventional methods because of its repetitive coverage, synoptical view, and high ratio of benefit to availability of data and costs in various ranges of the electromagnetic spectrum. GIS provides many tools to obtain an overview of groundwater conditions in the region through integrating information regarding soil, geologic structures, lithology, geomorphology, drainage, vegetation land use, etc. (Rawal et al., 2016). The structure of the GIS raster model is highly appropriate since it can connect GIS input data easily derived from satellite imagery with a mathematical model of groundwater flow. GIS data structures are applied efficiently since parameter data are stored in attribute tables while spatial data are stored in raster layers. New raster layers can be generated from the attributes to use in spatial evaluation. The attribute tables could easily define new soil and land cover and types, as well as parameter changes, to investigate future water and land management scenarios (Batelaan and De Smedt, 2007). A detailed review of applications of GIS in water resource management is presented by several researchers (Jha et al., 2007).

These reviews show that GIS applications in water management and hydrology are critical in modeling dominated context. Moreover, they provide several geoscientific applications of GIS and the function of geo-computation in the application and development of GIS technologies (Jha et al., 2007). GIS can be used in the hydrological models to prepare input data or to integrate them as an extension tool for developing the ArcGIS functionality. Batelaan and De Smedt (2001) have developed a tool that is used as an extension in ArcView GIS 3.3 in surface and sub-surface water balance modeling, and the other tool Arc SWAT which is an extension in ArcGIS for water balance. Developing distributed hydrological models remained a challenging and problematic task over the last decades due to the temporal and spatial and distribution of hydrologic processes. For this reason, the application of GIS has become a common and useful tool in numerous fields of science. Distributed hydrological models are often linked to GIS and use capabilities to estimate spatial parameters from topography and digital maps of soil type and land use. The powerful GIS tools give new possibilities for hydrological research in understanding the fundamental physical processes underlying the hydrological cycle and the solution of mathematical equations representing those processes.

2.10 Surface water-groundwater interactions

In most regions on the Earth, surface water and groundwater are in a continuous dynamic interaction that could influence the water quantity and quality of both, the surface-water and groundwater resources (Sophocleous, 2002). Nowadays, water resources management moves towards the challenge of integrating surface water and groundwater as one management unit (Ala-aho et al., 2015; Salem et al., 2018a). This paradigm shift needs a better understanding of the complex interactions between groundwater and surface water and reliable techniques to simulate these interactions. Among groundwater/surface-water interactions, probably the most complex and distinct interactions are those between lakes or reservoirs, and groundwater according to Chapman (1996) terminology. El-Rawy et al. (2020) developed modules for groundwater-surface water interaction as part of the STRIVE (stream river ecosystem)

package within the flexible environment for mathematically modelling the environment (FEMME) software.

Furman (2008) reviewed and discussed different techniques for coupling surface and subsurface flow processes. These techniques differ between physical models that conserve momentum and mass and numerical models. He reported five different categories of the physical models relying on the definition of the boundary conditions at the interface between surface and subsurface systems. The first category suggests continuous velocity and its gradient along the interface, the second suggests also the continuity of velocity but by weighting the kinematic viscosity with the velocity gradient with t, the third implies the velocity continuity along the interface but within the gradient involves a jump condition, the fourth category is a special case of the third one where a different representation form for the jump, and the fifth considering only the derivative form of the velocity from the fluid-free side.

Moreover, Furman (2008) discussed three different categories of numerical models: no-coupling, iterative coupling, and full coupling. No-coupling is the simplest approach in which solving the surface water system is the first step, then follows the definition of boundary condition and finally solving the subsurface system. The second category is similar to the first but the boundary condition is updated by the solution of the subsurface system in the same time step. The third category represents the most sophisticated approach that solves simultaneously the two systems with the internal boundary condition. International examples show that the integrated (conjunctive) use of surface water and groundwater within a proper management system increases the efficiency of water utilization (Cheng et al., 2009; Salem et al., 2019b), provides sufficient irrigation water for agriculture (El-Rawy et al., 2016; Seo et al., 2018; Singh et al., 2015), and improves the environmental conditions of irrigated lands (Liu et al., 2013). Construction of recharge dams and controlling the rate of groundwater abstraction are considered common practices (Healy and Scanlon, 2010; Krešić, 2009). Managed Aquifer Recharge (MAR) using treated wastewater is a feasible option for non-conventional water resources in arid and semiarid regions ((Abiye et al., 2009; Allam and Allam, 2007; Asano and Cotruvo, 2004; Gale, 2005; Khan et al., 2008).

2.11 Modeling lake-groundwater interactions

The interaction between lakes (subsurface reservoir) and groundwater is the most important part of lake water budget and it substantially influences lake water quality (Nakayama and Watanabe, 2008; Schwartz and Gallup, 1978; Stauffer, 1991). Modeling the interactions between surface water and groundwater in adjacent areas to rivers, lakes, and reservoirs was a topic of many studies, applying numerous approaches. The exchange between reservoir/lake water and groundwater is governed by the stratification, texture, and isotropy of sediments in the shoreline zone (J. Dezső et al., 2017; Salem et al., 2018b; Sanford, 2002). The most direct and simplest way of investigating a lake interaction with groundwater is by evaluating exchange seepage between lake water and groundwater by using methods of point field measurements such as potentio-manometers, piezometers, seepage meters, dye tracing, and thermic profiling (Lee, 1977; Ong and Zlotnik, 2011; Otz et al., 2003; Winter et al., 1988) or a combination of methods (Anibas et al., 2009; Owor et al., 2011; Su et al., 2016). However, such techniques are vulnerable to heterogeneity and hence difficult for spatial integration.

Mass-balance methods and geochemical analyses quantify groundwater inflow, which determines isotope or solute concentration in the lake (Sacks et al., 1998; Stauffer, 1985). The latter methods are complex, as they need a conservative tracer unaffected by land use such as stable isotopes (Brindha et al., 2014; Kanduč et al., 2014; Krabbenhoft et al., 1990; Sacks et al., 2014). Moreover, semi-analytical water balance models (Ghosh et al., 2015; Rudnick et al., 2015) include quite a number of assumptions to simplify spatial heterogeneity. Isotope-balance methods (Coplen, 2011) using $\delta 2H$ or $\delta 18O$ measurements of water were applied in several hydrological studies to evaluate groundwater inflow to lakes, with different degrees of success (Dinçer, 1968; Krabbenhoft et al., 1990; LaBaugh et al., 1997; Sacks, 2002; Turner et al., 1984). Increasingly sophisticated physically based distributed through integrated hydrological models represent the most reliable and complete tools for the assessment of lake water/groundwater interactions especially if based on solid features of hydrogeological conditions of a lake and its adjacent area and time series data (El-Zehairy et al., 2018).

Liuzzo et al. (2015) applied a lumped conceptual model (TOPDM) to assess the impacts of climate change on the availability of water resources in the Belice River Basin (Italy), in which Lake Garcia is situated. Fowe et al. (2015) applied a genetic algorithm model to couple Boura reservoir with the adjacent groundwater system and to optimize water allocation. Chhuon et al. (2016) coupled the MODSIM decision support system with semi-distributed hydrologic SWAT model to evaluate the effect of a future upland reservoir on the Prek Te River, Cambodia, on hydrological consequences. A Modular Three-Dimensional Finite-Difference Ground-Water Flow Model (MODFLOW) (McDonald and Harbaugh, 1988) is used widely to simulate this interaction from different approaches. Leblanc et al. (2007) simulated the lake as a constant stage source or sink through the river package. One of the disadvantages of this approach is that the river stage is constant during each stress period and not changing due to the interaction between the river (the lake) and the groundwater system. Another approach to simulate the water balance of lakes uses the General-Head Boundary (GHB) Package (Mylopoulos et al., 2007). Gurwin (2008) applied the General Head Boundary Package (GHB) for lake simulation. In his study, the lake bed sediment was simulated by adjusting the conductance of each cell simulated as a GHB. The main drawback of GHB approaches is that the lake stage is assumed to be constant during each stress period. Fenske et al. (1996) simulated the lake using the Reservoir Package. This approach does not differ much from the GHB approach except that the Reservoir Package allows the lake stage to vary according to the user specified limits. The disadvantage of this approach is that it requires prior knowledge of lakebed seepage to estimate the lake stages (Merritt and Konikow, 2000).

Another approach that represents the lake volume through high hydraulic conductivity cells (Lee, 1996) is called the “high-K” technique. The difficulty of simulating the connection between the lakes and streams is the main drawbacks of “high-K”. This method was applied by others including Lee (1996), Anderson et al. (2002), Chui and Freyberg (2008), and Yihdego and Becht (2013). Lee (1996) used the same approach to simulate the transient lake stage and groundwater interactions for Lake Barco, an acidic seepage lake in the mantled karst of north central Florida. Lee concluded that the model underestimated the groundwater inflow compared to the calculated inflow

from the hydrologic budget lake using the energy budget method. Yihdego and Becht (2013) used a three-D flow model with the high-K technique to simulate lake/groundwater interaction in Naivasha, Kenya. Yihdego and Becht (2013) found that this method is limited to seepage lakes such as Lake Naivasha which do not have outlet and lose water mainly by seepage through sides or bottom and it may lead to instability problems with groundwater heads solution. Moreover, this approach can be difficult to simulate accurately the connection between the lakes and streams (Merritt and Konikow, 2000).

Cheng and Anderson (1993) developed the MODFLOW lake package (LAK1) that solves the aforementioned problems. The main advantage of the lake package is that lake stages are not defined as hydraulic boundaries but determined as part of the simulation it allows the fluctuation of the lake stage. Also, the exchange of volumetric water between the lake and the aquifer is determined following the hydraulic gradient and explicitly defined lakebed conductance (El-Zehairy et al., 2018). The LAK1 Package was also incorporated with the Stream Flow Routing (STR1) Package (Prudic et al., 2004) to regulate inflow water to the lake and outflow from the lake to streams. The Lake Package LAK1 did not consider that some of the lakebed cells could become dry due to low lake stages. Also, it did not take into account the flow resistance within an aquifer, which could be substantial in magnitude and even larger than the lakebed resistance in the case of thin lakebeds (Merritt and Konikow, 2000). The most important addition in the next, LAK2, package can simulate more than one lake simultaneously. Lake representation as a volume of space within the model grid is the greatest improvement in the LAK3 Package (Merritt and Konikow, 2000), where a lake is represented which consists of inactive cells extending downward from the upper surface of the grid reviewed by Hunt (2003). Active model grid cells bordering this space and presenting the adjacent aquifer, exchange water with the lake at a rate determined by conductance and by the relative heads that are based on grid cell dimensions, user-specified leakance distributions and hydraulic conductivities of the aquifer material that represent the resistance to flow through the material of the lakebed. The simulation of solute transport is also added in LAK3. Kidmose et al. (2011) validated the LAK3 package through measurements by seepage meter. LAK3 package used in many studies

such as Vaeret et al. (2009). The advantages and disadvantages of three approaches for simulating lake–groundwater interactions (namely, fixed lake stages, high-K nodes, and LAK3 package) were compared by Hunt (2003).

Kidmose et al. (2011) a 3-D MODFLOW steady-state model including LAK3 Package to simulate lake-groundwater interaction to assess the spatial distribution of Lake seepage Hampen, Western Denmark. They compared the steady state model results with the seepage meter measurements and concluded that both results compared well if direct measurements of seepage from the nearshore were combined with measurements from deeper parts of the lake. Anderson et al. (2002) applied both, the Lake Package and the High-K approach to simulate lake levels in Pretty Lake, Wisconsin. The results show that the High-K method is more accurate than other methods, but it requires a longer run time and more post-processing at the same time. On the other hand, the review of Hunt (2003) stated that the LAK3 Package is superior to all other lake simulation approaches because any change in the lake stage, due to interaction with groundwater system and/or streams is appropriately stimulated by the Lake Package and not considered when using any other approaches. Besides, the LAK3 Package has been proved to be more stable in simulating lake- groundwater interaction than other techniques. It has also the capability of simulating multiple lakes within one model and simulates better the lake–stream connections. Another important improvement took place recently in the most up-to-date LAK7 Package, also used in this study. Water balance is simulated more realistically in the latest update LAK7 package (El-Zehairy et al., 2018). The experience gathered from the MODFLOW lake packages is utilized in the modeling of water balance for the reservoir planned in the Drava floodplain.

2.12 Proposed Research

The reviews presented in the above sections showed that a large number of studies have been conducted in the areas of assessment of groundwater recharge, surface water, and groundwater interaction with LULC change variables. The research is required to extend the knowledge of the effects of LULC on the hydrology of the basin. There is a lack of systematic studies that have measured the efficiency of natural reservoirs as

integrated water resources management approach. Processes like groundwater recharge, field water balance, and groundwater modeling are to be fairly well understood. Considering the above-mentioned aspects, an attempt is made to study the local and catchment scale effects of LULC change and developing a methodology to systematically assess the effects of surface water and groundwater interaction with LULC change variables in the watershed. Integrated water resources management aims to find an optimized approach to address, and balance the needs of multiple participants, stakeholders, as well as multiple natural components. Integration of computer modeling in Integrated Water Resources Management has become increasingly crucial as IWRM becomes more and more complex requiring more refined, detailed, and dynamic solutions to more challenging situations such as land use/land cover change and climate change effects.

In this study, the spatially distributed water balance model WetSpass-M (Abdollahi et al., 2017) is selected for the following reasons:

- It is a robust multidisciplinary basin model;
- It is a spatially distributed and time-dependent water balance model that can be used to model spatial heterogeneity of catchment characteristics even without the extensive data requirements of fully distributed models;
- It involves an optimized implementation of hydrologic processes;
- Simple data requirements still assure model accuracy and a rapid process of simulation (Dams et al., 2008; Dujardin et al., 2011; Tilahun and Merkel, 2009);
- It is user-friendly and easily compatible;
- It is possible to integrate this model with other models to develop a range of scenarios to be investigated and analyzed.

The WetSpass-M model is a physically based, basin-scale, spatially distributed, and time-dependent hydrological model that operates on a monthly step. This model is developed to estimate the long-term average, spatially distributed, water balance components: actual evapotranspiration surface runoff, and groundwater recharge. The WetSpass-M model is computationally efficient and capable of continuous simulation

over long periods which concerns water resources managers. The WetSpass-M model will be applied to create a hydrological model for the highly-regulated river basin, the Drava River basin in Hungary. The state-of-the-art interfacing of the WetSpass-M model with other environmental models has been achieved to develop a range of scenarios. One such example is the coupling with MODFLOW-NWT, the groundwater flow model, which has been carried out by many researchers such as Dams et al. (2008); (2013); Ghouili et al. (2017) and Zomlot et al. (2017).

The WetSpass-M model has a limitation in terms of dealing with groundwater since it excludes in-depth soil water balance and its groundwater module is lumped and accordingly, parameters such as hydraulic conductivity could not be spatially represented (Kim et al., 2008). On the other hand, in the MODFLOW model, an accurate and reliable estimation of recharge rates within the input data is the key component. The groundwater flow of MODFLOW often overlooks the precision of the recharge rates that are needed to be calculated into the model. In this study, the coupled WetSpass–MODFLOW model will be applied to a highly-regulated river basin, the Drava River basin in Hungary, to construct a monthly WetSpass–MODFLOW model to assess the impact of land use land cover changes in the study area on groundwater hydrology. This model will be applied to different management scenarios by simulating two natural reservoirs with different filling rates. The WetSpass–MODFLOW coupled fully distributed water resources model will be useful for decision-makers in water resources planning and management.

CHAPTER Three

3. DESCRIPTION OF THE STUDY AREA

3.1 Location

The Drava basin is located in southwestern Hungary along the lower section of the Drava River. It lies between latitudes 46°3'20.05" and 45°45'50.8" North and longitudes 17°26'13.05" and 18°21'38.71" East (Figure 3-1). This section of the river coincides with the national border between Hungary and Croatia in the axis of a 15-km-wide alluvial plain (Szalay, 2014). The Hungarian Drava section is 75 km long, and the corresponding catchment extends to 1.143 km^2 and it is more undulating with sand dunes in the west and flattens out towards the east. In the Hungarian section of the Drava River, there are twenty major side channels, thirteen tributary streams, hundreds of meander scars, and eighteen oxbow lakes (Pálfai, 2001). Borehole samples and Ground Penetration Radar (GPR) surveys show extreme spatial heterogeneity in the hydraulic properties of sediments in the Drava basin (J. Dezső et al., 2017). The Hungarian section of the basin is traditionally affected by floods prior to river regulation. Beginning with 1750, river channelization divided the area into an active and a morphological (in the terminology of Hungarian water management:" protected") basin. This channelization resulted in reducing river length by 50 % (Buchberger, 1975). The lowest-lying areas of the Drava basin, next to the Drava channels and its tributaries, almost entirely consist of silty deposits and are hardly suitable either for human settlement or intensive cultivation. The main features of the basin are oxbows, abandoned channels with natural levees, scroll bar systems, backswamps, and to the north elongated blown sand dunes of east to west strike (Lóczy, 2018).

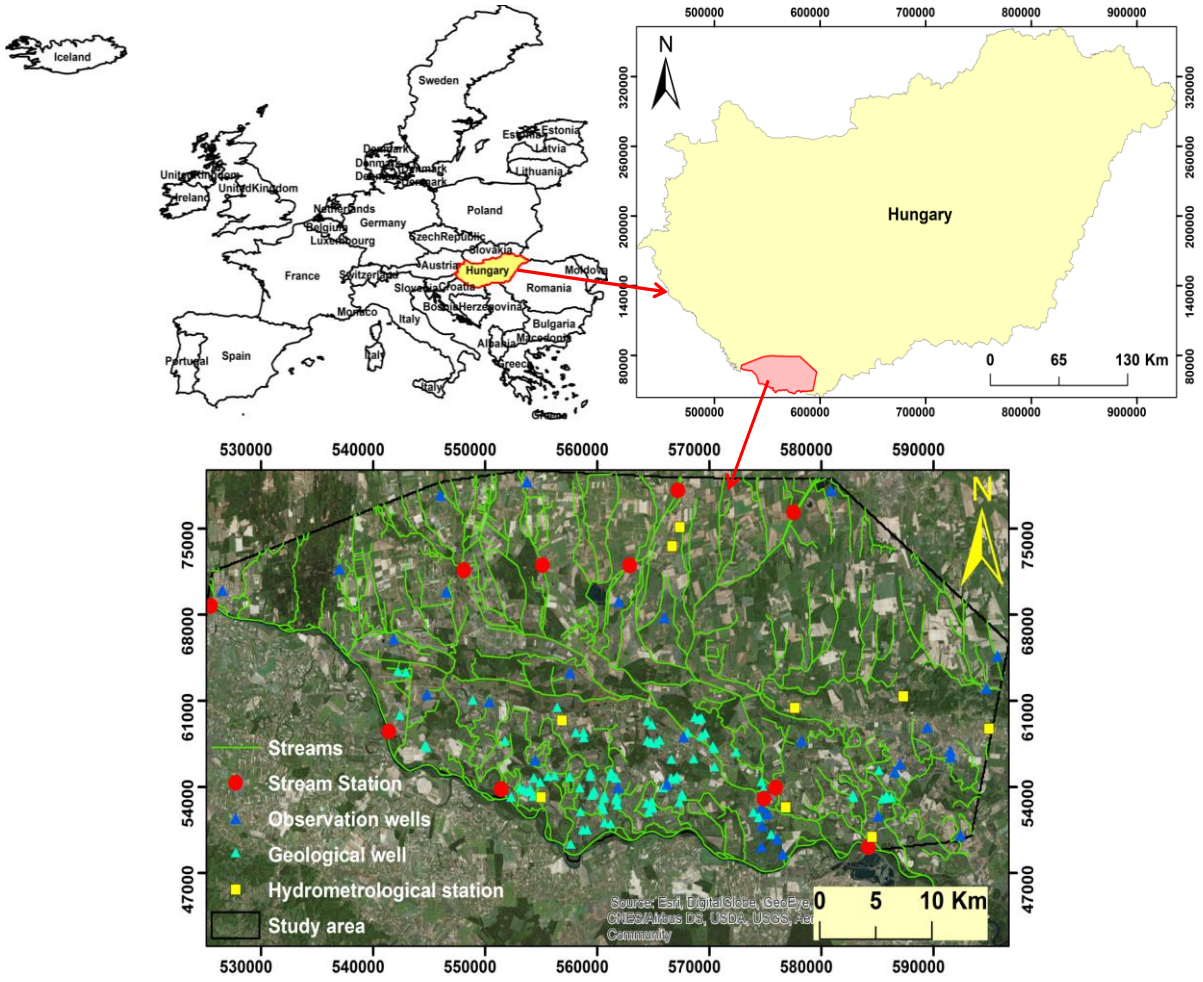

Figure 3-1: Location of the Drava basin, Hungary, with river gauges, observation wells, geological boreholes and hydrometrological stations

3.2 Hydromorphology

The hydromorphological features of the Drava river and their effects on the basin along the section under study are presented through the EU project REFORM indicators (Restoring Rivers for effective Catchment Management) (González del Tánago et al., 2016) The Drava is an important tributary of the Danube. Its length is 720 km and the total catchment area is estimated between 40,150 and 41,810 km^2, of which 6,160 km^2 (ca 15%) lies in Hungary (236 to 70.2 river kilometer), where it is a border river with Croatia (except for a 29-km section) (Sommerwerk et al., 2009; VKKI, 2010). The long-term average discharge of the Drava River is 595 m^3 s^{-1} at the Barcs gauge, where the

average water stage was 618 cm for the period 1896–2018 (Lóczy et al., 2017; VKKI, 2010). Basin storage during flood waves is responsible for a considerable difference between discharges measured at the upper and lower river gauge. The maximum discharge of 0.1 % probability is assumed to be 3070 $m^3 s^{-1}$ (reached during the flood of 1827), while 900 $m^3 s^{-1}$ and 170 $m^3 s^{-1}$ are accounted to bankfull and baseflow discharge, respectively (VKKI, 2010). As a possible source of water replenishment, the Fekete-víz stream is a tributary with an average discharge of Qav= 2–2.5 $m^3 s^{-1}$. High daily water level fluctuation results from the peak operation of the Dubrava hydroelectric power plant in Croatia. It accounts to 110-130 cm at Őrtilos, 30-40 cm at Drávaszabolcs, and 50-70 cm at Barcs. The dams on the Austrian and Croatian river sections created artificial conditions and make the selection of reference locations for rehabilitation extremely difficult.

3.3 Geological and Geomorphological Settings

The entire Drava basin consists of three main geological units of the southeastern foreland and their Eastern Alps: 1, the Southern Alpine Nappe System (with the eastern Dolomites); 2, the Austroalpine Nappe System (with a small portion of the High Tauern Window) and 3, the southwestern margin of the Pannonian (Carpathian) Basin (Lóczy, 2018). The basement of the Hungarian Drava basin is represented by carbonates and Triassic clastics in the eastern section and a graben built up of metamorphites in the west. The Drava Plain is a lowland along the Hungarian section of the Drava river between Drávatamási and Drávaszabolcs. Ethnographically named as “Ormánság”, which refers to small, separated mounds rising above the basin. The mounds have a few meters of relief and are continuously settled. Geologically, the Drava river basin was formed in a graben and is characterized by a variety of geological units from recent alluvial deposits to older rocks. During the late Pleistocene- Holocene the top 0-100 m sequence of the basin accumulated from unconsolidated fluvial sediments. Their textural character is represented by coarse sand to heavy clay series.

3.4 Active Floodplain

The average active floodplain width varies from 80 m to 1,800 m as the minimum and maximum values, with an average value of 650 m. On the other hand, the average morphological floodplain width is 3,500 m with a maximum width of 14,500 m which includes the active floodplain and the former, now flood-free, floodplain outside the levees. The sheer floodplain width could be considered as a primary factor in the assessment of rehabilitation potential (Lóczy, 2013). In the Hungarian bank of the active floodplain, the vegetation is softwood forest plantations and subordinately wet meadows, mainly in the oxbows vicinity (Ortmann-Ajkai et al., 2003). Today, flood-protection levees artificially restrict floodplain width. Therefore, active fluvial processes can only operate over the 1–10-km-wide artificially confined floodplain

3.5 Climate

The climate of the catchment is characterized by winter drought (January to March), wet summers (Atlantic influence in June-July) and autumns (Mediterranean influence in October-November) (Lovász, 1972). The basin climate is moderately wet and warm in the east and under a Mediterranean influence, while in the west it is under an Atlantic influence (Lóczy, 2019). The annual mean temperature for the period 2010 till 2018 is 11.6 °C, while the minimum and maximum extreme temperatures are respectively -12 °C and 33 °C. . The long-term mean annual temperature is 10.8 °C in the east and 10.2 °C in the west. The number of sunny hours is between 2000-2500; in the summer quarter 810-820, in the winter period 210 sunny hours are expected on average. The number of cold days (mean daily temperature below -10 °C) is 10, while the number of hot days (mean temperature above 30 °C) is 21. Winter is characterized by little snowfall. The number of snow covered days is around 30, and the average maximum snow thickness is 20-22 cm. The dominant wind direction is typically northwestern, but especially in the autumn months, southeastern wind is not uncommon either. Average wind speed is around 2.5 m s^{-1}. Mean yearly global radiation is 4600-

4700 MJ m^{-2}. The period April to June is characterized by higher discharges, attributed to snowmelt in the southern ranges of the Eastern Alps. The average runoff in the Drava basin is around 435 mm and precipitation is 720 mm, but the effect of this inflow on the Drava water regime is much more limited than that from the Alpine region. The climatic conditions are reflected in equable monthly and annual river regime, where only moderate variations are observed. The duration of river ice has considerably decreased due to global warming: in the 1930s the river was commonly frozen for 28-30 days, while in the 1990s only for 2-3 days. In the 21st century, it was almost free of ice cover. However, exceptionally huge amounts of snow (5.9 km^3) were recorded in the Alpine region in the winter of 2013-2014 (National Water Management Service).

3.5.1 Rainfall

Rainfall is considered one of the most important supplies of water in any region. The amount of water that is used for different purposes in the specific region depends on the amount of rainfall. Excess water means a waste of water which is so precious in any region. Moreover, it can raise the groundwater table that resulted in unsatisfactory saturation of the root zone. On the other hand, an extensive period with the absence of rainfall during the growing season leads to the wilting of plants. The availability of freshwater resources becomes a limiting factor for crop growth worldwide (Gat, 2004). Not only total annual rainfall is important, but the knowledge on the temporal, spatial variability and trends of precipitation is essential for the proper management and planning of water resources including quality preservation and evaluation, optimal water distribution, flood hazard mapping, proper design of hydro-related schemes such as clean water supply, construction of reservoirs and stormwater channels. The spatial distribution of monthly, seasonal and annual precipitation over the Drava basin for the study period is shown in Table 3-1. The long-term spatial distribution of average annual rainfall for the period from 2000 to 2018 is shown in Figure 3-2. The average annual precipitation displays great variation between 383 mm yr^{-1} and 1057 mm yr^{-1}, with a mean value of 673 mm yr^{-1} and a standard deviation of 152 mm yr^{-1}. The average long-term rainfall amounts in dry (winter and autumn) and wet (summer and spring) seasons

are 281.41 mm and 396.10 mm, respectively. The rainy season (summer and spring) has a share of 60 % of the annual rainfall, while the remaining 40 % falls in the (drier) season (winter and autumn) (Salem et al., 2019c).

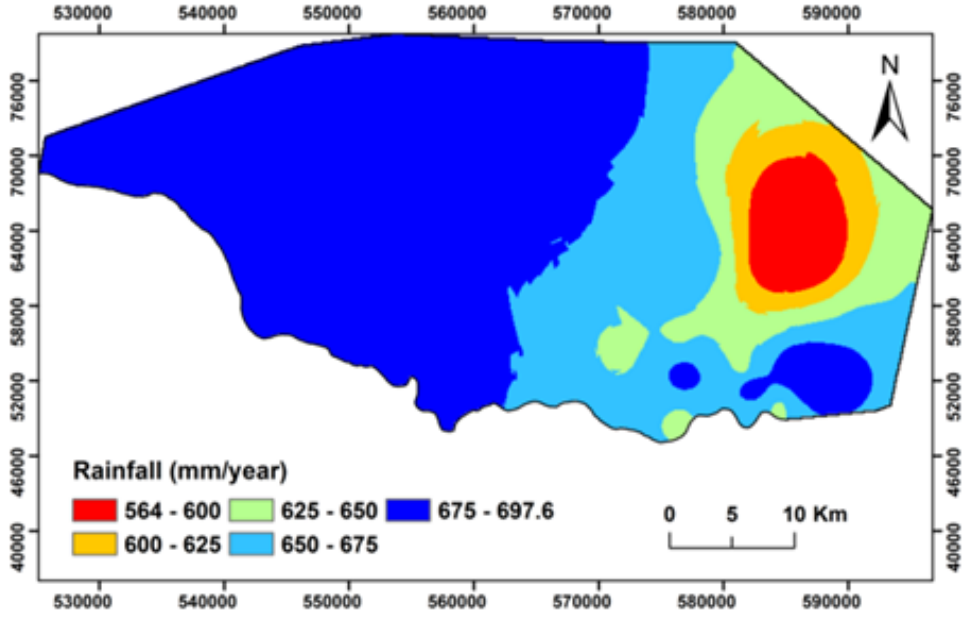

Figure 3-2: The spatial average annual rainfall distribution

Table 3-1: Long-term monthly, annual, and seasonal precipitation in (mm) for the Drava basin during 2000-2018

Time Scale	Min	Max	Mean	Std. dev.	% of annual precipitation
Monthly	0.23	228.58	56.63	28.14	
Annual	382.68	1056.66	672.91	152.36	
Winter	44.23	202.01	128.69	46.71	19.00 %
Spring	92.57	414.01	205.58	67.48	30.34 %
Summer	93.58	334.27	190.53	62.27	28.12 %
Autumn	82.16	227.54	152.72	38.18	22.54 %

The precipitation changes considerably from month to month as depicted in Figure 3-3. May is the month with maximum rainfall and it contributes to 16.8 % of mean annual

precipitation (Salem et al., 2019c). The average monthly precipitation of the basin ranged from 0.23 mm month^{-1} to 228.58 mm month^{-1} as the minimum and maximum values respectively, the mean and standard deviation of this distribution are 56.63 mm and 28.14 mm, respectively. May precipitation is followed in order by October (12.6 %, secondary maximum), September (12.4 %), and July (10.3 %). Least amounts of rainfall are observed during December (17.6 mm) followed by March (35.5 mm), which contribute only 2.2 and 4.4 % to the annual rainfall, respectively.

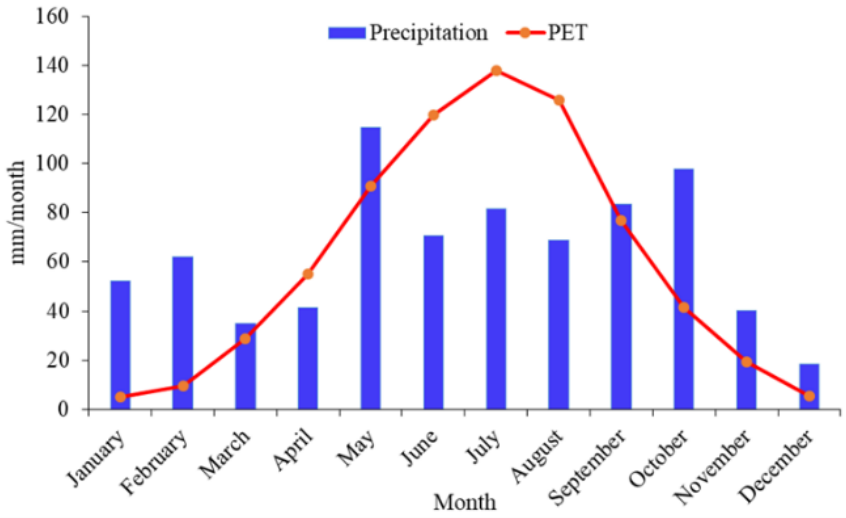

Figure 3-3: Long-term average monthly precipitation and potential evapotranspiration (1981-2018)

Regarding daily precipitation, the result clearly indicate that peak daily precipitation was 85 mm and the maximum number of precipitation events in a year were 12 events. From Figure 3-4, it can be observed that rainfall is usually at its peak from the end of April to mid of May, the end of October, Mid-July, and all September, and minimum daily rainfall was observed in December and March. These findings are essential for the assessment of runoff and infiltration because when precipitation intensity is larger than the ability of the soil to absorb moisture, surface runoff happens.

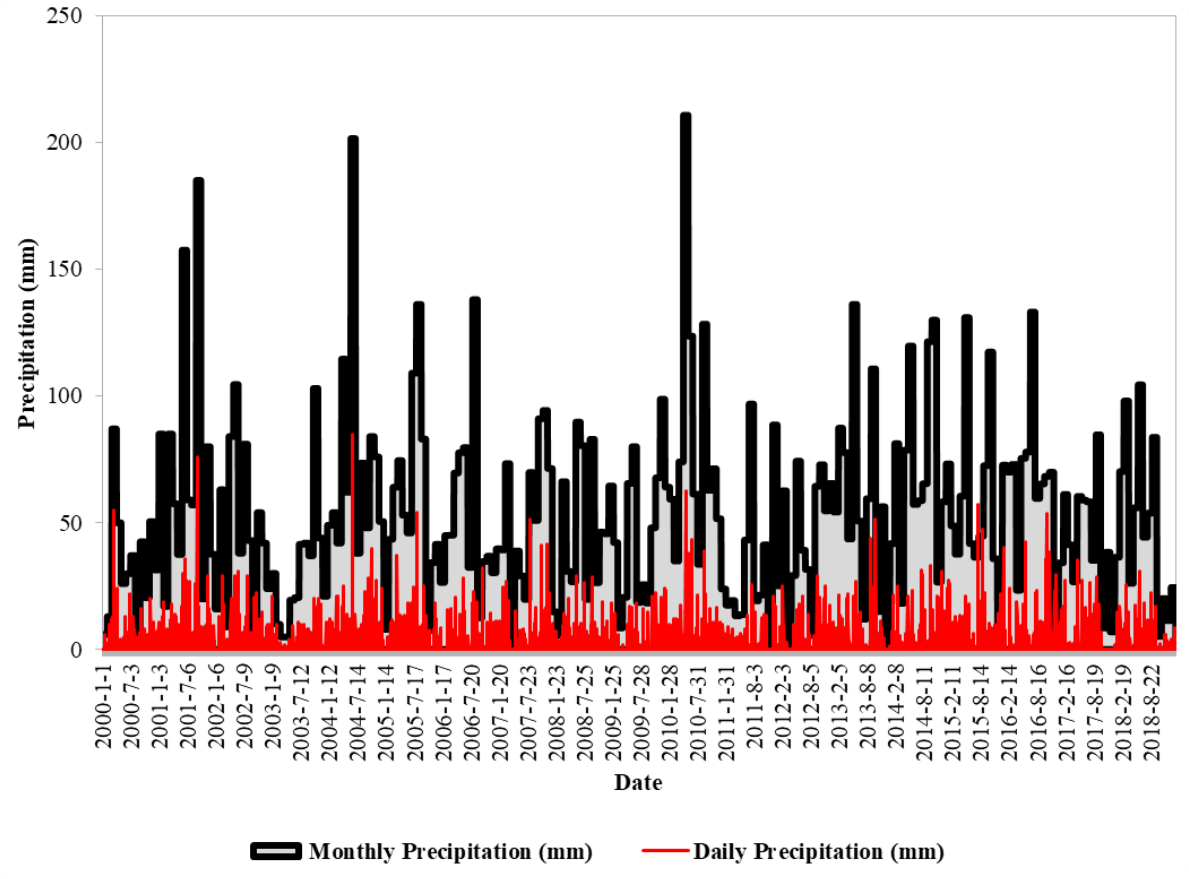

Figure 3-4: Fluctuation of rainfall for the basin at daily and monthly scales (2000-2018**)**

3.5.2 Potential evapotranspiration (PET)

Daily potential evapotranspiration (PET) was calculated from meteorological data (soil heat flux, hourly incoming solar radiation, wind speed, and relative humidity) using the FAO-Penman-Monteith method (Allen et al., 1998)) Equation (3-1).

$$PET = \frac{0.408\Delta(R_n - G) + \gamma \frac{900}{T+273} u_2 (e_s - e_a)}{\Delta + \gamma(1 + 0.34\, u_2)}, \quad (3\text{-}1)$$

where PET is the potential evapotranspiration (mm d^{-1}), R_n is the net radiation (MJ m^{-2} d^{-1}), Δ is the slope of the saturation vapor pressure function (kPa $°C^{-1}$), G is the soil heat flux density (MJ m^{-2} d^{-1}), u_2 is the wind speed at 2 m height (m s^{-1}), T is the daily average air temperature (°C), e_s is the saturation vapor pressure (kPa), e_a is the actual

vapor pressure (kPa), and γ is the psychometric constant (kPa ◦C^{-1}). Daily PET varies from 0.0 mm to 46 mm, with an average of 19.8 mm. Figure 3-4 presents the average monthly PET, which varies from 5.1 mm to 138 mm with an average of 60 mm. The highest PET occurs in July, 138 mm, while January has the lowest, 5.7 mm. The average annual PET of the basin is 674 mm yr-1. About 88 % of the PET is associated with the summer half-year, while the remaining 12 % with the winter half-year.

3.5.3 Lake evaporation

The Penman open-water equation (Penman, 1948) was applied to determine open-surface water evaporation. Daily evaporation from the lake surface using the Penman approach is based on hourly incoming solar radiation, relative humidity, air temperature, and wind-speed and can be determined from Equation (3-2) (McMahon et al., 2013):

$$E_{OW} = \frac{\Delta}{\Delta + \gamma} . \frac{R_n}{\lambda} + \frac{\gamma}{\Delta + \gamma} . E_w \tag{3-2}$$

where E_{OW} is the daily open-surface water evaporation (mm d^{-1} = kg m^{-2} d^{-1}), Rn is the net daily radiation at the water surface (MJ m^{-2} d^{-1}), λ latent heat of vaporization (MJ kg^{-1}), and other terms have been previously defined. In the present study, the water albedo was assumed to be fixed and equal to 0.1 as recommended by Govaerts (2013). E_w is a function of the average daily wind speed and can be determined from Equations (3-3) and (3-4)

$$E_w = f(w) . (e_s - e_a) \tag{3-3}$$

$$f(w) = a + b. w_2 \tag{3-4}$$

where $f(w)$ is wind function, $(e_s - e_a)$ is vapor pressure deficit (kPa), w_2 is the daily average wind speed (m s^{-1}), a and b are wind speed function constants (values of a = 1.313 and b = 1.381 are recommended by McMahon et al. (2013). Evaporation from the Cún-Szaporca Lake is concentrated on the summer months and shows a large variation between 0.0 mm d^{-1} and 6.8 mm d^{-1}, with a mean value of 1.85 mm d^{-1}.

3.6 Topography and Slope

The Digital Elevation Model (DEM) of the investigated area is used with a cell size of 10 m. The DEM is processed to derive topographic, stream network, and slope angle maps of the investigated area (Figure 3-5)(Salem et al., 2019a). A Digital Elevation Model (DEM) (Figure 3-5a) is obtained from the South-Transdanubian Water Management Directorate (DDVÍZIG), Pécs, at 10 m resolution. The highest point in the basin is 407 m, in the eastern part of Villány Hills, while the lowest point is 81m in the southwestern part of the basin. The mean elevation of the basin is found to be 114 m.asl. The slope map is derived directly from the DEM using Spatial Analyst Tools within ArcGIS. Slope angles vary from 0 % to 23 % with an average value of 0.7 % (Figure 3-5b).

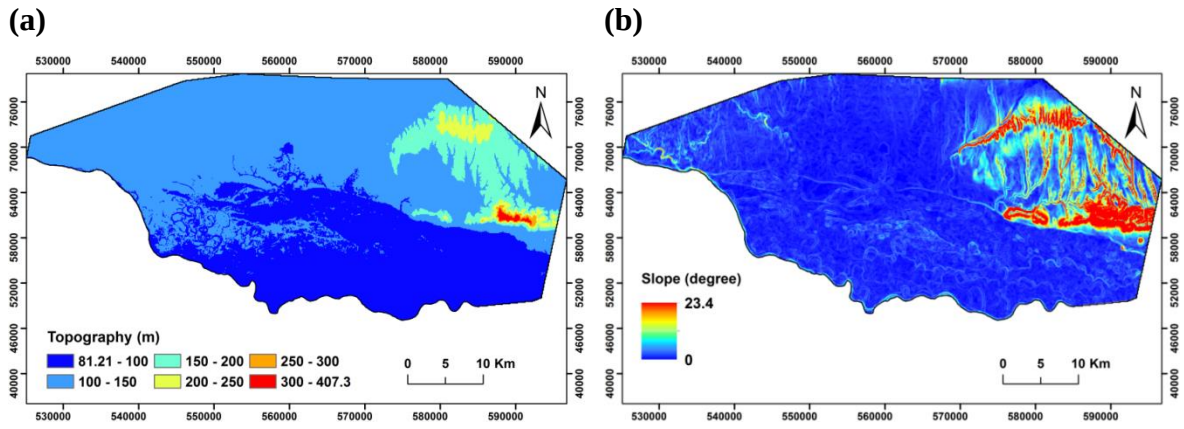

Figure 3-5: a) Topography; b) slope.

3.7 Soil and Sediment Data

Figure 3-6a shows the vertical distribution and frequency of the different sediment textures and their thicknesses by a box diagram for the top 100 m. The CMu (clayey mud) layers mostly occur at around 25–30 m depths (ranging from 20 to 40 m) and their average thickness is 5 m (2 to 8 m). All texture classes occur in the top 20 m of the modeling space. These sediments were deposited in point bars, channels, and oxbows (Słowik et al., 2018). During the Late Pleistocene-Holocene in the top 100 m fluvial coarse-sand–heavy clay series deposited in the basin (Figure 3-6a). Subsurface water

flow and capillary rise are influenced by the above-mentioned landforms and deposits. In the research area, fluvisols occur, which were formed under periodically surplus water conditions and forest vegetation. The investigation of soils was based on GPR (Ground Penetrating Radar) satellite image analysis and particle size distribution studies. Along with paleo-channels the basin is built up of dunes, point bars, and other forms of accretion (Dezső et al., 2017; Lóczy, 2019; Słowik et al., 2018). Subsurface water flow and capillarity are influenced by the above mentioned forms.

Soil samples were taken at 89 sampling sites manually (Figure 3-1)(Salem et al., 2019a). Samples were dried in the oven at 60 °C till they reach constant weight. Malvern MasterSizer 3000HS particle size analyzer was used to perform the particle size analysis. The samples were classified into five textural classes of the spatial distribution of soils that were interpolated using Thiessen polygon tools within ArcGIS (Figure 3-6b). The missing part of the study area is obtained from the AGROTOPE base (MTA ATK TAKI, 2013). In the Drava basin, five soil textures occur (Figure 3-6b): the northern part of the Drava basin is mainly covered by loamy soil, while in the south sandy soils dominate. The soil textures that are the most common are loam and sand, 53% and 27%, respectively, followed by sandy loam (9%), clay loam (7%), and clay (<4%).

a) b)

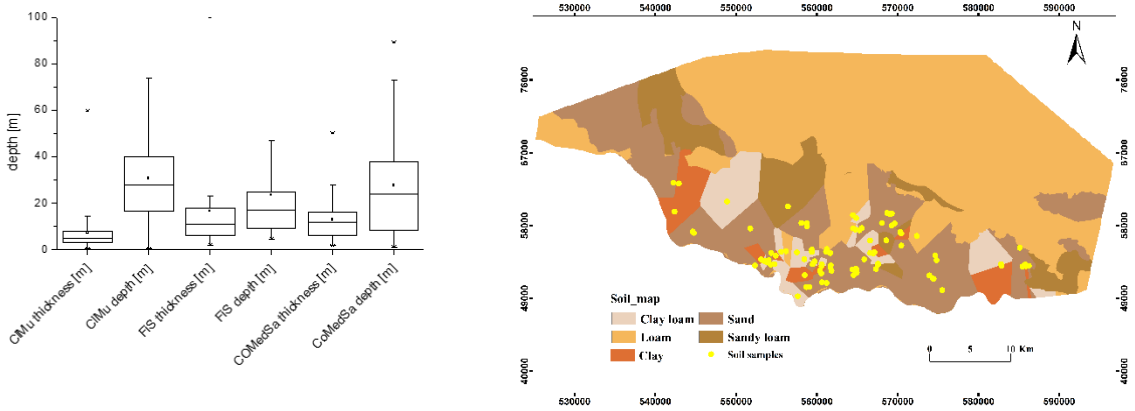

Figure 3-6: a) Vertical distribution of sediment textures in the top 100 m. ClMu: clayey mud; FiS: fine sand; COMedSa: coarse to medium sand, b) Spatial distribution of soil textures in the Drava basin

3.8 Land use

Land use is associated with both surface and groundwater patterns and influences groundwater recharge by altering infiltration rates (Jinno et al., 2009). Land use data for the Drava basin in 2018 is obtained from the CORINE database (CLC, 2018)(https://land.copernicus.eu/pan-european/corine-land-cover/clc2018).The investigated area is characterized by 17 land cover forms as depicted in (Figure 3-7a). It is dominated by agricultural land (69 %), forests (25 %), and artificial surfaces (4 %), while the total area of wetlands and water bodies amounts to 2 %.

3.9 Groundwater Assessment

The groundwater can be found virtually at 2-4 m depth. In the Dráva Basin, it is not possible to distinguish the water bodies at shallower depths from the groundwater. The water reserves which are contained in the sand layers of the Upper Pannonian sediment sequence represent a significant part of underground water resources. Currently, only 10-20 % is utilized from the utilizable water resources of the Dráva valley area downstream of Barcs. The artesian wells provide more than 500 l min-1 water below 100 m depth, which is limited in usefulness by its high iron content. There are still operating vulnerable drinking water bases in the region, but the wells of shallower depths are only used as observation wells to keep deeper wells safe. Thirty-five observation wells (Figure 3-1) for daily groundwater depth data are obtained from the South-Transdanubian Water Management Directorate for the period from 2000 to 2018. Groundwater levels range from 91.3 m to 117.8 m with an average of 99.3 m for the whole Drava basin (Salem et al., 2019d). Figure 3-7b presents the average annual groundwater level for the 35 observation wells for 2000-2018.

(**a**) (**b**)

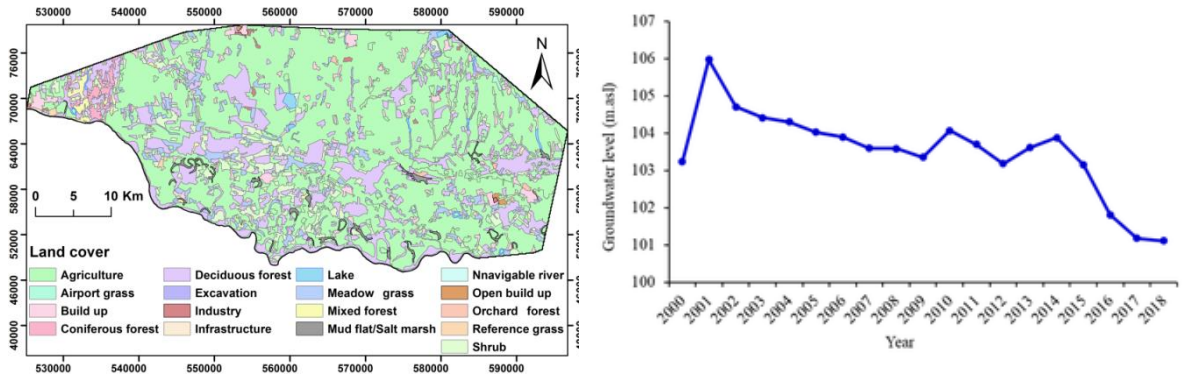

Figure 3-7: a) Land-cover map of Drava Basin, and b) Average annual groundwater level for 38 observation welss (2000-2018)

3.10 Surface Waters in the Environment of the Oxbow System

The 18 Drava oxbows can be characterized with a total of 150 ha surface, moreover, there are 3 natural lakes, 5 ha and 3 reservoirs with a total of 137 ha surface. The region's largest river is the Drava with the largest tributaries of the Black water (Fekete-víz) and the Pécs water (Pécsi-víz). The Dráva river has potential floods in the summer (June-July) and autumn (October-November) alike, while its low water levels occur mainly in September and between December and February. The local watercourses bring plenty of water mainly in early summer, but they can flood in other periods as well. They are the Korcsina channel (length: 38 km, catchment area: 167 km^2), the Sellyei-Gürü (11 km, 76 km^2), the Black-water (Fekete-víz) (76 km, 2021 km^2 – only its 18 km section under Baranyahidvég belongs to the landscape), the Gordisa-channel (7 km, 43 km^2) and the Lanka-channel (25 km, 132 km^2) (DDKÖVÍZIG, 2012). The Pécsi-water feeds into the Black-water (Fekete-víz) below the Kémes bridge.

CHAPTER Four

4. HYDROLOGICAL MODELLING OF A HIGHLY-REGULATED RIVER BASIN

As reviewed in Chapter 2, the first group of computer models (e.g. hydrological models, hydrodynamic models, and hydraulic models) is typically applied to studying natural processes in the water cycle. The hydrological models are used to simulate the physical processes of the natural water system to evaluate the available surface and groundwater resources with different initial and boundary conditions and to form the basis for a further 'what-if' analysis. Although many river floodplains in question already have flow regulations in place which makes it difficult to model the hydrological process, stakeholders become increasingly keen for more accurate information when it comes to human impacts, such as spatially distributed water resources under different management practices. In this chapter, the spatially distributed water balance quasi-steady-state WetSpass -M model is applied as an example of a hydrological model to describe a highly-regulated river basin.

4.1 Introduction

The Hungarian Drava floodplain is characterized by alternations of floods and drought periods. On the lower sections of the Drava River, incision and entrenchment of the river led to dropping groundwater level by 1.5 to 2.5 m in the adjacent basin and increasing drought hazard (Dezső et al., 2019; Lóczy et al., 2017). Indeed, the human interventions (extraction gravel from the river bed, regulator constructions, improved water retention in the hydroelectric dams and reservoirs etc.) resulted in decreasing water stages (Burián et al., 2019). The water budget of the Drava basin is unbalanced; available water resources are not efficient and sufficient for agricultural productivity (Lóczy et

al., 2014). Protecting groundwater resources in the Drava basin is especially essential for the provision of ecosystem services, natural conservation, landscape management, and economic development through improving agricultural productivity. Hence, an accurate assessment of spatial and temporal variations of water balance components, especially groundwater recharge and evapotranspiration, is crucial for developing a groundwater flow model for the Drava basin and, consequently, for optimal long-term planning and management of the available water resources (discussed later in the upcoming chapters).

In this chapter, a hydrological model built for a highly-regulated river basin is presented. The Drava river basin, Hungary is modeled using the spatial distributed water balance quasi-steady-state WetSpass model (WetSpass-M). The model is then calibrated against the observed data using the water table fluctuation method (WTF). The method can be readily extended to study future climate and land use change impact

4.2 Study Area

The study area is presented in Chapter 3.

4.3 Data Collection

The required data to build an application of the WetSpass-M model can be categorized into two groups. There are GIS grid maps and parameter tables (Batelaan and Smedt, 2001). The GIS grid maps include meteorological data (precipitation, potential evapotranspiration (PET), average temperature, and wind speed), topography, slope, land use, soil type, and groundwater depth. The model makes use of grid GIS technology and digital data to partition the precipitation into actual evapotranspiration, surface runoff, evapotranspiration, and groundwater recharge. Parameters such as soil type and related land use are connected to the model using attribute tables of soil and land-use raster maps. The attribute tables also allow defining new soil types or land cover easily, as well as changes in the parameter values, which permits analysis of future land and water management scenarios (Batelaan and De Smedt, 2007). All input data

were prepared as raster mapS in ESRI ASCII grid format with a resolution based on the digital elevation model (DEM) with a cell size of 100x100 m totaling 547,249 raster cells. Table 4-1 present the input parameters and their sources for WetSpass-M model. South-Transdanubian Water Management Directorate (TWMD).

Table 4-1: Input data and sources for WetSpass-M model

ID	Input parameter	Sources	Resolution
1	DEM and slope	TWMD and own processing	100 × 100 m
2	Daily temperature	TWMD and own processing	100 × 100 m
3	Daily precipitation	TWMD and own processing	100 × 100 m
4	Daily wind speed	TWMD and own processing	100 × 100 m
5	Daily PET	TWMD and FAO-Penman-Monteith method	100 × 100 m
6	LULC maps	Corine data base (CLC 1990, 2000, 2006, 2012 and 2018)	100 × 100 m
7	Soil texture	Map based on soil sample analysis and AGROTOPO data base	100 × 100 m
8	Groundwater depth	TWMD and own processing	100 × 100 m
9	Land-use parameters lookup table	WetSpass-M model	
10	Runoff coefficient lookup table	WetSpass-M model	
11	Soil parameter lookup table	WetSpass-M model	

4.4 Methodology

As mentioned above, the hydrological modeling of river basins is widely used to reveal regional water resources and their variability. The selection of the model relies on the scale of the problem, data availability, robustness of the model, and computational cost. In this study, Water and Energy Transfer between Soil, Plants and Atmosphere under quasi-steady state WetSpass (Batelaan and Smedt, 2001) is chosen as it has been

most frequently used in large scale modelling studies to investigate the relative impact of LULC changes, climate, and management practices on available water resources. This model is widely used to successfully investigate the impact of catchment management on:

1. Water availability (e.g. Gebremeskel and Kebede, 2017);
2. Irrigation return flow (e.g. Mustafa et al., 2016);
3. Climate change (e.g. (Gebremeskel and Kebede, 2018; Kahsay et al., 2019; Tam et al., 2016);
4. Drought and overexploitation (e.g. Soleimani-Motlagh et al., 2020);
5. Urbanization (e.g. (Zhang et al., 2017); and
6. Land-use/land-cover change on variable soil textures (Batelaan et al., 2003; Dams et al., 2008; Wang et al., 2012).

4.4.1 Modelling Using WetSpass-M

Spatially distributed water balance quasi-steady state, WetSpass model (Batelaan and De Smedt, 2007; Batelaan and Smedt, 2001) stands for water and energy transfer among plants, soil, and atmosphere. In this study, a semi-physically based distributed water balance model (WetSpass-M) is utilized to estimate the spatial groundwater recharge on monthly, seasonal, and annual scales. The model considers the spatial distribution of land use, soil texture, elevation, slope, and meteorological parameters for each raster cell. The wetSpass model treats a region or basin as a regular pattern of raster cells (Batelaan and De Smedt, 2007). The total water balance for a raster cell (Figure 4-1: Schematic representation of water balance after (Batelaan and Smedt, 2001)) is split into independent water balances for the vegetated, bare-soil, open-water, and impervious parts of each cell. This allows one to account for the non-uniformity of the land-use per cell, which is dependent on the resolution of the raster cell, and the processes in each part of a cell are set in a cascading way (Batelaan and Smedt, 2001). The total components of the water balance of the vegetated, bare soil, open-water, and impervious fraction per raster cell are calculated using the following equations

$$ET_{raster} = a_v ET_v + a_s E_s + a_o E_o + a_i E_i, \quad (4\text{-}1)$$

$$S_{raster} = a_v S_v + a_s S_s + a_o S_o + a_i S_i, \quad (4\text{-}2)$$

$$R_{raster} = a_v R_v + a_s R_s + a_o R_o + a_i R_i, \quad (4\text{-}3)$$

where ET_{raster}, S_{raster} and R_{raster} are total evapotranspiration, surface runoff, and groundwater recharge of a grid cell, respectively, each having a (v) vegetated, (s) bare-soil, (o) open-water, and (i) impervious area, respectively. The terms av, as, ao, and ai are the fraction areas of vegetated, bare-soil, open-water, and impervious areas, respectively. The mathematical formula of WetSpass-M is described in Appendix A.

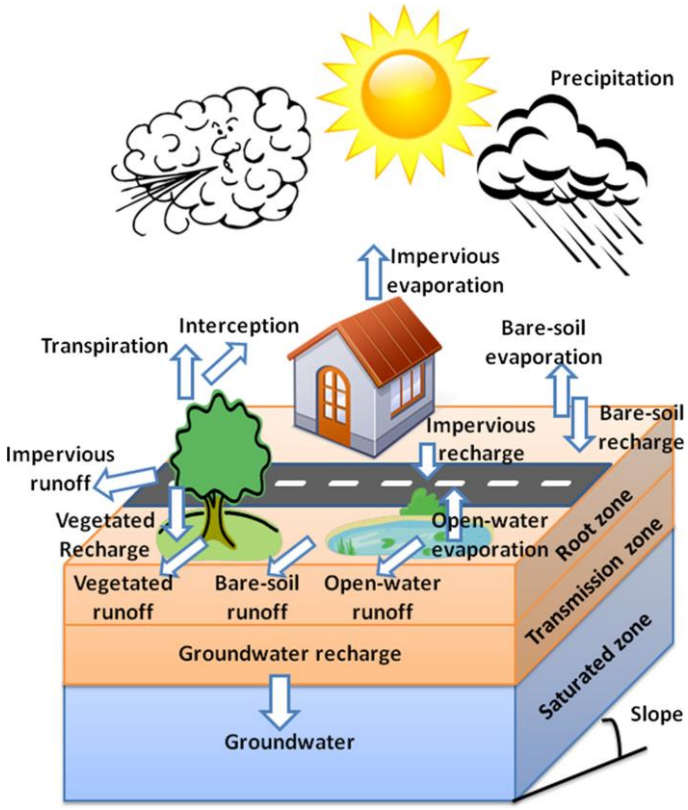

Figure 4-1: Schematic representation of water balance after (Batelaan and Smedt, 2001)

4.4.2 Model validation

The WetSpass model is validated using the water-table fluctuation method (WTF). WTF is one of the most widely used techniques to estimate groundwater recharge (Healy and Cook, 2002; Kubicz et al., 2019; Martin, 2005; Moon et al., 2004). The method is more scientific and considers the response of specific yield and groundwater level fluctuation, which are more realistic and directly measurable, unlike other approaches where assumptions are to be made for most of the components. Recharge is then calculated by the following formula:

$$\mathbf{R = S_y \times \Delta h} \quad (4\text{-}4)$$

where R is recharge, S_y is specific yield, and Δh is the change in water table height with time.

A gravimetric method (Singhal and Gupta, 2010) was used to measure the specific yield of undisturbed samples for the investigated area. First, the samples were dried in an oven at 105 ºC for 24 hours and filled with water until full saturation. Then, the samples were placed on a sand bed for 24 hours so that the gravitational water was lost from the soil. In this period, the amount of capillarity lost from the undisturbed samples, and the difference represents the specific yield. The measured values of specific yield for different lithologies are presented in Table 4-2. The observed daily groundwater levels for 18 observation wells were obtained from the South-Transdanubian Water Management Directorate. Table B1 presents the coordinates and annual change in groundwater level and specific yield for each of the observation wells.

Table 4-2: The measured values of specific yield for different lithologies

Lithology	Specific Yield
Sand	0.27
Sandy Loam	0.22
Loam	0.20
Clay Loam	0.13
Clay	0.07

4.5 Results and discussion

4.5.1 Validation of the WetSpass-M Model

The calculated groundwater recharge from Water Fluctuation Method is used to validate the WetSpass-M model. The simulated groundwater recharge for the WetSpass-M model at the corresponding observed wells were extracted from the spatially distributed results in GIS. Figure 4-2 shows that the simulated groundwater recharge by WetSpass-M matches the calculated recharge by WTF with $R^2 = 0.91$, a mean error of 7 mm yr^{-1}, and an absolute mean error of 18 mm yr^{-1}. The simulated recharge by the WetSpass-M model was then considered conditionally validated.

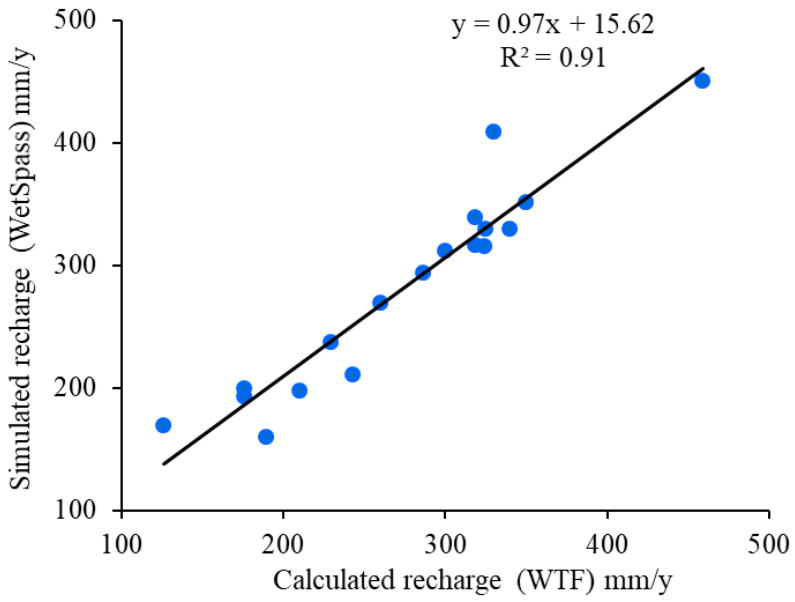

Figure 4-2: Scatter plot for the simulated values (WetSpass) and calculated values (WTF) of groundwater recharge for 18 monitoring points

4.5.2 Water balance components

The main outputs of the WetSpass-M model are raster maps of monthly groundwater recharge, surface runoff, actual evapotranspiration, and interception for the period 2000 to 2018 (223-time steps). In these maps, every pixel represents the magnitude of the water budget

component (in mm). A WetSpass-M model calculates the total actual evapotranspiration per pixel as a sum of evaporations from open water, impervious surface area, bare soil, interception of vegetated area, and the transpiration of the vegetative cover (Abdollahi et al., 2017; Batelaan et al., 2003). This research presents the first study to assess the spatial and temporal distribution of groundwater recharge in the Drava basin. The WetSpass results for water balance components will be used as integrated groundwater modeling inputs and boundary conditions in the Drava basin.

4.5.2.1 Actual evapotranspiration

The spatial distribution of monthly, seasonal and annual actual evapotranspiration, simulated by the WetSpass model is presented in Table 4-3. An assessment of water balance components on the annual scale is required to evaluate the total water budget of the Drava basin, also for monthly and seasonal scales to determine the agriculture water requirements. The simulated monthly long-term actual evapotranspiration of the Drava basin ranges from 0 mm $month^{-1}$ to 67 mm $month^{-1}$ as the lowest and highest values. The mean and standard deviations are 16 mm and 14 mm, respectively. The total annual actual evapotranspiration is determined by accumulating the simulated monthly actual evapotranspiration in the Drava basin. The annual average of evapotranspiration varies from 127 mm yr^{-1} to 263 mm yr^{-1} as the minimum and maximum values, respectively, with an average value of 190 mm yr^{-1} and a standard deviation of 39 mm yr^{-1} (Table 4-3). Average actual evapotranspiration represents 27 % of annual average rainfall (Figure 4-3b), of which an average of 158 mm (83 %) falls during the wet season (spring and summer), while the remaining 32 mm (17 %) occurs in the dry season (winter and autumn) (Table 4-3). This variation is due to rainfall differences within the two seasons. High annual and seasonal actual evapotranspiration are observed in the northwest of the Drava basin because of the higher rainfall while the northeast part that receives less precipitation shows lower evapotranspiration as depicted in Figure 4-3b.

Table 4-3: Long-term monthly, annual, and seasonal WetSpass simulated components of the Drava basin, 2000-2018

Period	Value	Precipitation (mm)	Recharge (mm)	Evapotranspiration (mm)	Runoff (mm)

Monthly	**Range**	0–229	0–58	0–67	0–114
	Average	58	25	16	17
	Std. dev.	28	10	14	13
Annual	**Range**	398 – 1072	175 – 412	127 – 263	77–418
	Average	696	307	190	199
	Std. dev.	161	55	39	81
Winter	**Range**	44–202	30–121	6–16	9–71
	Average	129	81	11	37
	Std. dev.	47	28	3	18
Spring	**Range**	93–414	48–102	41–138	10–187
	Average	215	72	83	59
	Std. dev.	67	14	23	39
Summer	**Range**	94–334	50–104	40–152	9–123
	Average	200	76	76	46
	Std. dev.	62	14	24	32
Autumn	**Range**	82–228	49–110	13–31	22–96
	Average	153	77	21	57
	Std. dev.	38	17	4	23

4.5.2.2 Interception

The spatial distribution of annual average interception is given in Figure 4-3d. Such annual average interception ranges from 10 mm yr^{-1} to 15 mm yr^{-1}, with an average interception rate of 13 mm yr^{-1}. The southern part of the Drava basin has the highest interception due to the presence of a dense vegetation cover (Figure 4-3d). About 91 % of the

simulated interception occurs in wet seasons (spring and summer) while the remaining 9 % takes place in dry seasons (winter and autumn).

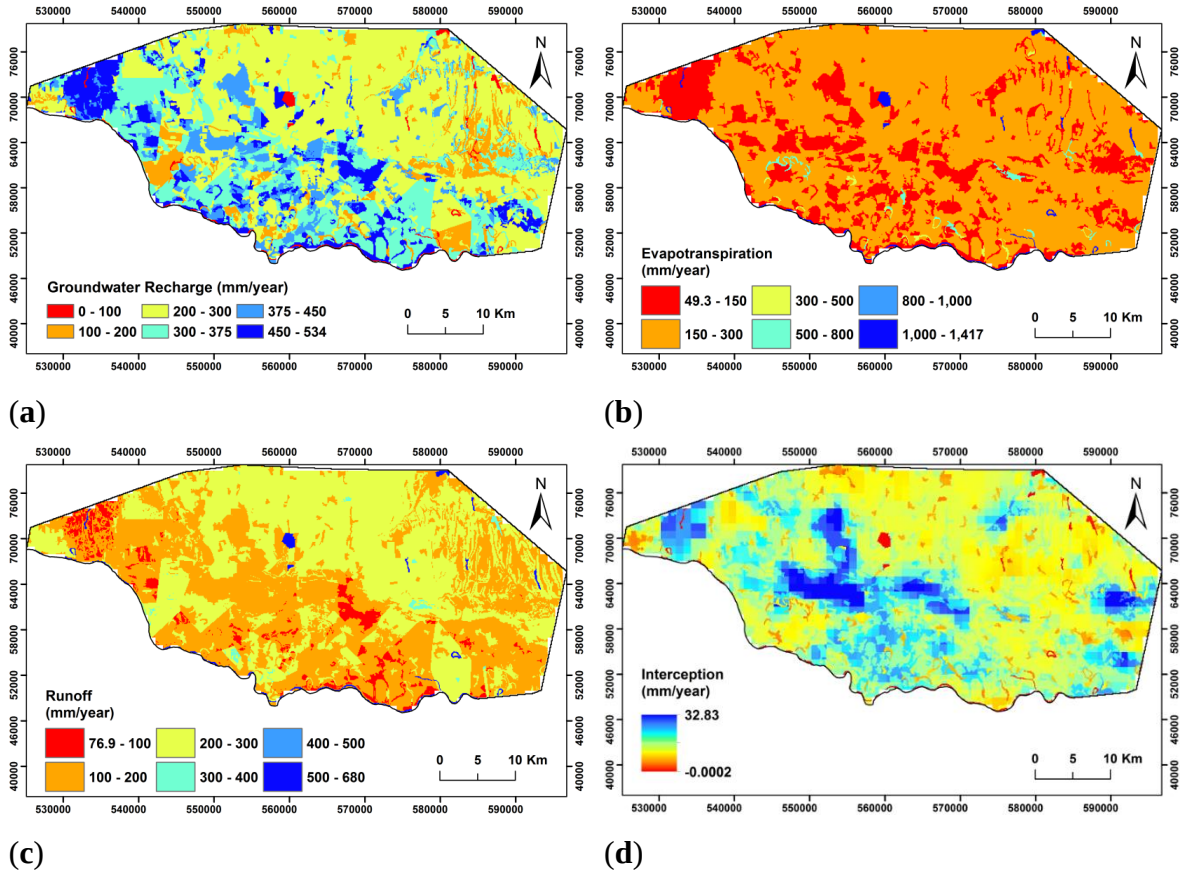

Figure 4-3: Spatial distribution of simulated mean water balance component (a) groundwater recharge; (b) actual evapotranspiration; (c) surface runoff; and (d) interception.

4.5.2.3 Surface runoff

The used WetSpass-M model calculates monthly surface runoff (in mm month^{-1}) using a rational method through an actual surface runoff and soil moisture coefficient (Abdollahi et al., 2017). The monthly, seasonal and annual WetSpass simulated runoffs in the basin are presented in Table 4-3. Estimated monthly surface runoff varies from 0 mm month^{-1} to a maximum of 114 mm month^{-1} with an average value of 17 mm month^{-1} and a standard deviation of 13 mm month^{-1}. Annual surface runoff is calculated by accumulating the simulated monthly values over the whole period. Annual actual surface runoff shows a large spatial variation with values between 77 mm and 418 mm. The average and standard deviation

of this distribution are 199 mm yr^{-1} and 81 mm y^{-1}, respectively (Table 4-3). Mean surface runoff in the basin constitutes about 29 % of annual mean rainfall. Mean surface runoff in summer and spring seasons is 105 mm, while average runoff in winter and autumn seasons is approximately 94 mm. As presented in Figure 4-3c, the northeastern mounds have high seasonal and annual surface runoff rates attributed to their gentle slopes. The highest mean seasonal and annual surface runoff values of the Drava basin are observed in the northern part attributed to the presence of clay, clay loam, and loam soils with low permeability, which increases surface runoff. On the other hand, the lowest runoff occurs in the southwestern and central areas due to the presence of sand and sandy loam soils. This confirms that the soil map is an important source of information on the spatial distribution of surface runoff.

4.5.2.4 Groundwater recharge

Groundwater recharge is essential to assess groundwater resources; however, it is difficult to evaluate groundwater recharge (Alley, 2002; Healy and Scanlon, 2010). The WetSpass-M model evaluates the long-term spatial distribution of monthly groundwater recharge for the Drava basin as a residual term of the water budget components by subtracting the monthly surface runoff and actual evapotranspiration from the monthly rainfall. The spatial distribution of groundwater recharge depends on topography, slope, soil type, land cover/land use, and climatological conditions (Batelaan and Woldeamlak, 2007). Winter, spring, summer, and autumn groundwater recharge of the Drava basin changes spatially with the basin characteristics and topography (Figure 4-4a–d). The WetSpass-M model evaluates the monthly long-term groundwater recharge of the Drava basin to be 0 mm and 58 mm as minimum and maximum values, respectively, with a standard deviation of 10 mm $month^{-1}$ and mean value of 25 mm $month^{-1}$ (Table 4-3). The average annual groundwater recharge is determined based on monthly simulated data. The maximum, minimum and mean values of annual groundwater recharge for the whole period are 412 mm, 175 mm, and 307 mm, respectively. Average recharge attributes to 44 % of the total average annual rainfall (Figure 4-3a). Average long-term groundwater recharge values for the dry (winter and autumn) and wet (summer and spring) seasons are 158 mm, and 148 mm, respectively.

About 52 % of the annual groundwater recharge takes place in the winter and autumn seasons (Figure 4-4a, d), while the remaining 48 % happens in the summer and spring seasons (Figure 4-4b, c). As shown in Figure 4-3a, the central-western part of the Drava basin that receives a high value of precipitation has higher annual and seasonal groundwater recharges. Also, forests and agricultural areas in the southern and central parts of the Drava basin are characterized by high groundwater recharge due to the presence of permeable (sand and sandy loam) soils with apparently flat topography. On the other hand, the northern part accounted for a lower rate of annual and seasonal groundwater recharge attributed to the presence of shrub and mudflat cover with less permeable loam soil (Figure 4-4a-d). In general, the groundwater recharge analysis reveals that higher values are observed in agricultural land with permeable soils.

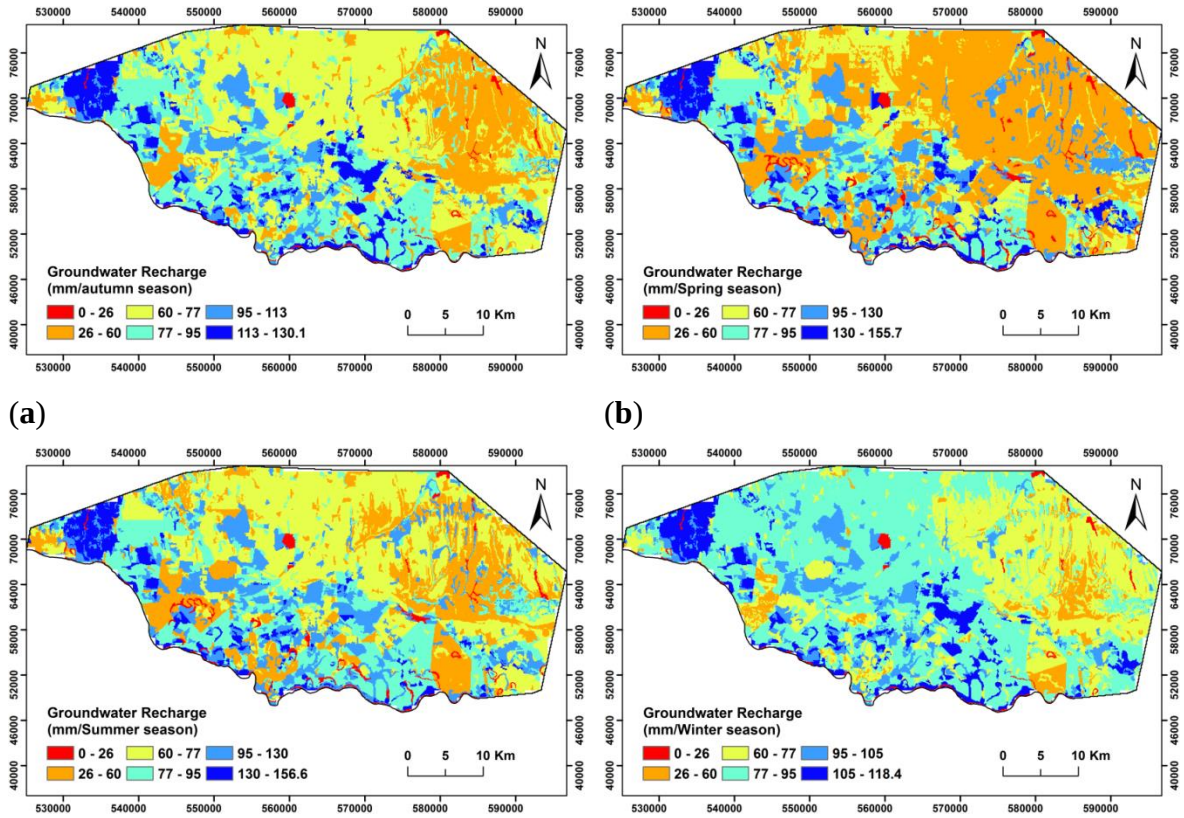

Figure 4-4: Simulated spatial distribution of average groundwater recharge in the Drava basin (a) Winter; (b) Spring; (c) Summer; and (d) Autumn.

4.6 Summary

Numerous river basins around the world are highly-regulated with several physical flow control and a range of regulations and storage structures. One such river basin is the Drava River basin in Hungary. Developing a groundwater model for the Drava basin requires an accurate estimation of groundwater recharge and evapotranspiration as input data and boundary conditions. This study evaluates temporal and spatial distributions of actual evapotranspiration, surface runoff, and recharge by applying the WetSpass - M model, which is crucial for integrated groundwater modeling of the Drava basin and optimal long-term planning and management of the available water resources in the basin. The basic relevant input data form for the WetSpass-M model is prepared in grid maps using the tool ArcGIS tool. It comprises monthly climatological recordings (e.g., rainfall, temperature, wind speed), distributed land cover, soil map, groundwater depth, topography, and slope. The spatial variability of groundwater recharge depends on climate conditions, groundwater depth, distributed land cover, soil texture, topography, and slope. The outputs of the WetSpass-M model revealed a favorable structure of water balance in the Drava basin, with the dominance of groundwater recharge.

CHAPTER Five

5. GROUNDWATER FLOW MODELING

Groundwater is one of the main components of the hydrological cycle but has not been well modeled by surface hydrological models such as WetSpass. An accurate simulation of both land surface and groundwater hydrological processes in the river basin is a fundamental step for integrated water resources management, particularly for watersheds where both surface water and groundwater resources are used conjunctively. In this chapter MODFLOW-NWT with ModelMuse as a graphical user interface is used to simulate groundwater flow to model a complex river catchment, the Drava River basin, thereby serving the IWRM goals of optimizing the conjunctive use of surface and groundwater.

5.1 Introduction

Groundwater modeling is the way of representing reality in a simplified form without making invalid assumptions or compromising the accuracy to investigate the system response under certain phenomena or to predict the behavior of the system in the future (Baalousha, 2009). Groundwater models use mathematical equations to simulate groundwater flow and transport processes according to certain simplifying assumptions. These assumptions include the flow direction, the anisotropy or heterogeneity of bedrock or sediments within the aquifer, aquifer geometry, chemical reactions, and contaminant transport mechanisms. Models should be represented as an approximation and not an exact representation of real conditions because of the uncertainties in the required data by the model and the embedded assumptions in the mathematical equations. A better understanding of hydrogeology in a given area is achieved by integrating the information on the aquifer boundaries, hydrochemistry and groundwater flow to build a 3-D conceptual, hydrogeological model (Yihdego, 2005).

Figure 5-1 presents the main steps of methodology in groundwater modeling. The first step in modeling is defining the model's purpose. Data collection represents a major issue in the modeling process. The conceptualization of the model is another fundamental step in modeling followed by setting up the numerical model. Model calibration and validation, and sensitivity analysis can be performed after model completion. The last step is preparing and running simulations for prediction scenarios.

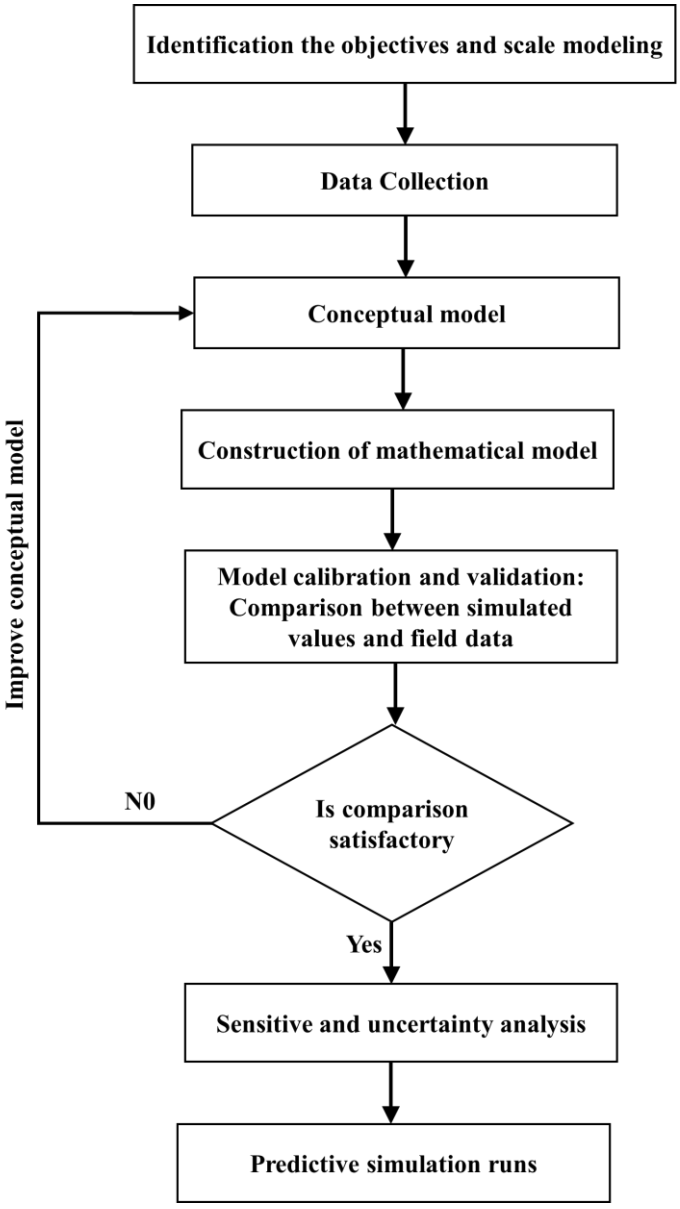

Figure 5-1: Flow diagram of stepwise methodology in groundwater modeling

5.2 Materials and methods

5.2.1 Study Area

The investigated area covers part of the Drava basin region in the southwest part of Hungary, as shown in Figure 5-2. The floodplain extends from 45.74°–46°N latitude and 17.44°–18.15°E longitude with a total area of 538.46 km^2. The elevation of the floodplain ranges between 133 m.asl and 83 m.asl, with an average elevation of 100.3 m. The floodplain is flat, with an average relative relief of 0.26 m km^{-1} (Figure 5-2). Settlements were built on elevated terrain.

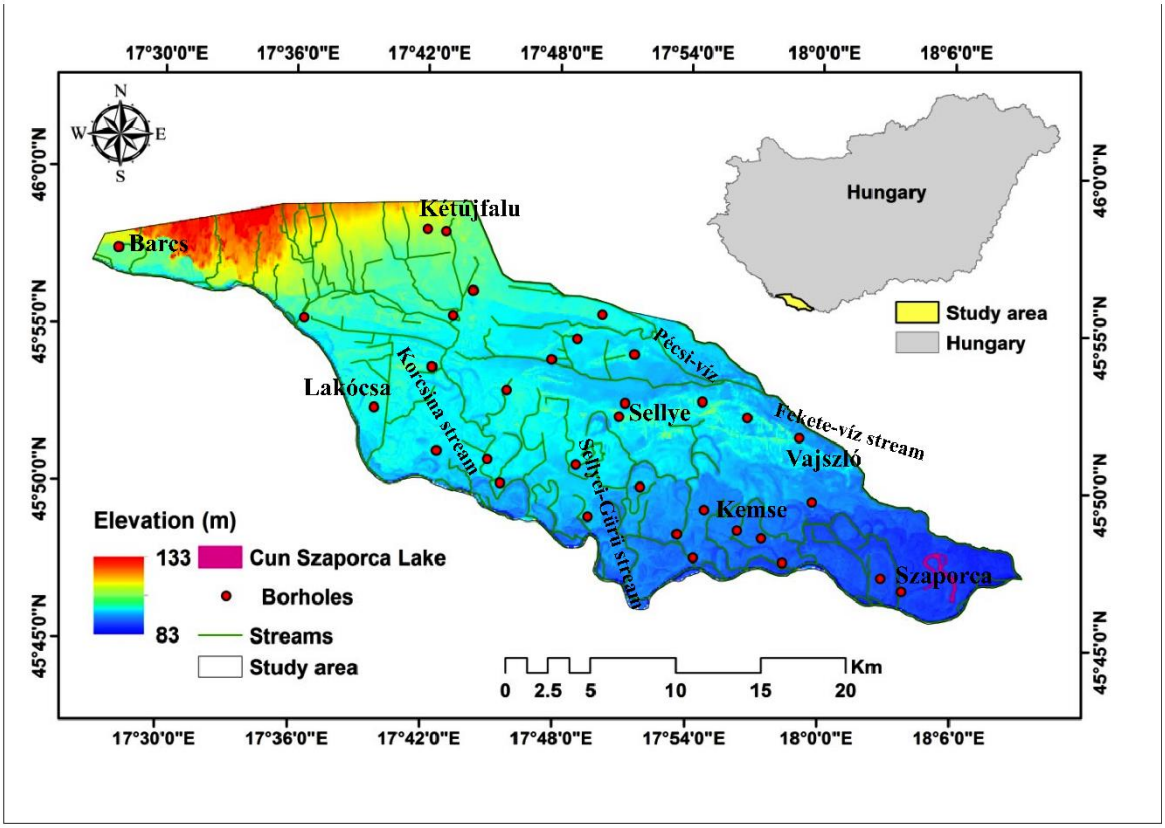

Figure 5-2: Location of the Drava River floodplain, SW Hungary, with watercourses, existing (Cún-Szaporca) lake, and topography.

5.2.2 Groundwater data

The data used to create the groundwater flow model, MODFLOW, are demonstrated in this section. There are also two categories of data collected for modeling the catchment, namely:

1) The static dataset, such as DEM (used as the elevation of ground surface), depth of groundwater from the ground surface (used to estimate initial groundwater head), aquifer designation data and soil type map (for horizontal permeability values) that are assumed to be static over the study period;

2) The historical observations of daily groundwater level; and daily lake stages

5.2.3 Defining modeling objectives

The model approach, extent and model type may vary depending on modeling objectives. Groundwater models can be applied as predictive, interpretive, or generic (Anderson and Woessner, 1992). The main objectives of groundwater modeling in this study are:

- Predicting the temporal and spatial distribution of groundwater head and groundwater flow.
- Investigating different fluvial sediment structures scenarios to assess the exchange between surface flow (from the Drava river and the Cún-Szaporca oxbow lake) and aquifer.
- Evaluating the impacts of LULC changes from 1990 to 2018 on groundwater systems.
- Investigating different management scenarios on hydrological processes and groundwater systems.

5.2.4 Conceptual model

A conceptual model represents the most important part of groundwater modeling and builds on an understanding of how a groundwater system works. It consists of

understanding the groundwater system characteristics and their spatiotemporal evaluation and provides a descriptive representation of the hydrogeologic system. A good conceptual model should simplify the complexity of the reality in a way that meets management requirements and achieves modeling objectives (Bear and Verruijt, 1987). Simplification relies on the objectives, the amount of available data, the scale of the model, and the current level of understanding. The conceptual model describes factors which include:

- Model domain and aquifer geometry
- Aquifer parameters such as hydraulic conductivity, porosity, transmissibility, specific yield, specific storage, etc
- Boundary conditions
- Evapotranspiration and groundwater recharge
- Identification of sources and sinks
- Water balance

According to evidence from geological boreholes, pumping tests and GPR surveys, the groundwater flow system consists of four layers. Since the sediments in the area range from coarse sand to clay, the four layers are highly heterogeneous in space. The records of GPR, supplemented with auger holes, presented high heterogeneity in the hydraulic proprieties of the sediment depending on particle size (ranging from coarse sand to clay). The fall head method was applied to calculate the hydraulic conductivity for each borehole. According to boreholes data, the first layer consisted of four K-zones of hydraulic conductivity (Figure 5-3), varying from 375 to 0.15 m d^{-1}, while the second layer was characterized by three zones with a range of 375 and 75 m d^{-1}. The third and fourth layers were described by two zones, with a range from between 375 and 75 m d^{-1} and 0.15 to 3 m d^{-1}, respectively (Figure 5-3). Although all the hydraulic parameters were determined in the field, because of limited spatial representativeness and the influence of modeling scale in accordance with Guimerà et al. (1995), Zhang et al. (2006) and Zhang et al. (2007), they still had to be adjusted in the calibration process. Fortunately, the majority of the units had natural boundaries. The upper layer of the aquifer is under the effect of lake level fluctuations, whereas at high stages, the aquifer is recharged from the lake, and at low stages, groundwater system discharge into the

lake. Lake stages variability affects seepage from the lake and the leakage through the aquifer in upward direction. Inputs to the groundwater system are groundwater recharge from precipitation, river seepage and lake seepage, lateral groundwater inflow from part of the northern boundary, while the output from the groundwater system includes groundwater seepage to rivers and lakes, lateral groundwater outflow from the south western boundary and, evaporation from groundwater.

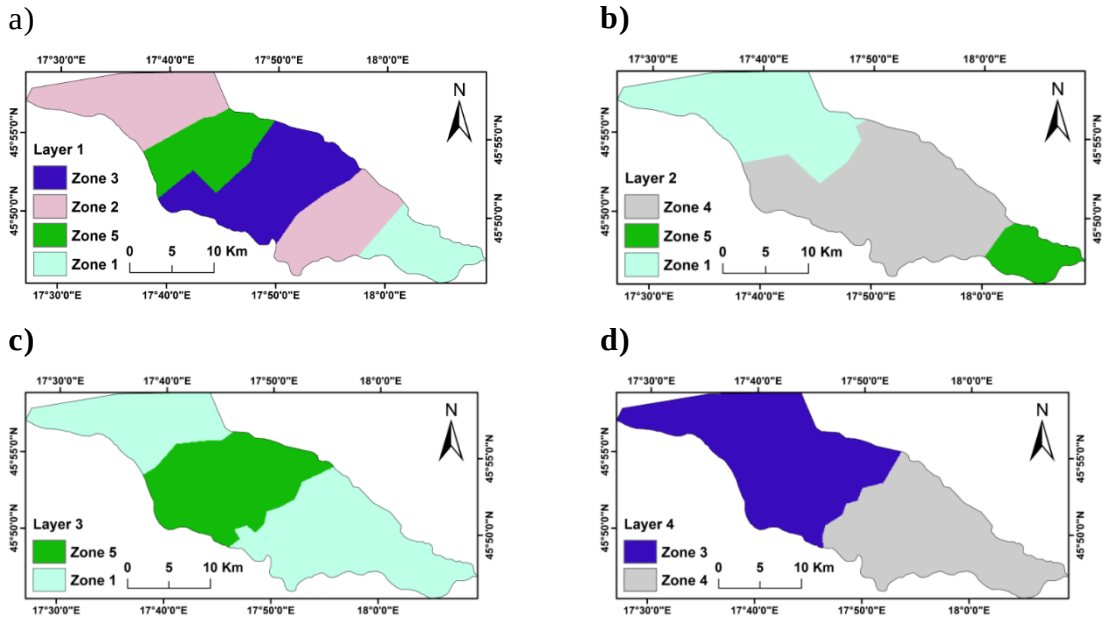

Figure 5-3: Hydraulic conductivity zones for (a) layer 1; (b) layer 2; (c) layer 3; (d) layer 4.

5.2.5 Numerical Groundwater Modeling (Software Description)

Modular Finite-Difference Ground-Water Flow Model (MODFLOW) is developed by the U.S. Geological Survey and used a cell-centered FDM to simulate three-dimensional groundwater flow in three dimensions for both steady-state and transient conditions. It went through several versions, MODFLOW-88 (McDonald and Harbaugh 1988) MODFLOW-96, MODFLOW-2000 (Harbaugh et al., 2000; Hill et al., 2000), and the current version is MODFLOW-2005 (Harbaugh, 2005). The MODFLOW model is built based on the combination of two basic equations the principle of momentum conservation and mass conservation (Trescott and Larson, 1977). The three-dimensional

groundwater flow with a constant density of an anisotropic and a heterogeneous porous medium can be described by the partial-differential equation of Freeze and Cherry (1979).

5.2.5.1 The groundwater flow equation

The partial-differential equation of groundwater flow used in MODFLOW is (McDonald and Harbaugh, 1988):

$$\frac{\partial}{\partial x}\left(K_x.\frac{\partial h}{\partial x}\right)+\frac{\partial}{\partial x}\left(K_x.\frac{\partial h}{\partial y}\right)+\frac{\partial}{\partial x}\left(K_x.\frac{\partial h}{\partial z}\right)+W=\ S_x.\frac{\partial h}{\partial t} \qquad \textbf{(5-1)}$$

where h (L) is the hydraulic head in the porous medium; K_x, K_y, and K_z (LT^{-1}) are anisotropic hydraulic conductivity for the porous medium in x, y, and z directions, respectively W (T^{-1}) is the volumetric flux per unit volume at sources or sinks of the porous medium, W < 0.0 for flow out of the ground-water system, and W > 0.0; Ss (L^{-1}) is the specific storage for the porous medium and t is time (T). In this study, MODFLOW-NWT (Niswonger et al., 2011) with ModelMuse (Winston, 2009) as a graphical user interface was applied to simulate groundwater flow. MODFLOW-NWT was mainly developed to run models suffering from nonlinearities of drying and rewetting of the unconfined aquifer. This is in contrast with other versions of MODFLOW, which exclude dry cells from calculation.

5.2.6 Boundary conditions

5.2.6.1 General-Head Boundary (GHB) Package

MODFLOW General-Head Boundary (GHB) was assigned to the southwestern and part of the northern boundary (Figure 5-4**)** to simulate lateral groundwater inflow and outflow of the system based on the time series of groundwater level from the available observation wells. Initially, the conductance of GHB was set to be 20 $m^2\ d^{-1}$, based on geological boreholes and adjusted during the calibration process.

5.2.6.2 River boundary simulation

The River Package is designed to simulate volumetric river interactions with groundwater. In this study, all rivers and streams were simulated by the river package. River reaches within the model domain are imported from their shape files as polylines. Elevations of river bottom are set at ground level, i.e. the top of the grid cell as given by the DEM. The water depths of the Drava river, Fekete-víz, and Okor are obtained from the Water Directorate management for the period 2000-2018 while the water stages in the other streams were assigned under the ground level by 0.75m. The southern boundary is represented by the Drava River and assigned as a river package. Based on data available from observation wells, the general direction of groundwater flow is from north to south. The Fekete-víz and Okor streams comprise the northern, eastern, and part of the western boundary and they are parameterized by the River package (Figure 5-4). All streams in the floodplain are assigned by a river package. The conductance of the riverbed was initially set to 5 $m^2 d^{-1}$, and then adjusted during the calibration process. (Riverbed conductance for the main streams is set to 0.3 and 0.2 for the secondary streams and adjusted during the calibration process. Flow between the river and the groundwater system for reach n is given by:

$$Q_{RIV} = C_{RIV} (H_{RIV} - h_a) \qquad h_a > h_{rivbot} \qquad (5\text{-}2)$$

$$Q_{RIV} = C_{RIV} (H_{RIV} - h_{rivbot}) \qquad h_a \leq h_{rivbot} \qquad (5\text{-}3)$$

Q_{RIV} is the flow between the river and the aquifer; C_{RIV} is the hydraulic conductance of the riverbed(L^2T^{-1}); H_{RIV} is the river stage(L); h_a is the head in the aquifer beneath the riverbed; and h_{rivbot} is the level of the river bottom. Therefore, when the head in the aquifer is higher than the river stage, the aquifer recharges water to the river, represented as a negative inflow to the aquifer. When the head in the aquifer is lower than the river stage, flow is recharge to the aquifer. This flow increases linearly as the head in the aquifer decreases, until the aquifer head reaches the river bottom the flow remains constant. Riverbed conductance, C_{RIV} $(\frac{m2}{day})$ can be computed as follows (McDonald and Harbaugh, 1988):

$$C_{RIV} = \frac{K.W.L}{d} \qquad (5\text{-}4)$$

K is the hydraulic conductivity of riverbed sediments (L T^{-1}), w is the width of a river reach (L), L is the length of river reach corresponding to a volume of aquifer (L), d is the thickness of the streambed deposits (L),

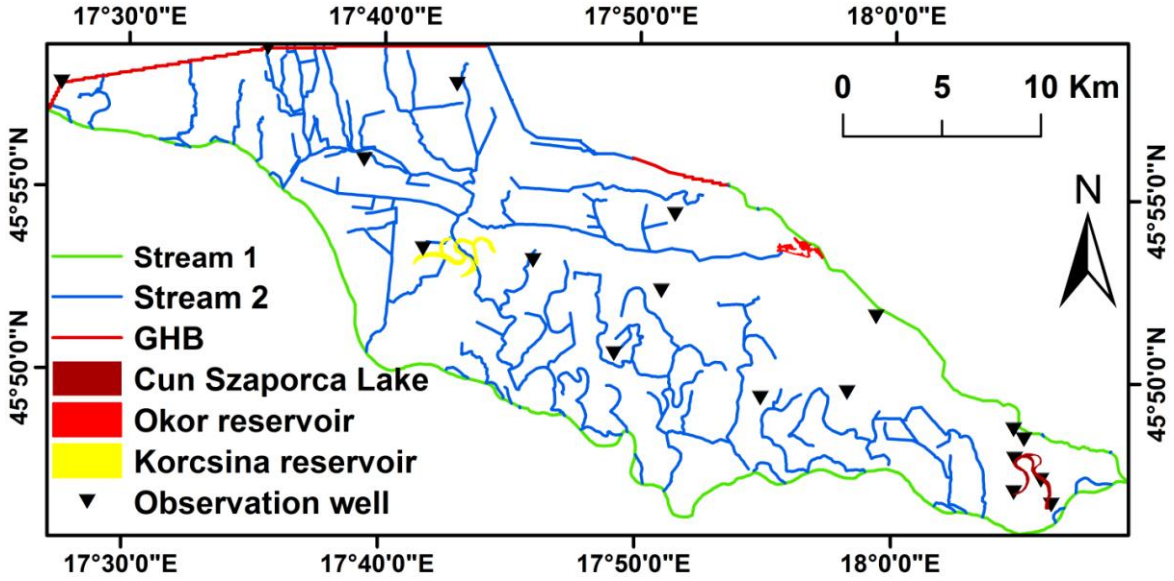

Figure 5-4: Boundary conditions, observation wells, and planned reservoirs

5.2.6.3 Lake Package

Using the LAK package to simulate lake/groundwater interactions is one of the advantages of using MODFLOW-NWT under ModelMuse. Unlike the Reservoir package, the lake stage in the Lake Package can rise or fall due to interaction with groundwater and/or with streams. The Lake Package is integrated into MODFLOW-NWT by specifying lake nodes in the model finite-difference grid, then, the lake stage is determined based on the exchanges of volumetric water in and out of the lake and the overall water balance of the lake (Hunt, 2003). The seepage between a lake and its groundwater system depends on lake stage, lakebed leakage in grid cell dimensions, the hydraulic conductivity of the lakebed material, the adjacent aquifer, and hydraulic heads in the groundwater system. The seepage is calculated by Darcy's law (Merritt and Konikow, 2000), as follows:

$$q = K\,(h_1 - h_a)/d, \qquad (5\text{-}5)$$

where q is the seepage rate (L T^{-1}); K is the hydraulic conductivity (L T^{-1}) of materials between the lake and the aquifer; h_1 is the stage of the lake (L); h_a is the aquifer head (L); d is the distance (L) between the points at which h_1 and h_a are measured; and the volumetric flux Q (L^3 T^{-1}) is established by the following equation:

$$Q = q\,A = (K\,(h_1 - h_a)/d)\,A = C\,(h_1 - h_a), \quad (5\text{-}6)$$

where c = KA/d is the conductance (L^2 T^{-1}) and K/d is the leakage (T^{-1}).

Estimating a lake water budget requires quantifying the gains and losses of water from the lake, such as gains from precipitation, overland runoff, and inflowing streams, and losses due to evaporation and outflowing streams, besides any other types of anthropogenic gains and losses. The updated lake stage in the Lake Package is calculated through the water budget procedure by the explicit form of Equation 2.26.

$$h_1^n = h_1^{n-1} + \Delta t\,\frac{P - E - SR - W - SP + Q_{in} - Q_{out}}{A_s} \quad (5\text{-}7)$$

where h_1^n and h_1^{n-1} are the lake stages (L) during the present and previous time step, Δt is the time step length (T), P is the precipitation rate (L^3T^{-1}) on the lake during the time step, E is the evaporation rate (L^3T^{-1}) from the lake during the time step, SR is the surface runoff rate (L^3T^{-1}) to the lake during the time step, W is the withdrawal rate (L^3T^{-1}) from the lake, SP is the net rate of seepage (L^3T^{-1}) between the lake and the aquifer, Q_{in} is the rate of inflow from streams and $and\ Q_{out}$ is the rate of outflow (L^3T^{-1}) to streams during the time step, and A_s is the surface area of the lake (L^2) at the beginning of the time step.

Cún-Szaporca Lake was assigned in the model through the LAK7 package (Figure 5-5). The lake simulation was performed using a separate additional inactive layer (Merritt and Konikow, 2000) with variable thickness. The top of the inactive layer had a 1.0 m thickness outside the lake and the top equaled the maximum lake stage within the lake area. The bottom was equal to the bathymetrically defined lake bottom. To represent the lakebed leakance, three undisturbed sediment samples were taken from the oxbow lake bed for laboratory analyses in PVC pipes of 45 mm diameter (Figure 5-5). The hydraulic conductivity of three intact samples from the oxbow lake was calculated in our laboratory experiment using the falling head method (Landon et al., 2001). Following the hydraulic measurements, grain size distribution analyses were carried out on undisturbed samples with a Malvern Mastersizer 3000 Hydro LW (Malvern Inc.,

Malvern, United Kingdom) particle size analyzer. Geologically, the sediments of the oxbow bed can fundamentally be subdivided into two types: a calcareous sandy and a clayey-silty unit. Hydraulic conductivity was 8.3 x 10^{-8} m s^{-1} for KP1 and 2.82 x 10^{-7} m s^{-1} for the sediment samples of KP2 and KP3. The modi of the PSD curves were markedly different, 10 μm in the deepest part of the lake and 80 μm along the shoreline. Thus, lake bed leakance was assigned by 0.05 d^{-1} for the deepest part (former thalweg) of the oxbow and 5 d^{-1} for the remaining lakebed area.

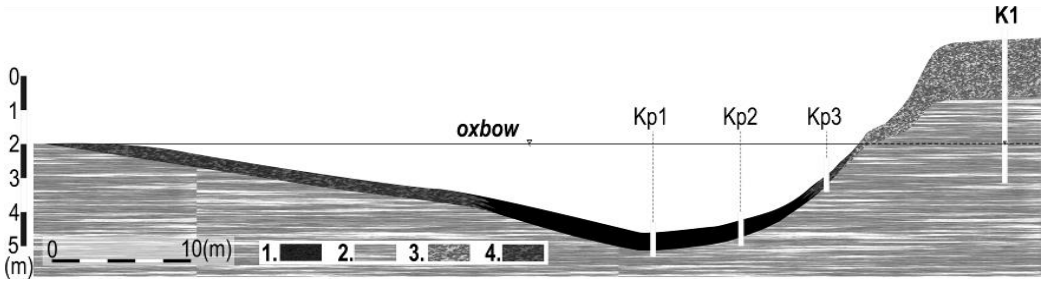

Figure 5-5: Cross section of Lake Kisinc with sites of the sampling (Kp1, Kp2, Kp3) and K1 well tests. 1, fine oxbow bed material, 2, alluvium (clayey, silty, sandy deposits), 3, brown topsoil with root canals, 4, mixed lacustrine sediments

5.2.6.4 Stream Flow Routing Package

In this study, the feeding canal to the oxbow lakes was simulated using the Stream Flow Routing Package (SFR). One of the main advantages of the SFR package is that it is linked to the lake package, and it was developed to accommodate streams that discharge water into and from lakes (Prudic et al., 2004). Unlike River Package or Drain Package, the SFR Package is able to simulate volumetric surface water discharges. The feeding canal of oxbow lake was simulated by rectangular section, the hydraulic conductivity for the streambed was initially assigned as and adjusted during the calibration process the stream bed thickness was assigned as 1.0 m, the Manning coefficient was assumed equal to 0.0354, the canal width was set equal to 1.5 m.

5.2.6.5 Recharge (RCH) and Evapotranspiration (ET) Packages

Recharge and evapotranspiration are estimated using the WetSpass-M model, as explained in section A.1 of Chapter 3. The spatial distribution of groundwater recharge

and evapotranspiration are imported in the form of a shape file into ModelMuse. Inputs to the groundwater system are groundwater recharge from precipitation, river seepage and lake seepage, lateral groundwater inflow from a part of the northern boundary, while output from the groundwater system includes groundwater seepage to rivers and lakes, lateral groundwater outflow from the southwestern boundary, and evaporation from groundwater.

5.2.6.6 ZONEBUDGET

ModelMuse can provide the overall volumetric groundwater balance, but it cannot produce the water balance for a specific region in the model or for each simulated layer alone. Harbaugh (1990) developed the ZONEBUDGET, which is capable of calculating the water budget for any zone. The ZONEBUDGET is also available under ModelMuse environment. It reduces the calculations that may be done by the user through providing the water budget for any single zone and for composite zones.

5.2.6.7 The Head Observation (HOB)

The Head Observation (HOB) Package was applied to simulate the time series head records. For each piezometer, the required data are the piezometer name, the observed head, and the time step. The piezometer coordinates were imported to ModelMuse as points. After activating the HOB Package, and then the data were assigned to each point individually.

5.2.7 Model Computational Grid

The conceptual model is converted to the numerical model by defining the grid size, whereas the grid size relies on the problem type. In the current study, the model was discretized by a 100 m by 100 m grid, and the model was refined for lake area with 30 m by 30 m, resulting in a domain of 361 rows and 742 columns, and 4 layers with a total number of 1,339,310 cells, 655,390 of which were active cells. Once the model is

converted from conceptual to numerical by assigning the grid type, the model is to be translated and simulated with all the given inputs (including boundary conditions and observed wells).

5.2.8 Defining Initial Groundwater Head

The initial heads are required for both the steady-state and the transient state mode. The initial groundwater head map was constructed using observed measurements of depth to water table converted to hydraulic heads from the available 18 observation wells. A nearest-neighbor technique was used to interpolate those observations. The initial head map was imported to ModelMuse as a shape file and initial heads have been assigned to each grid cell. The observed average lake level stage was 98 m.

5.3 Water balance

To establish the water balance of reservoirs is a complex task due to intricate interactions between surface and groundwater components. The water balance of each model zone is important to assess the interaction between the natural reservoir and aquifer system. The water balance equation of the whole model is

$$P + GHB_{in} + Q_{in} = ET + GHB_{out} + Q_{out} + \Delta S, \quad (5\text{-}8)$$

where P is precipitation, ET is total evapotranspiration, Q_{in} is stream inflows, Q_{out} is stream outflows, GHB_{in} is lateral groundwater inflow by GHB boundaries, GHB_{out} is lateral groundwater outflow by the GHB boundaries, and ΔS is a total change of storage.

The water balance equation of the Lake Package can be expressed as follows:

$$P + S + LAK_{in} + QLAK_{in} = ELAK + LAK_{out} + QLAK_{out} + \Delta SLAK, \quad (5\text{-}9)$$

where S is surface runoff, $QLAK_{in}$ is inflow from stream to the lake, $QLAK_{out}$ is the outflow from stream to the lake, LAK_{in} is a discharge from the aquifer to the lake, and LAK_{out} is aquifer recharge from the lake. In the equation, ELAK is lake evaporation. Daily lake evaporation is calculated using the Penman open-water equation (Penman, 1948) based on wind speed, hourly incoming solar radiation, air temperature, relative humidity, air temperature, and wind speed. ΔSLAK is a change in lake storage.

The water balance equation of the unsaturated zone is calculated using water and energy transfer between soil, plants, and atmosphere under quasi-steady state conditions WetSpass (Batelaan and De Smedt, 2001) see equations in chapter four.

The water balance of the saturated zone for four aquifers is expressed as follows:

$$R + LAK_{out} + QGW_{in} + GHB_{in} = ET + LAK_{in} + GHB_{out} + QGW_{out} + S_{sat}, \quad (5\text{-}10)$$

where QGW_{in} is groundwater recharge from stream, QGW_{out} is the discharge from groundwater to streams, and S_{sat} is the change in saturated zone storage.

5.4 Calibration Process

The model calibration process is aimed to match the model results with the measurements in the field within some acceptable criteria. In groundwater models the simulated groundwater head and fluxes are forced to match the field measured values at observed points with a range of acceptable error. This process requires changing model parameters (i.e. hydraulic conductivity, specific yield, specific storage), boundary conditions, and hydrologic stresses to obtain the optimal match. Proper field characterization and sufficient data are required to achieve a well-calibrated model..

In this study, the steady-state and transient models were calibrated manually in a forward way because of its high complexity involving long simulation time when using optimization codes such as UCODE (Hill and Tiedeman, 2007) or PEST (Doherty and Hunt, 2010), and forward calibration procedure enables the modelers to understand model behavior. A steady-state model was developed to represent an initial case for the transient model by applying long-term average parameters, i.e., mean precipitation, mean groundwater levels, mean PET, and mean groundwater recharge for the period from 1 January 2010 to 20 September 2018. The steady-state oxbow lake stage was calculated as an average for the whole lake stages during the study period (173.77 m a.s.l.) (the model parameters). Several statistic indices have been recommended for assessing the performance of a model, of which Mean Error (ME), Mean Absolute Error (MAE), and Root Mean Square Error (RMSE) are used as measures of groundwater head and lake stages calibration. They are mathematically presented as follows:

$$\text{ME} = \frac{1}{n}\sum_{i=1}^{n}(h_m - h_s)_i \quad (5\text{-}11)$$

$$\text{MAE} = \frac{1}{n}\sum_{i=1}^{n}|h_m - h_s|_i \quad (5\text{-}12)$$

$$\text{RMSE} = \left[\frac{1}{n}\sum_{i=1}^{n}(h_m - h_s)_i^2\right]^{0.5} \quad (5\text{-}13)$$

where n is the number of observations; h_m is observed groundwater level, h_s is simulated groundwater level and $\bar{h}_m$ is the mean observed groundwater level. ME provides a general description of model bias as both positive and negative differences are involved in the mean, the errors may eliminate each other, and thus decreasing the overall error (Anderson et al., 2015). MAE measures the average error in the model. RMSE is the average of the squared differences in observed and simulated heads.

5.5 Sensitivity analysis

A sensitivity analysis is a process of changing model input parameters through a reasonable range and evaluating the relative variation in model response (Kumar, 2004) and measuring the effect of these variations on the model outputs. There are a large number of uncertain parameters, boundary conditions, and stresses in regional groundwater models. Sensitivity analysis quantifies the impacts of uncertainty on the estimates of model parameters, on model results and provides which parameters have a greater impact on the output. Parameters with a high effect on model results should get the most attention in the data collection and the calibration process. In this study, sensitivity analysis was achieved using computer code for universal sensitivity analysis, calibration, and uncertainty evaluation (UCODE-2005) (Poeter et al., 2006) with the help of ModelMate (Banta, 2011). It was applied to groundwater recharge (RCH), hydraulic conductivity (HK), which was divided into five zones, evapotranspiration (EVT), river conductance (RIVC), and general head boundary (GHB) parameters.

5.6 Transient model calibration

The transient state solution represents a set of solutions corresponding to time steps of a specific stress period, while the steady-state solution produces an average solution

for the analyzed problem (Shakya, 2001). However, starting the transient model by steady-state model as an initial condition proved to be unsuccessful due to a large difference between the steady-state parameters and the measured daily values at the start-up of the transient model on 1 January 2010. Thus, the steady-state model was abandoned and the first three hydrological years from which data were available, i.e., from 1 January 2010 until 31 December 2012, were used as a warm-up period, after which the model was run (calibrated) throughout the following six hydrological years from 1 January 2013 to 20 September 2018. Daily stress periods, each including one single-day time step, were assigned the time domain of the final transient model. There were 18 daily piezometric records (Figure 5-4); two of them were used for assigning the head of the general head boundary at the western side. The same parameters in the steady-state model were applied in the transient model, and they were adjusted during the calibration process. The calibration process was conducted mainly by adjusting the number of initially assigned K-zones, their areas and the associated hydraulic conductivities (Kh), groundwater recharge, and evapotranspiration boundary conditions. Some minor changes were made in the initially assigned riverbed conductance, and GHB conductance at the western boundary was slightly adjusted.

5.7 Results and Discussions

5.7.1 Results of steady-state calibration and sensitivity analysis

Calibrated results of the steady-state model showed a good agreement between observed and simulated groundwater heads, with $R^2 = 0.98$. Mean error was −0.016 m, and mean absolute error was 0.09 m as shown in Figure 5-6a. The calibrated values of hydraulic conductivity result in six zones: 550, 1.25, 0.1, 5, 60, and 170 m d^{-1}. The river bed conductance for the main streams was found 30 m^2 d^{-1}, and for secondary streams 3 m^2 d^{-1}. The conductance of the GHB boundary was changed to 40 m^2 d^{-1}. The calibrated groundwater recharge is 0.95 times of the obtained average of groundwater recharge from WetSpass. The parameters of groundwater recharge (RCH), hydraulic conductivity

(HKZ1), and evapotranspiration (EVT) had the highest composite scaled sensitivity values and were therefore the most sensitive parameters (Figure 5-6b).

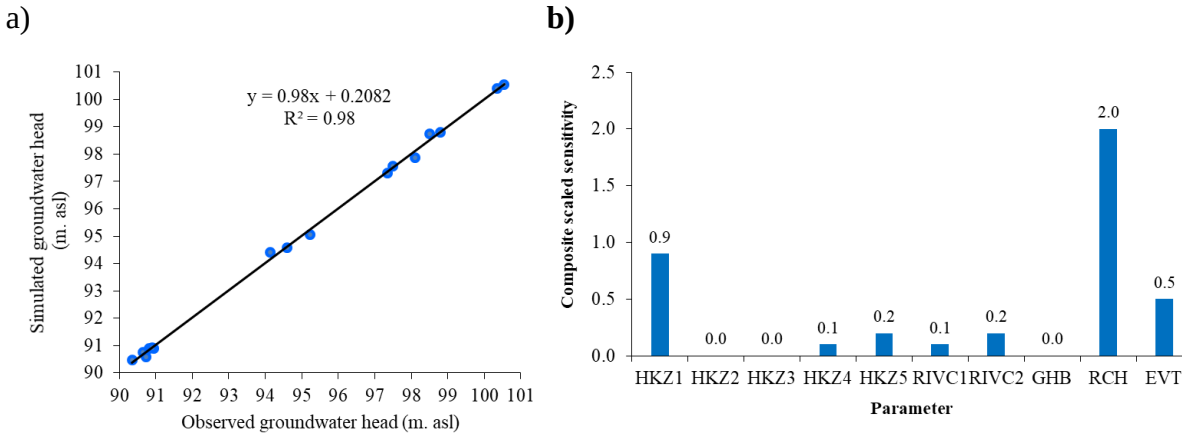

Figure 5-6: a) Scatter plot for simulated versus observed heads of steady-state using 18 observations; b) composite scaled sensitivities calculated with the parameter values

5.7.2 Transient Calibration

However, starting the transient model by steady-state model as an initial condition proved to be unsuccessful due to a large difference between the steady-state parameters and the measured daily values at the start-up of the transient model on 1 January 2010. The first three hydrological years from which data were available, i.e., from 1 January 2010 until 31 December 2012, were used as a warm-up period, after which the model was run (calibrated) throughout the following six hydrological years from 1 January 2013 to 20 September 2018 with a daily time step. The calibrated results of the transient model against the time series of observation well heads and the stages of the Cún-Szaporca Lake are shown in Figure 5-7. The calibration process of groundwater head was carried out using 16-time series of daily groundwater levels from observation wells extending over 10 years. Calibrated results showed a good match between observed and simulated groundwater heads, with $R^2 = 0.98$. The mean error was −0.08 m, and the root mean square error was 0.4 m (Figure 5-7a). Additionally, the calibration of lake stages showed a good agreement between simulated and observed stages with a correlation coefficient of 0.90, a mean error of −0.07 m, mean absolute error of 0.15 m, and root mean square error of 0.2 m (Figure 5-7b). The calibrated parameters of hydraulic

conductivity, river conductance, general head conductance, and groundwater recharge are shown in Table 5-1

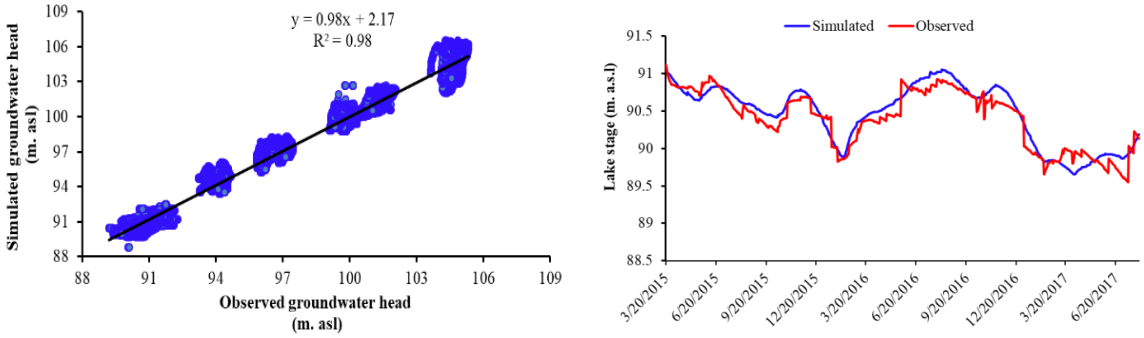

(**a**) (**b**)

Figure 5-7: Model calibration. (a) Scatter plot for simulated versus observed groundwater piezometric heads; (b) simulated and observed daily variability of lake stages

Table 5-1: Calibrated parameters for the calibrated model. R represents the spatial distribution map of the average groundwater recharge

Parameter	Value	Unit	Description
HKZ1	360	m d^{-1}	Hydraulic conductivity of zone 1
HKZ2	25	m d^{-1}	Hydraulic conductivity of zone 2
HKZ3	0.10	m d^{-1}	Hydraulic conductivity of zone 3
HKZ4	5	m d^{-1}	Hydraulic conductivity of zone 4
HKZ5	60	m d^{-1}	Hydraulic conductivity of zone 5
RIVC1	300	m^2 d^{-1}	River conductance of streams 1
RIVC2	5	m^2 d^{-1}	River conductance of streams 2
GHB	40	m^2 d^{-1}	Conductance of general head boundary
RCH	0.95R	mm d^{-1}	Groundwater recharge

5.7.3 Water Budget of the Groundwater Flow Model

The water balance at the end stress of the calibrated transient model is shown in Table 5-2. The inflow rate from GHB boundary to the aquifer represents 42.25 % of the total inflow to the aquifer through 627,789.00 m^3 d^{-1}. Both groundwater recharge from precipitation, streams, and the Cún-Szaporca Lake are represented by 41 % of the total inflow to the aquifer through 609,169 m^3 d^{-1}. The total water budget of the floodplain

proves the importance of groundwater recharge in maintaining groundwater levels. Groundwater discharge from the aquifer to streams is 1,275,244.38 m^3 d^{-1}, which amounts to 85.82 % of the total outflow from the groundwater system as the area characterized by shallow groundwater table, while evapotranspiration represents 10 % of total outflow.

Table 5-2: Water balance at the end stress of the calibrated transient model

	Input		**Output**		**Input−Output**
	(m^3 d^{-1})	**%**	**(m^3 d^{-1})**	**%**	**(m^3 d^{-1})**
Recharge	546,403	36.8	457	0.0	545,946
Evapotranspiration	0	0.0	149,992	10.1	−149,992
GHB boundary	627,789	42.3	10,949	0.7	616,840
River	62,766	4.2	1,275,244	85.8	−1,212,478
Lake	6868	0.5	4967	0.3	1901
Storage	242,055	16.3	44,265	3.0	197,783
Total	1,485,881	100.0	1,485,874	100.0	0

5.8 Summary

Developing a groundwater model of the floodplain is crucial to assess the interactions between surface water and groundwater at a critical part of this system under different hydrological conditions, also to evaluate the water retention and water budget under different management scenarios in the lower parts of the floodplain to sustain agricultural production and wetland habitat. A regional steady and transient groundwater model was constructed using MODFLOW-NWT with ModelMuse as a graphical interface to simulate the flow of water. The steady-state and transient state model calibration indicated a good correlation between the computed and observed water levels with a correlation coefficient of 0.96, a mean error of −0.016 m, and a mean absolute error of 0.4 m. The sensitivity analysis was conducted using (UCODE-2005) with the help of ModelMate.

CHAPTER Six

6. INTEGRATED ASSESSMENT OF THE IMPACT OF LAND-USE/LAND-COVER CHANGES ON HYDROLOGY

Land-use/land-cover (LULC) change is considered to be a key human factor influencing groundwater recharge in floodplains. Without accurate estimations, the impact of LULC change on water balance components may be either understated or exaggerated. Nevertheless, the effects of LULC changes on the surface hydrology has not been investigated in the Drava Basin. In this chapter, a coupled surface hydrological model, i.e. a spatially-distributed water balance model (WetSpass-M), coupled with a groundwater flow model (MODFLOW-NWT) were integrated to assess the impacts of LULC changes with different soil textures from 1990 to 2018 on the hydrology of the complex river catchment, the Drava basin, where human interference has led to a critical environmental situation. The results show that the coupled model significantly improves the overall simulation of water balance including groundwater conditions under the effect of LULC changes.

6.1 Introduction

LULC changes are among the major human interventions altering the regional hydrological cycle and the groundwater flow systems (Calder, 1993). Changes in the water regimes of rivers are predicted to be damaging to these ecosystems under extensive human pressure, exploitation, and pollution. Intensive human exploitation of land resources throughout the entire human history leads to significant changes of LULC (Bronstert, 2004). Groundwater system is an important part of the regional hydrological cycle, and it has been strongly affected by LULC changes (Alley et al., 1999; Calow et al., 1997). Moreover, the water balance components (i.e., groundwater recharge, actual

evapotranspiration, and surface runoff) respond differently to LULC classes according to soil texture and climate conditions (Han et al., 2017).

More specifically, the lower section of the Drava floodplain is substantially impacted by diverse human activities and the provision of ecosystem services has declined. Therefore, managers need to know and understand how land-use decisions and allocation will affect the flow of water to protect and improve water resources generally, and groundwater in particular, (Brauman et al., 2012). Hence, the spatial distribution of groundwater recharge for areas with different soil texture types affected by LULC is considered essential for both planners and stakeholders to estimate the sustainable yields of groundwater systems (Sophocleous, 2005) and to reach sustainable and efficient management of water resources in the Drava floodplain.

6.2 Integrated surface water- groundwater models

A physically-based WetSpass model simulates only the surface processes based on topography, slope, soil type, land cover/land use, and climatological conditions (Batelaan and Woldeamlak, 2007). It does not consider a two-way exchange between surface processes and groundwater, ignores run-on/runoff dynamics in recharge contribution. On the other hand, MODFLOW simulates flow processes occurring in the saturated zone defined by three-dimensional cells and the hydrogeological properties. MODFLOW use a finite difference approach to solve the groundwater flow differential equation, and integrates groundwater systems with other hydrological sub-system components (e.g. surface drainage, vadose zone, transport phenomena, etc.) through the incorporation of 'packages' using a gridded spatial discretization. However, it does not directly account for hydrologic processes that occur on the surface or in the root zone.

For that reason, most recent research focuses on the development and application of integrated models that handling surface-groundwater interactions. The key goal of model integration is to bridge the multi-disciplinary knowledge gap to support the quantitative ability to accurately assess hypotheses and system response under dynamic scenarios (Arnold, 2013). Therefore, an integrated WetSpass-M and MODFLOW is

essential to better represent feedback fluxes spatially within the surface and groundwater domains. This will improve simulation of the effects of long-term stressors, such as climate change, and LULC change. This chapter demonstrates the coupling of WetSpass and MODFLOW to assesses the impacts of LULC changes on the hydrology of the Drava river floodplain.

6.3 Materials and Methods

6.3.1 Study Area

The study area is presented in Chapter 5.

6.3.2 LULC Data

Land use and land cover patterns of the Drava basin for years 1990, 2000, 2006, 2012, and 2018 are obtained from the CORINE database for Land Cover (CLC (1990), CLC (2000), CLC (2006), CLC (2012) and CLC (2018)). As depicted in Figure B1, around half of the total area is under agriculture use, which is scattered over the whole floodplain. Agricultural areas are dominated by arable land (cereals and row crops). The extension of grassland (grazing land, meadow) is limited since animal husbandry has declined in the region. Forest areas are composed of coniferous forest, deciduous forest, and mixed forest with the dominance of deciduous forest. Coniferous forests are found in the southern part of the floodplain, while deciduous forests show a scattered pattern (Figure B1). A comparison of LULC maps for the years 1990, 2000, 2006, 2012, and 2018 shows that the major changes observed in six LULC classes: Agriculture, forest, willow-poplar shrubs, urban, meadow, and mudflat during 1990 - 2018 (Figure 6-1). The proportional extent of forest and mudflat and willow-poplar shrubs increased from 24 % to 27 % and from 5.8 % to 8.1 %, respectively, from 1990 to 2000 while they decreased to 24.0 % and 7.0 %, respectively, in 2012 and then they increased to 28.1 % and 12.4 %, respectively, in 2018 (Figure 6-1). Arable land-areas gradually decreased from 56.3

% to 43.7 % from 1990 to 2018. Built-up areas were relatively stable between 2000 and 2012 while they increased from 3.2 % to 6.1 % between 2012 and 2018 (Figure 6-1). The extent of meadows decreased by 3.2 % and 3.1 % between LCLU in 1990-2000 and 2012 – 2018, respectively (Figure 6-1). The expansion of forests and mudflats occurred at the expense of arable land and meadow areas. Moreover, herbaceous vegetation is replaced gradually by willow and poplar shrubs (Salem et al., 2022).

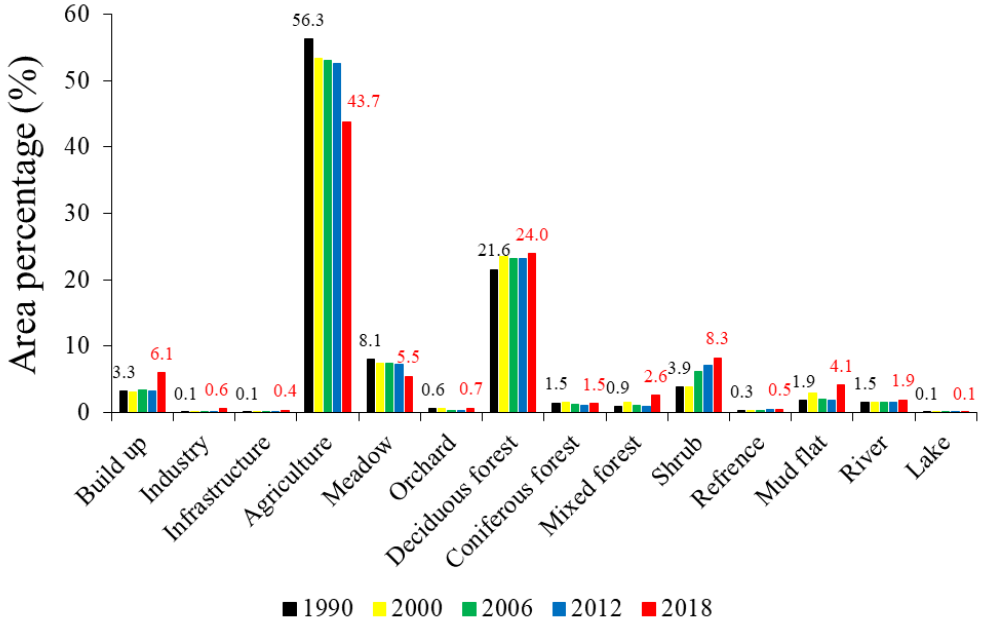

Figure 6-1: Area percentage of LULC classes in 1990, 2000, 2006, 2012, and 2018

6.3.2.1Assessment of CORINE Land Cover (CLC)

The European CORINE Land Cover (CLC) mapping scheme is a project managed by the European Environment Agency. The CLC inventory was initiated in 1985, and updates have been issued in 2000, 2006, 2012, and 2018. The standard CLC nomenclature comprises of 44 land cover classes. These are classified in a three-level hierarchy. The first level consists of five main classes: 1) agricultural areas, 2) artificial surfaces, 3) wetlands, 4) forests and semi-natural areas, 5) water bodies (Heymann et al., 2014), the second level consists of 15 headings and the third, most detailed, level includes 44 thematic classes (Feranec et al., 2007). The satellite imagery, from which CLC vector layers were drawn, consists of single date LANDSAT 5 MSS/TM (for

CLC1990 LANDSAT -7 Enhanced Thematic Mapper (ETM)ETM (for CLC (2000)), SPOT-4/5 and IRS P6 LISS III imagery (for CLC (2006)), IRS P6 LISS III and RapidEye (for CLC (2012)), and lastly, Sentinel 2 and LANDSAT 8, for CLC (2018) (CORINE Land Cover, 2020). CORINE provides a European scale map at 1:100,000, with a minimum mapping unit (MMU = 25 ha) for areal phenomena, 5 ha for change in land cover every six years (Kallimanis and Koutsias, 2013), minimum width of linear phenomena (MMW = 100 m) and thematic accuracy is higher than 85%. Those technical parameters are regarded as suitable for national or regional studies (Falťan et al., 2020). However, the CLC database has a particular limitation in spatial resolution. It has become the primary spatial data source on land for EEA. CLC is widely applied for environmental modeling, indicator development, and land use land cover change analysis in the European context (Büttner, 2014).

CLC is considered one of the most important sources of the land cover database from a European perspective attributed to its applicability to large regions and the comparability of the landscape dynamics development of various landscape types (Falťan et al., 2020). The Corine Land Cover program is a reliable source for assessing the effects of human activities on the Natura 2000 protected sites (Ursu et al., 2020). The Lucas survey (2003) used Eurostat LUCAS data for the reinterpretation of IMAGE2000 around LUCAS sampling points and automatic comparison of CLC (2000) codes with LUCAS land use and land cover codes to validate CLC (2000). Their results showed that the overall reliability of CLC (2000)was 87 % and 74.8 % for the reinterpretation approach and automatic comparison, respectively. The CLC (2000) and CLC (2006) database was validated using stratified random sampling through the re-interpretation of Google Earth imagery for IMAGE2000 and IMAGE2006. 17 of the 25 change type groups showed accuracy higher than 85 %, 13 types of which had an accuracy higher than 90 %, including the largest level change class (Büttner, 2014).

6.3.3 WetSpass-MODFLOW coupling

WetSpass model is basically limited in terms of dealing with groundwater flow because of its lumped nature. On the other hand, MODFLOW has difficulty in determining the distributed evapotranspiration and groundwater recharge that are the main input for the groundwater model. Consequently, it is promising that the hydrological variables are realistically computed if a WetSpass-based evapotranspiration and groundwater recharge are applied for input data in MODFLOW and the groundwater level is determined and exchanged to WetSpass, then the spatiotemporal features in the investigated area will be appropriately represented. In this study, the coupled WetSpass-MODFLOW framework links calibrated hydrological modeling (WetSpass-M) in Chapter Four with calibrated groundwater flow model (MODFLOW-NWT) in Chapter Five, applying ModelMuse as a graphical user interface, as shown in Figure 6-2. In this framework, WetSpass simulates water balance components. Meanwhile, MODFLOW-NWT simulates three-dimensional groundwater flow and all associated sources and sinks (e.g. recharge, discharge to drains, interaction with lakes, and interaction with stream networks). Using this approach, the outputs of the WetSpass-M model were used as inputs to MODFLOW-NWT. MODFLLOW- NWT computes groundwater hydraulic head and groundwater-surface water interactions, which are passed to WetSpass. Such a coupled model was applied to assess the impacts of changing LULC on the hydrology (water balance components, water budget of the system, and groundwater level) of the Drava floodplain.

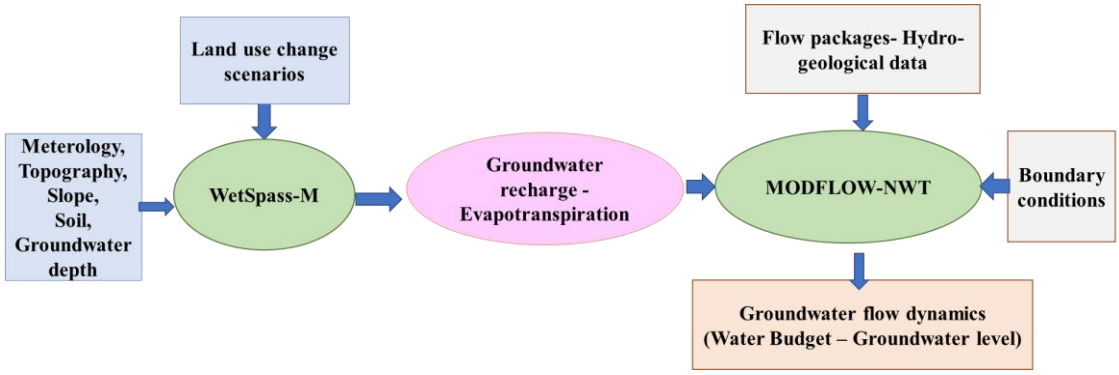

Figure 6-2: Adopted modeling framework

We launched five different runs, each corresponding to one LULC map from the years 1990, 2000, 2006, 2012, and 2018, respectively. To isolate, and yet capture, the effect of LULC changes, other input parameters such as meteorological data, topography (DEM and slope), distributed groundwater depth, and soil types were kept constant among the five runs. For the simulation meteorological variables for the period 2010-2018 was used as climate input, as well as the DEM, slope and soil of the study area for all the five runs. Each run simulated the long-term average water balance components in the 9 years from 2000 to 2018 (223 time steps).

6.4 Results and discussion

6.4.1 Impacts of LULC changes on water balance components

The simulated annual average water balance of Drava floodplain for each LULC maps of the years 1990, 2000, 2006, 2012, and 2018 is presented in Figure 6-3. For the LULC base scenario in 1990, groundwater recharge accounts for 48% of annual precipitation (688 mm yr^{-1}). It mainly takes place during the winter half-year. Both evapotranspiration and surface runoff amount to 26% of the total annual precipitation. Almost 89% of evapotranspiration occurs in the summer half-year. The statistical analysis (minimum, maximum, average, standard deviation) for LULC of 1990, 2000, 2006, 2012, and 2018 is presented in Table 6-1. Compared to LULC in 1990, the average annual groundwater recharge over the floodplain is 8 mm lower in 2000, 4 mm higher in 2006, 6 mm higher in 2012, and 8 mm lower in 2018 (Figure 6-3). Similar to groundwater recharge, average annual surface runoff decreased from 182 mm for LULC in year 1990 to 177 mm for LULC in 2000 and surface runoff values for LULC in 2006 and 2012 were similar to that in 1990 (Figure 6-3). For LULC in 2018, average annual surface runoff increased by 8 mm yr^{-1} with respect to LULC in 2012. In contrast, the average annual actual evapotranspiration for LULC in 2000 was 19 mm higher than that in 1990 but evapotranspiration for LULC in 2006 and 2012 decreased by 4 mm and 11 mm, respectively compared with LULC in 1990 (Figure 6-3). The average annual actual

evapotranspiration increased from 169 mm with LULC in 2012 to 192 mm with LULC in 2018 (Figure 6-3). The spatial distribution of water balance components for the current scenario 2018 is presented in Figure B2 of the appendix.

Table 6-1: The statistical analysis (min, max, average, standard deviation) for LULC scenarios of 1990, 2000, 2006, 2012, and 2018

Scenario	Value	Recharge (mm)	Runoff (mm)	Evapotranspiration (mm)
	Min-Max	0-533	80-680	50-1393
Land-use 1990	**Average**	325	183	180
	Std. dev.	100	70	140
	Min-Max	0-533	42-756	79-1435
Land-use 2000	**Average**	317	177	200
	Std. dev.	100	80	159
	Min-Max	0-533	80-680	50-1393
Land-use 2006	**Average**	329	182	177
	Std. dev.	100	71	142
	Min-Max	0-533	80-680	49-1393
Land-use 2012	**Average**	333	180	169
	Std. dev.	100	71	138
	Min-Max	0-533	80-680	50-1393
Land-use 2018	**Average**	317	189	192
	Std. dev.	106	80	170

The variability of surface runoff matches the trend of changes in LULC. As shown in Figure 6-1 and Figure 6-3, the decrease in surface runoff from 1990 and 2000 matches the decrease of built-up areas in this period. The comparison of changes in surface runoff and LULC maps indicates that the increase of average annual surface runoff by 9 mm yr^{-1} can be attributed to built-up areas (sealed surface) expansion between 2012 and 2018. These areas are characterized by a partially or fully impervious surface and were considered as having a negative impact on the Drava floodplain. Changes in built-up

areas were observed as the primary contributors for the change of surface runoff from 1990 to 2018.

The comparison between changes in actual evapotranspiration and groundwater recharge and LULC changes indicated that changes of forest, willow - poplar shrubs, mudflat, meadow and arable land were the strongest contributor to modified recharge and evapotranspiration, suggesting that the primary increase of evapotranspiration and decrease of recharge can be attributed to the increase of forest, willow-poplar shrubs and mudflats and decrease of meadow areas and arable lands from 1990 to 2000 and 2012 to 2018 in the Drava floodplain. The replacement of arable and meadow lands by forest, mudflats, with expanding willow shrub areas was identified as the strongest contributor to the major increase in evapotranspiration by 19 and 23 mm yr^{-1} and a decrease in groundwater recharge by 8 and 16 mm yr^{-1} between LCLU in 1990-2000 and 2012 – 2018, respectively (Figure 6-3). Conversely, from 2000 to 2012, the decrease of forest areas by 3% (27 % - 24 %), mudflat and shrubs areas from by 1.1% (8.1%-7.0%), with expanding meadow areas by 2.7% (5.9%-8.6 %) (Figure 6-1) contributed to the major decrease in evapotranspiration by 31mm yr^{-1} and an increase in groundwater recharge by 16 mm yr^{-1} (Figure 6-3).

Unlike arable lands, riparian willow shrubs have permanent access to shallow soil water and groundwater system (Doody et al., 2006; Yin et al., 2014), increasing total leaf area of the canopy, evaporative, and transpiration losses (Doody et al., 2006; Marttila et al., 2018). This property of willow shrubs resulted in less water recharged. Indeed, mudflat areas are seasonally inundated by the river and have high groundwater levels, which enhanced transpiration and resulted in changes in the water balance of the floodplain by reducing groundwater recharge and increasing evapotranspiration. Moreover, urbanization leads to a decrease in groundwater recharge. Because of low groundwater and high drought hazard ecosystem services are provided at a lower level, and agricultural productivity is reduced because of the water deficit. Thus, the ecosystem services and agricultural productivity in the Drava floodplain reached a critical situation and, hence, human activities have a net negative effect on groundwater recharge in the

floodplain. Thus, understanding the spatial distribution of groundwater recharge changes is crucial for water resources management in the Drava floodplain.

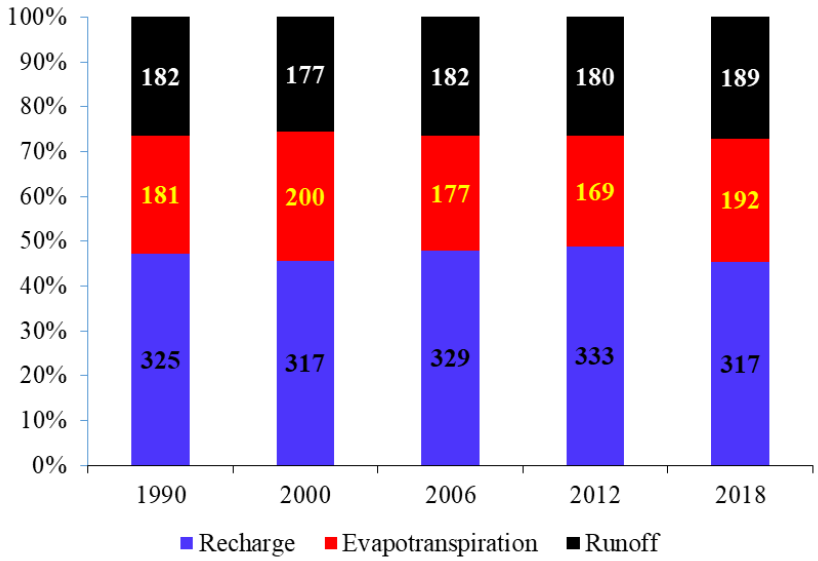

Figure 6-3: Average yearly water balance components for the Drava floodplain from 1990-2018 (values are in mm yr^{-1})

6.4.1.1 Impacts of LULC changes on groundwater recharge

Minimum, maximum, average, and standard deviation percentages of change in groundwater recharge of the simulated LULC scenarios (2000, 2006, 2012, and 2018) with respect to the base year 1990 are presented in Table 6-2. The range of change in groundwater recharge between 1990 and 2000 was from -100% to 256.8%, respectively, with a mean decrease of -2.5% (Table 6-2). In the period 1990–2006, groundwater recharge slightly increased by 1.3% on average (Table 6-2). The average increase in groundwater recharge was 2.4% during the period 1990-2012 (Table 6-2). The difference in groundwater recharge which occurred between the year 1990 and the year 2018 ranged from -100% to 289.7% with an average decrease of -2.6%. The spatial distribution of the change in simulated groundwater recharge for the LULC scenarios is shown in Figure B3 of the appendix.

Table 6-2: Minimum, maximum, average, and standard deviation values of the change in groundwater recharge in % of the simulated LULC scenarios (2000, 2006, 2012, and 2018) with respect to the base LULC in1990

	Change in groundwater recharge			
	2000 - 1990	**2006 - 1990**	**2012 - 1990**	**2018 - 1990**
		%		
Minimum	-100	-100	-100	-100
Maximum	256.8	273.6	273.6	289.7
Average	-2.5	1.3	2.4	-2.6

We also investigated the change in groundwater recharge in the following period with an interval of 6 years. In a period from 2000 to 2006, the change in groundwater recharge varied from a minimum of -72% to a maximum of 126% with an average value of 4% and a standard deviation of 8% (Figure 6-4a). This variation of groundwater recharge is associated with changes in arable lands, mudflat, forest, and meadow. A small variation in groundwater recharge was observed during the period 2006–2012 with an average ratio of 1% due to small changes in LULC for this period. Groundwater recharge decreased from 2012 to 2018 (Figure 6-4b). As depicted in Figure 6-4c, the simulated changes in groundwater recharge showed a large variation between -100% and 256%, at a pixel scale, with an average value of -5% and a standard deviation of 28%. This means that the total annual groundwater recharge decreased by 5.3×10^{7} m^{3} with respect to LULC in 2012. This reduction in groundwater recharge is associated with the expansion of built-up areas, forest, mudflat, and growing of willow shrubs with shrinkage of agriculture areas. The results clearly indicate that LULC changes affect the overall water budget of the floodplain.

a) **b)**

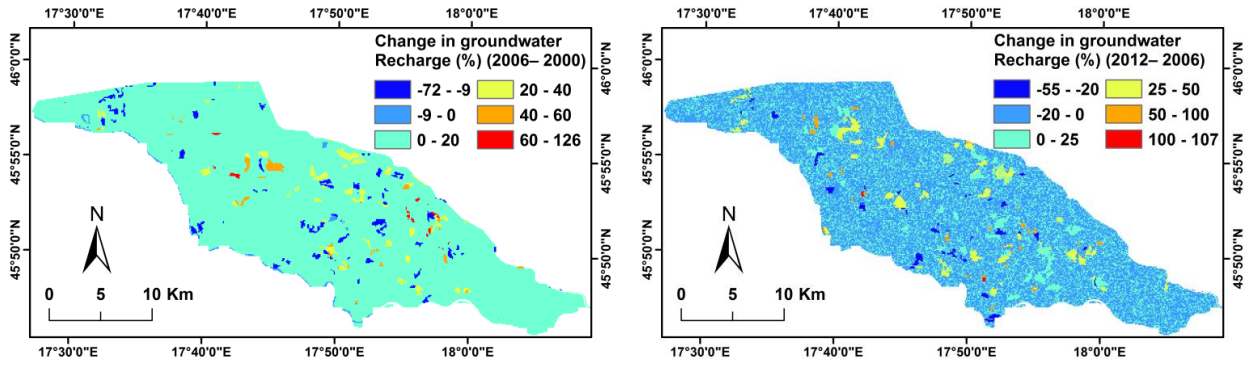

c)

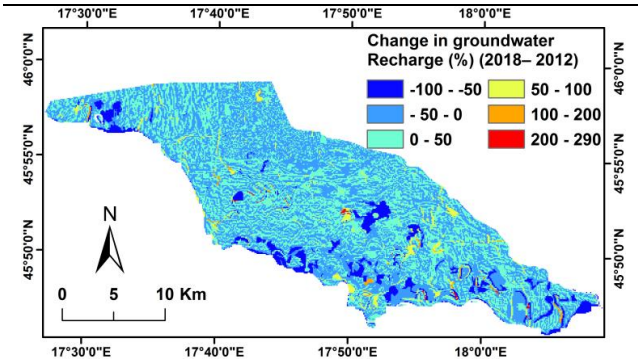

Figure 6-4: Change in groundwater recharge: a) 2006 – 2000; b) 2012 – 2006; c) 2018 – 2012

6.4.2 Water Balance components under different LULC and soil textures

LULC changes from 1990 to 2018 are considered the major factor contributing to the spatial variation of groundwater recharge, actual evapotranspiration, and surface runoff in the Drava floodplain. To quantify these impacts, we assessed water balance components under different LULC classes. Figure 6-5 shows the average annual groundwater recharge, runoff, and actual evapotranspiration, as a function of LULC classes under LULC of 2018 in the Drava floodplain. Groundwater recharge, actual evapotranspiration, and surface runoff are strongly dependent on LULC. Agricultural land comprises 44 % of the Drava floodplain and it is scattered over the investigated area. Deciduous forest covers 24% of the total area of the floodplain. Mudflats (deeper lying areas which are seasonally inundated by the river and have high groundwater levels) and forests show high average actual evapotranspiration by 499 and 322 mm yr^{-1}, respectively, while they have average groundwater recharges of 133 and 251 mm yr^{-1}, respectively (Figure 6-5). Groundwater recharge is assigned to a value of zero for open water surfaces (i.e., rivers and lakes) in the WetSpass-M model since the open water surfaces are assumed to be groundwater discharge locations (Singhal and Gupta, 2010). Similar to a study of the southern Moravian floodplain forest (Čermák and Prax, 2001), forest areas are characterized by high actual evapotranspiration with an average of 322 mm yr^{-1}. The coniferous forest has the lowest surface runoff with an average of 130 mm yr^{-1}. Built-up areas show a low groundwater recharge and actual evapotranspiration with

an average of 204 and 231 mm yr^{-1}, respectively, as these areas are characterized by a partially or fully impervious surface.

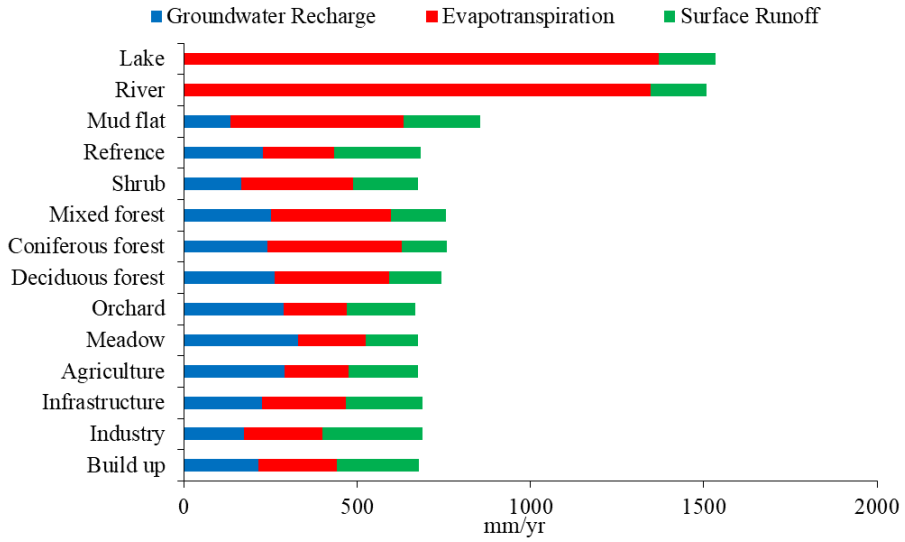

Figure 6-5: Average annual groundwater recharge, surface runoff, and evapotranspiration as a function of LULC in 2018

Figure 6-6 presents the water balance components for 2018 as a function of different soil textures in the Drava floodplain. The spatial variability of soil types comes from fluvial land features and strongly influence local/regional hydraulic properties (Dezső et al., 2019). Hydraulic conductivity, porosity, specific yield, and capillarity depend on textural properties. For the light soil texture, sandy soils of natural levees show the highest average annual groundwater recharge rate because of their high conductivity, while heavy soils (clay) in the swales between point bar ridges have the lowest rate of 210 mm yr^{-1}. The simulated average annual recharge of the sandy soil is 343 mm yr^{-1} (Figure 6-6). Clearly, the groundwater recharge values for sandy loam, loam, and clay loam fall between the values for sand and clay soils. Evaporation strongly depends on the depth of the groundwater table, which is within 1 m in the study area. Heavy soils (clay and clay loam) in abandoned river channels and the riparian zone have the highest evapotranspiration and surface runoff as they are located in the deepest morphological position with shallow groundwater and intensive capillary rise. In contrast, sand and sandy loam soils have the lowest surface runoff. The WetSpass-M model indicates the average annual actual evapotranspiration of soils of clay texture to

be 235 mm yr^{-1} while the simulated average annual surface runoff of sandy soils is 160 mm yr^{-1} (Figure 6-6).

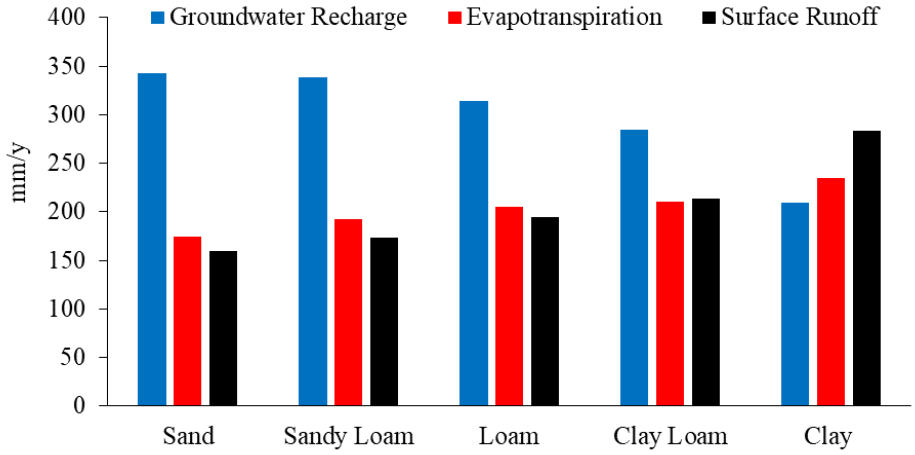

Figure 6-6: Average annual groundwater recharge, evapotranspiration, and runoff as a function of soil texture for LULC in 2018

This study shows that water balance components have been influenced by both soil texture and LULC classes. Table 6-3 presents the average annual groundwater recharge (mm) across different combinations of land-use and soil types to assess the spatial variations of the groundwater recharge as a function of LULC class and soil textures in the Drava floodplain. A higher groundwater recharge was observed in forest and arable areas with sandy soils due to the high permeability of sandy textured soil. On the contrary, areas predominantly with clay and clay loam soils showed a lower amount of groundwater recharge because of the less permeability and shallow groundwater system of such soils. The highest average groundwater recharge of 411 mm was accounted to forest areas with sandy soil type while mudflat land with clay soils show the lowest average groundwater recharge of 123 mm followed by built-up areas (Table 6-3). The results indicated that groundwater recharge was more effected by land-use than soil type as the standard deviation of the groundwater recharge for the different land-use classes is higher than the standard deviation of groundwater recharge for the different soil textures (Table 6-3).

Groundwater recharge variability with soil textures and LULC classes similar to the present findings have been reported for the Guishui River Basin, China by Pan et al. (2011), for the upper San Pedro watershed, Mexico and USA, by Nie et al. (2011), for

Flanders (Belgium) by Zomlot et al. (2015) and a catchment in northern Ethiopia by Kahsay et al. (2019) and Gebru and Tesfahunegn (2020). A higher evapotranspiration rate was observed in sites where the predominant cover is water body, mudflat, grassland, and forest with clay loam and clay soils that could be due to the high transpiration demand of vegetation cover and water availability of soil type (Table B2 in the appendix B). Similar findings of the influences of LULC and soil texture on evapotranspiration variability were reported by Graf and Przybyłek (2014), Singh et al. (2013), Zomlot et al. (2015), and Kahsay et al. (2019). The largest amount of surface runoff was detected in built-up areas with clay soil texture characterized by lower infiltration capacity, while sand and sandy loam soils with forest, meadow, orchard, and shrubland land use have the lowest amount of surface runoff because of their high permeability (Table B2 in the appendix). Moreover, the present results indicated that LULC variability affects more the spatial variability of surface runoff than the effect of soil type in the study area. Zhang et al. (2017), Kahsay et al. (2019), and Gebru and Tesfahunegn (2020) have reported similar results of the impacts of soil texture and LULC classes on surface runoff variability.

Table 6-3: Average annual groundwater recharge across different combinations of soil texture and LULC in 2018

	Soil texture						
LULC classes	**Sand**	**Sandy Loam**	**Loam**	**Clay Loam**	**Clay**	**Average**	**St.dev**
Build up	231	208	197	181	149	193	27
Industry	184	177	162	149	126	159	21
Infrastructure	275	-	218	195	157	211	43
Agriculture	344	297	279	245	190	271	52
Meadow	393	340	319	266	206	305	64
Orchard	366	-	306	270	210	288	57

Deciduous forest	302	272	255	240	235	261	24
Coniferous forest	250	-	232	-	-	241	9
Mixed forest	284	261	241	236	230	250	20
Shrub	139	161	167	180	183	166	16
Reference		-	276		180	228	48
Mud flat	143	127	123	116	94	121	16
River	0	0	0	0	0	0	0
Lake	-	-	0	-	-	0	0
Average	243	205	198	189	163		
St.dev	107	97	97	76	63		

-, (no value) as there is no such LULC for a given soil texture

6.4.3 Impacts of impervious cover changes on water balance components

The share of built-up areas in the Drava floodplain did not change considerably between 1990 and 2012. From 2012 to 2018, the built-up areas increased from 3.2% to 6.1%, mostly converting from arable land, thus, change in recharge, evapotranspiration, and surface runoff under built-up areas for this period were assessed to reveal the impacts of urbanization on water balance (Table 6-4). Both evapotranspiration and surface runoff presented increasing trends while groundwater recharge decreased from 2012 to 2018. Under built-up areas, the annual average groundwater recharge had the maximum variation rate with –10%, while the variation rates for annual average evapotranspiration and surface runoff were +7% and +6%, respectively, from 2012 to 2018.

Table 6-4: Annual water balance components in the Drava floodplain under built-up areas from 2012 to 2018

Parameter	Value	Recharge mm yr^{--1}	Evapotranspiration mm yr^{--1}	Surface runoff mm yr^{--1}
2012	**Range**	137 - 358	133-383	158 - 301
	Average	214	211	249
	Standard deviation	53	22	37
2018	**Range**	133 - 218	211 - 260	232 - 328
	Average	193	227	263
	Standard deviation	21	13	20
Variation		- 10 %	+ 7 %	+ 6 %

6.4.4 Effect of LULC changes on groundwater quantity and average groundwater level

To assess the impacts of the LULC changes on groundwater quantity, a groundwater flow model for each of the years (1990, 2000, 2006, 2012, and 2018) was built using the WetSpass-M results of groundwater recharge and evapotranspiration. The water balance components for simulated LULC scenarios are shown in Table 6-5. Aquifer recharge from precipitation, recharge from the rivers to the aquifer, discharge from the aquifer to river, evapotranspiration, inflow and outflow through, and changes in groundwater levels compared to the base scenario (1990) were used as indicators to quantify the impact of LULC changes on the water budget of the Drava floodplain. The spatial distribution effect of the LULC change (1990-2018) on the groundwater level of the floodplain for all scenarios with regard to the base case (1990) is presented in Figure 6-7.

Table 6-5: Water balance components (in m^3 d^{-1}) and changes in average groundwater level with respect to the base case (in m)

Scenario	Inflow through GHB boundary	Outflow through GHB boundary	Discharge from aquifer to river	Aquifer recharge from rivers	Aquifer recharge from precipitation	Evapo – transpiration	Average change in GW level (m)
1990	812,061	293,247	1,482,103	498,063	550,555	83,287	0.0
2000	812,977	292,507	1,469,941	499,736	536,821	86,139	- 0.04
2006	812,396	293,948	1,488,173	497,428	557,846	83,557	0.02
2012	812,235	294,675	1,494,416	496,679	563,799	81,612	0.06
2018	813,408	294,696	1,472,552	502,269	538,317	84,095	-0.04

The results clearly reveal a cycle of rising and falling averages of groundwater level for the different scenarios of LULC changes of the floodplain. The variations in groundwater recharge, evapotranspiration, and groundwater level were associated with changes in LULC classes. Compared to LULC in 1990, in 2000 the recharge rate from precipitation to aquifer decreased by 13,743 m^3 d^{-1}, while actual evapotranspiration increased by 2,852 m^3 d^{-1} (Table 6-5). Consequently, the average groundwater level decreased by 0.04 m (in Figure 6-7a). With respect to the scenario of year 2006, the recharge rate from precipitation to aquifer increased by 443,869 m^3 d^{-1} (Table 6-5), while the spatial distribution of change in groundwater level ranged from 2.1 m to -3.7 m with an average rise of 0.02 m compared to LULC in 1990 (in Figure 6-7b). Regarding the scenario for 2012, the simulated change in groundwater level ranged from -2.6 m to 1.9 m with a mean value of 0.06 m compared to the base scenario (in Figure 6-7c). In the 2018 scenario, the groundwater recharge from precipitation dropped by 25,482 m^3 d^{-1} and the evapotranspiration increased by 2483 m^3 d^{-1} with respect to scenario 2012 (Table 6-5). Thus, the lower amount of groundwater recharge and higher value of evapotranspiration for the current scenario (2018) led to average groundwater levels reduced by -0.1 m over this period. The simulated change in groundwater levels showed a large variation between -2 m and 5.4 m, with a mean decrease of -0.04 m between 2018 and the base case 1990 (in Figure 6-7d). Dropping groundwater levels reduced the

variety of crops which could be grown in the Drava floodplain and thus reduced the profitability of agriculture. At the same time, the water supply of nature conservation areas also became insufficient.

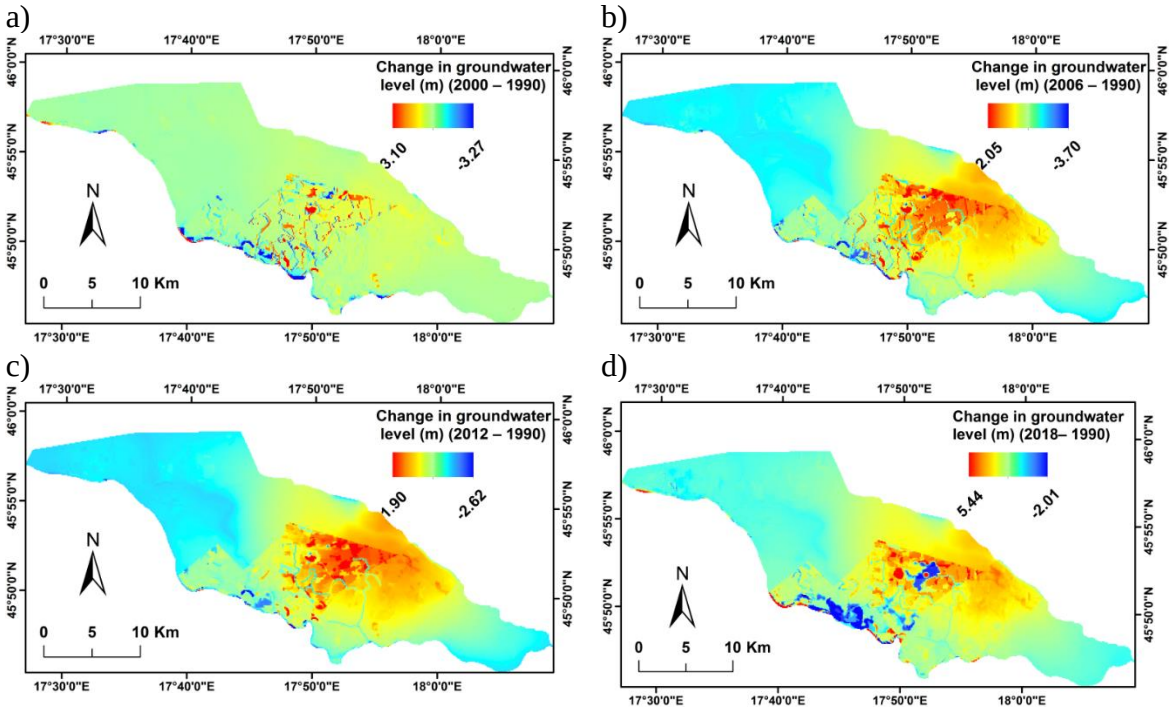

Figure 6-7: Change in groundwater level of the simulated LULC scenarios with respect to the base case (1990): a) 2000 – 1990; b) 2006 – 1990; c) 2012 – 1990; and d) 2018 – 1990

6.5 Summary

In this chapter, an integrated framework model which couples the water balance model (WetSpass-M) with the groundwater flow model (MODFLOW-NWT) is developed to assess the spatial distribution and the range of LULC change impacts on the hydrology of the Drava River basin. The interactions between natural hydrological processes and changes in energy fluxes, water, and storage attributable to human interventions are essential for water resources managers for the understanding of how these systems might respond to LULC change among other drivers for change. LULC change either has a positive or a negative effect on water balance components. . The results showed that water balance components have been influenced by both soil texture and LULC classes. Moreover, LULC changes have a direct effect on groundwater

recharge and the provision of floodplain ecosystem services. The coupled model proved to be a valuable assessment tool for assessing the impacts of long-term stressors such as LULC changes. Decision-makers should take measures to minimize the negative effects of further LULC change: restricting surface sealing, encouraging the cultivation of crops with reduced water demand on arable land, preservation of grazing land and meadows, and checking their overgrowth with shrubs. The approach tested in this research allows temporal and spatial estimation of hydrological components under the changes of LULC, providing quantitative information for decision-makers to implement a sustainable management of water resources in the Drava floodplain.

CHAPTER Seven

7. RANDOMLY LAYERED FLUVIAL SEDIMENTS INFLUENCE GROUNDWATER-SURFACE WATER INTERACTION/ ASSESSMENT OF WATER REPLENISHMENT TO A FLOODPLAIN LAKE

For the rehabilitation measures (focusing on water replenishment to oxbows) with the purpose of enhancing ecosystem services, the detailed hydrogeological study of alluvial deposits and soils is indispensable. In this chapter, the investigation covers the area lying between the Cún-Szaporca oxbow lake system, under rehabilitation, and the Drava River, which controls groundwater flow. A 3-D groundwater flow model is developed for the Cún-Szaporca oxbow of the Drava floodplain to gain a better understanding of the water budget of the whole system through different fluvial sediment structures scenarios. The model was applied to investigate the exchange between surface flow (from river and lake) and aquifer under the normal situation and for different lake replenishment scenarios. The results may be inspiring in understanding subsurface water dynamics in the lake–river systems influenced by complex sediment structures.

7.1 INTRODUCTION

Floodplain/ channel connectivity is a decisive factor for supplying water to oxbow lakes and represents the main ecological requirement for floodplain restoration (Wren et al., 2008). Hydrologists warn that surface and subsurface water have to be regarded as actively communicating components of a single system (Winter et al., 1988). Alluvial sediments indicate an extreme degree of heterogeneity in the hydraulic properties of sediment (Miall, 2006). The exchange between the alluvial aquifer system and surface

water will be affected by the degree of subsurface heterogeneity (Woessner, 2000). Although many studies address the interaction between groundwater and surface water (Sophocleous, 2002; Rudnick et al., 2015; El-Rawy et al., 2016), the degree of subsurface heterogeneity for aquifer was rarely addressed. The multi-layered sediments are of crucial importance as geological background related to subsurface water dynamics. The knowledge of the role (in a hydrogeological sense) of these layers is limited. Obviously, the randomly layered geological units cause anisotropy. Their position and extension modify the velocity of subsurface flow.

To improve the water availability and land management of the floodplain, a large-scale landscape rehabilitation project, the Old Drava Programme (ODP), was launched in 2013. The main objective of the ODP (AQUAPROFIT, 2005), implemented by the Hungarian Government, is to provide a holistic approach to water policy along the Drava river floodplain depending on the nature conservation and sustainable management of lake ecosystems and land. In this project, one of the most important plans envisages water replenishment to oxbow lakes by raising their level from different sources. During the program hydrological structures (feeder canals, reservoirs, dams, and sluices) were constructed to achieve the set goals. The length of the feeder canal is 3.1 km and it has a capacity of 0.4 $m^3 s^{-1}$. The Fekete-víz reservoir has to be filled to a minimum level of 93.1 m to ensure gravitational flow from the canal to the level of the oxbow lake by at least 0.5% slope. Unfortunately, the ambitious plans often go wrong because they neglected the hydrogeological reality (Dezső et al., 2017) and did not take into account the clogging of the feeding canal bottom. The first replenishment took place in March 2016 and not more than a 20 cm increase in lake level has been achieved.

In this chapter, a groundwater model of the Cún-Szapora Lake is developed to assess the exchanges between surface water and groundwater at a critical part of this system under different hydrological conditions and to quantify the water budget and water retention, under different management scenarios of oxbow lake(s) replenishment to protect the wetland habitat and agricultural production.

7.2 Study area

To evaluate the potential river–lake-groundwater interactions and to assess the potential replenishment options, an abandoned meander of the Drava of 257 ha total area (the Cún-Szaporca oxbow) was selected as a case study (including ca 140 ha of oxbow lakes,). The meander was partially cut off from the new Drava channel during the first stage of channelization between 1842 and 1846 (Dezső et al., 2015). In a period of drought summer, the Cún-Szaporca oxbow system separated into five lakes. The study area is Lake Kisinc which is the largest oxbow lake of 20 ha area, with a maximum water depth of 2.4 m and an average water depth of 1.12 m (DDKÖVÍZIG, 2012) (Figure 7-1). The width of the semi-natural riparian zone of the oxbow lakes is merely 10-20 m. This wetland area is part of the Danube-Drava National Park and is registered as a Ramsar Convention site.

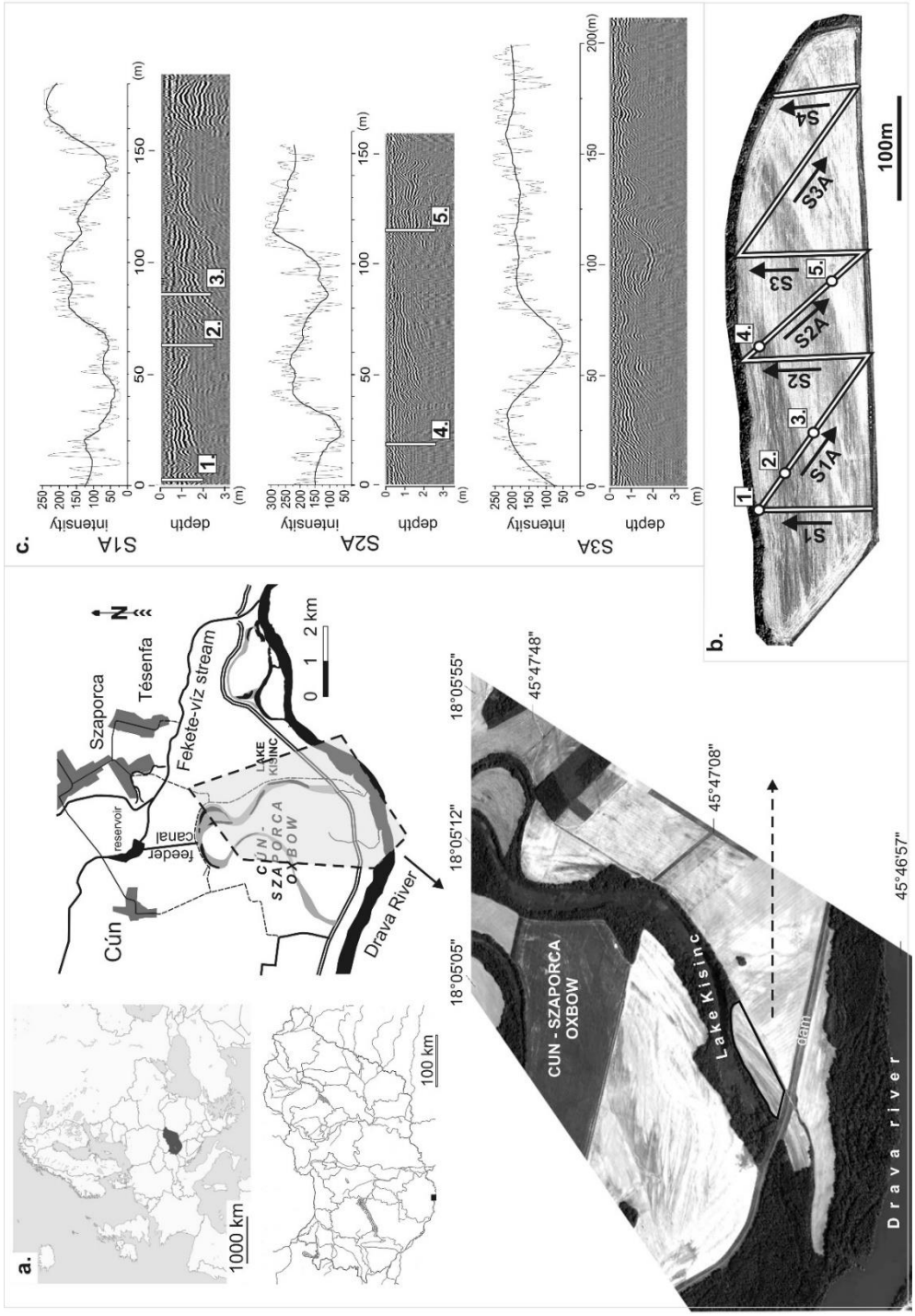

Figure 7-1: a) Location of the research area with case study (sub)area; b) direction and codes of GPR records, augering sites in the case study area, c) the sections of three important GPR records appended the result of the satellite image analyses

7.3 Methodology

7.3.1 Holistic investigation of sediment sequences

Pedo- and sediment diversity was characterized by satellite images, Ground Penetrating Radar (GPR) survey (conducted by Marcin Słowik as a s part of a project 2016/23/B/ST10/01027 "Processes forming anabranching and meandering rivers: examples of selected rivers from Wielkopolska Lowland and Transdanubia" supported by the National Science Centre, Poland), and augering. First, morphological features were identified from satellite images (Google Earth). The images were transformed to 8bit type and evaluated using signal processing (smoothing) by Origin8 software. Fieldwork augering and GPR surveys were implemented to study the sediment layers in detail. Augering-based subsurface layering was compared with a GPR survey. Particle size analyses were performed using a Malvern MasterSizer 3000HS (Malvern Inc., Malvern, England, United Kingdom) particle size analyzer. The in situ investigation hydraulic conductivity of each augering was implemented by falling head method (Juhász, 2002). Pumping test results (Dezső et al., 2017) and borehole information were compared with GPR records (as depicted in Figure 7-1). Surface water (lake and river) groundwater interactions were characterized by subdued ridge-and-swale topography in the paleomeander systems. Albeit the area is topographically relatively uniform, borehole sampling and GPR records showed extreme heterogeneity in the hydraulic properties of sediments. It was found that the fluvial landforms of the area have four zones with different hydraulic conductivities. In situ saturated hydraulic conductivity for each borehole was measured using the fall head method (Landon et al., 2001) by using the following formula:

$$k = \frac{L}{(t_2 - t_1)} * ln\left(\frac{h_1}{h_2}\right) \quad (7.1)$$

where k is saturated hydraulic conductivity, L is the height of the soil core, t1 and t2 are initial and final times of the experiment, respectively, h1 and h2 are the

corresponding pressure heads. Geographic Information System (ArcGIS v10.3) was used to prepare the groundwater model data and to visualize the model outputs.

7.3.2 Groundwater flow model setup

The finite-difference code MODFLOW-2005 (McDonald and Harbaugh, 1988), with ModelMuse (Winston, 2009) as a pre-processor graphical user interface, was applied to simulate groundwater flow. The model was discretized with a finite-difference grid that consists of 60 rows, 14 columns, and 10 layers with a cell size of 10 m by 10 m and with a total of 8400 cells, out of which 6540 are active cells. The top boundary of the model was represented by a 10-meter resolution Digital Elevation Model (DEM). The eastern and western boundaries were assigned with constant head values (interpolation between 89.68 and 90.69 m) and (interpolation between 89.8 and 90.91 m), respectively, based on initial groundwater level (see Figure 7-2). The groundwater recharge was found to be $2.5E^{-05}$ m d^{-1} and the average daily evapotranspiration was estimated at 13 mm.

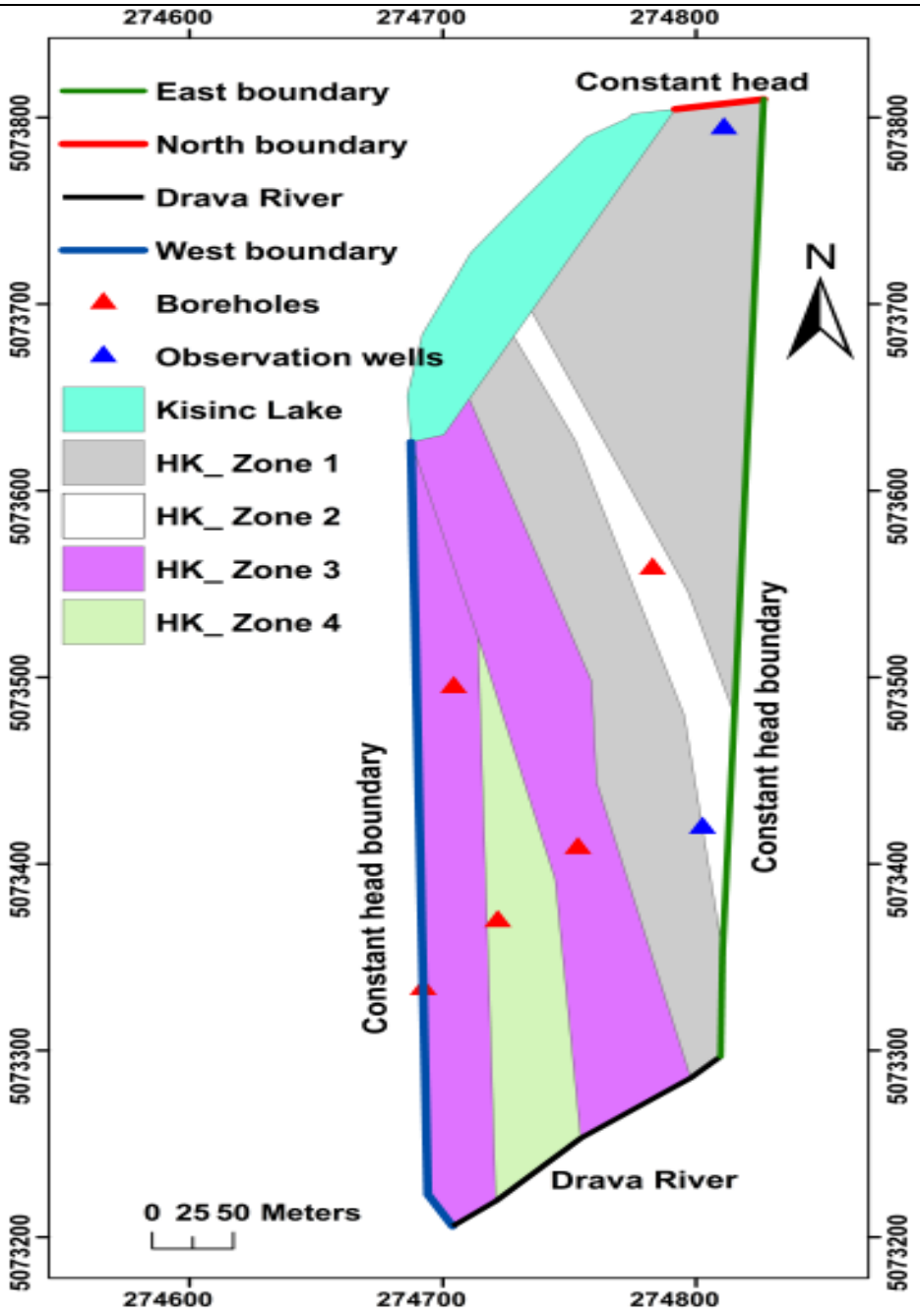

Figure 7-2: Hydraulic conductivity zonation, observation wells and the boundary conditions of the study area

7.3.3 Replenishment Scenarios

The baseline scenario represents the existing situation of the lake without replenishment, with water level at 90.5 m above sea level. This case is applied to

calibrate the steady-state model and to compare the results with replenishment scenarios. Two hydrological scenarios of lake envision replenishment by setting two different lake water levels.

7.4 Results and Discussion

7.4.1 Model calibration

The model is calibrated for steady state using data from 3 boreholes and 2 observation wells (see Figure 7-3). The calibrated recharge is $1.35E^{-05}$ m d^{-1}, the conductance of riverbed is 150 m^2 d^{-1} and the hydraulic conductivity of zone 1, zone 2, zone 3 and zone 4 are 6.75, 60, 6.75, 500 m d^{-1}, respectively. The results match with observed values with a correlation coefficient of R^2 = 0.94 as depicted in Figure 7-3. Mean error is 0.03 m, while the absolute mean error is 0.08 m. Moreover, simulated and observed heads are scattered around the mean values of observation heads which represent a reliable model.

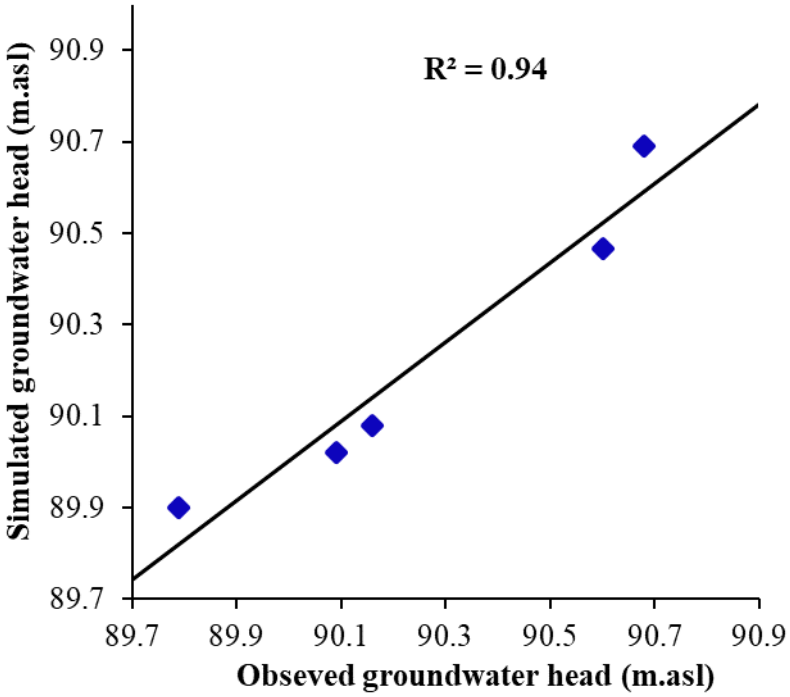

Figure 7-3: Scatter plot for simulated versus observed groundwater heads of steady states using five observation wells

7.4.2 Water Balance

Table 7-1shows the water balance of the calibrated model. The total amount of inflow from lake to aquifer is 891 m^3 d^{-1} which represents 37% of the total inflow to aquifer and groundwater recharge from precipitation is 0.85 m^3 d^{-1}. The water budget of the system showed the importance of replenishment of oxbow lakes as a source to recharge the aquifer and preserve the sustainability of groundwater. The total discharge from the aquifer to the river is 321.63 m^3 d^{-1} while evapotranspiration accounted for 223.95 m^3 d^{-1}. An amount of 1167.50 m^3 d^{-1} (or 48.87%) recharges the aquifer from the western boundary and 329.38 (only 13.79%) from the northern boundary. An amount of 1843.40 m^3 d^{-1} (77.16%) flows out the aquifer through the eastern boundary. This coincides with a real situation that flows come from northern western direction to the eastern direction.

Table 7-1: Water balance for the simulated steady-state model

	In		**Out**		**In-Out**
	(m^3 d^{-1})	**%**	**(m^3 d^{-1})**	**%**	**(m^3 d^{-1})**
Eastern Boundary	0.00	0.00	1843.4	77.16	-1843.4
Northern Boundary	329.38	13.79	0.00	0.00	329.38
Western Boundary	1167.50	48.87	0.00	0.00	1167.5
Lake	891.00	37.30	0.00	0.00	891.00
River	0.00	0.00	321.63	13.46	-321.63
Recharge	0.85	0.04	0.00	0.00	0.85
Evapotranspiration	0.00	0.00	223.95	9.38	-223.95
Total	2388.98	100	2388.98	100	0.00

7.4.3 Fluvial sediment structures scenarios

River–groundwater–lake interactions were identified in paleomeander systems with subdued ridge-and-swale topography. Albeit the area is topographically relatively uniform, field borehole sampling, GPR surveying, and model runs indicated extreme spatial heterogeneity in the hydraulic properties of sediments down to 10 m below fluvial landforms detected by remote sensing. Analyzing swales, it was found that darker (lower-intensity) units on the grayscale denote sedimentologically relatively homogeneous fine sandy–silty deposits, while the lighter colored units are characterized by the random alternation of loamy sand subunits of 20–50 cm thickness. The relatively homogeneous units are bordered by erosional features like vertical stackings, scour channel fills, or as coastal sediments of the river. They are intercalated with the previously mentioned layers with low (less than 10°) angles. From the aspect of the buildup of the model space, the relative positions of the two subunits are random, both for the case study and the entire floodplain.

Based on field observations, the hydrological scenarios are constructed in an ever more complex way as shown in Figure 7-4. Seepage from the lake into deeper layers and storage in sediments or occasionally percolation into deeper layers has also been analyzed (Table 7-2) The theory for creating our modeling space is that the generated (sub)structures which are characterized by different hydraulic properties and formed during sedimentation are analogous with fluvial features such as point bars, traces of lateral migration of river channel, and lateral accretion.

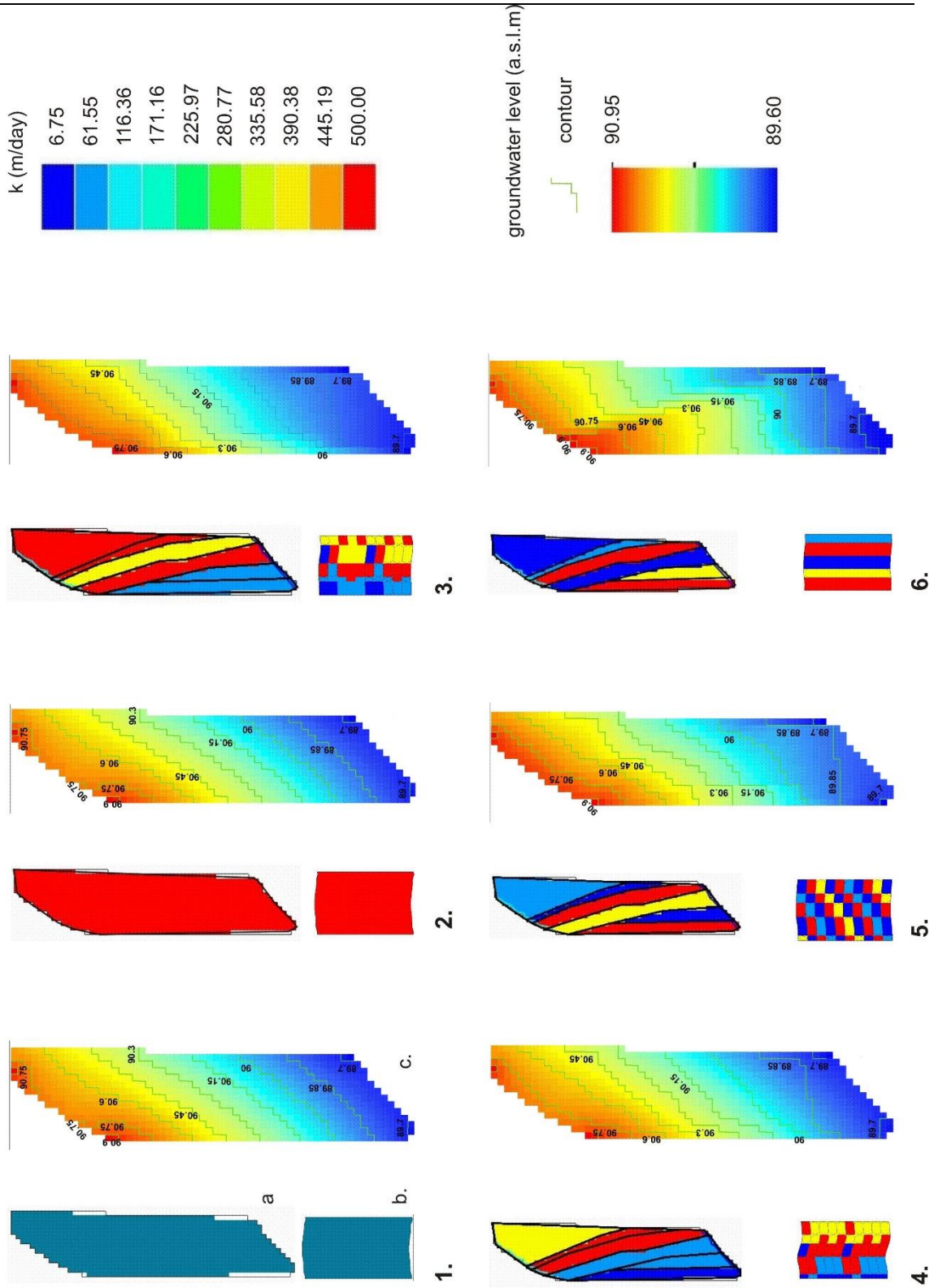

Figure 7-4: Result of six scenarios of modeling. Arrangement for each case: a) plan view; b) profile; c) distribution of groundwater level

Table 7-2: The result of seepage from the lake and recharge to the river for fluvial sediment structures scenarios

Case	Water loss from lake (m^3d^{-1})	Recharge to river (m^3d^{-1})	Description
1	344.29	176.34	Aquifer represented by one layer (loam k = 60 md^{-1})
2	1468.95	1477.15	Aquifer defined by one layer (sand k = 500 md^{-1})
3	1464.76	482.22	Aquifer characterized by multilayered zones for half of the aquifer and the same properties repeated for the second half
4	1425.45	250.98	Random pattern for variable zones defined half of the aquifer layers and this structure repeated for the second half
5	1464.96	512.29	Aquifer represented by 6 zones which distributed for every layer according to GPR records
6	347.79	707.74	On satellite images, 6 continuous zones from the first to the last layer represented the vertical discretization of the aquifer

The application of a simple structure was inadequate. Water loss in Case 1 is too low, in Case 2 seepage and recharge values are virtually identical, for which unreal rapid interaction should be assumed. Thus, the simplification of the sediment structure leads to an erroneous result. In Cases 3 and 4, the layering revealed by GPR was repeated. For this, it was assumed that sedimentation processes are periodically repeated during the alluviation of the floodplain. Water retention is calculated from the difference between seepage and recharge. The values received are now realistic.

The stepped arrangement in Case 5 represents the “vertical stacking” structure disclosed by GPR studies. The depicted water transfers are also realistic.

For Case 6 the surface structures revealed by satellite images were arranged vertically down to the bottom of the model space, disregarding the sediment structure reflected by the GPR investigation. The result was unrealistic.

7.4.4 Effect of model discretization

To study the effect of the model discretization, various models were built. Summary of the simulated model discretization scenarios, water balance components, and average groundwater level for every scenario are presented in Table 7-3.

Table 7-3: Water balance components compared to the base case situation

Case	Inflow through constant head boundary	outflow through constant head boundary	Aquifer recharge (from lake)	Discharge from aquifer to river	Evapo- transpira-tion	Aquifer recharge from precipitation	Average ground- water level
	m^3d^{-1}						
(1) Model defined by 6 zones and 10 layers in vertical discretization	1497.12	1843.39	891	321	223.95	0.85	90.26
(2) Model defined 6 zones and one layer for vertical discretization	496.41	4195.83	4382.0	412.49	271.23	0.84	90.3

(3) Model characterized by grid cell 5 m by 5 m	1910.10	2161.9	989.11	506.17	231.97	0.84	90.274

Contour lines of the simulated groundwater levels of the model discretization scenarios with the base case are shown in Figure 7-5. The results clearly pointed to a major effect on the groundwater levels and water balance between all scenarios. In case 2, the vertical discretization of the aquifer is characterized by one layer with average vertical hydraulic conductivity, disregarding the sediment structure that is reflected by the GPR survey. Water leakage from the lake increases by 3491 m^3 d^{-1} with respect to the first case, resulting in the average groundwater level rise by 4 cm and increases in the amount of outflow through constant boundaries and ET increase. In case 3, the cell size of the model was changed to 5 m by 5 m. The water balance component is quite similar to the base case, in which the recharge rate from the lakes to the aquifer increases by 98.11 m^3 $d^{-1}$and discharge of aquifer to the river increases by 185.17 m^3 d^{-1}. The average groundwater level rises by 1.5 cm with respect to the base case (Table 7-3). In case 4, the surface of the model defined by one zone with average horizontal hydraulic conductivity and one layer in vertical discretization, the simplification of sediments structure leads to increases in the seepage of the lake to the groundwater system by 2846.23 m^3 d^{-1} and discharge from aquifer to river increases by 2135.71 m^3 d^{-1}. The average water table rises by 8 cm in comparison to first case.

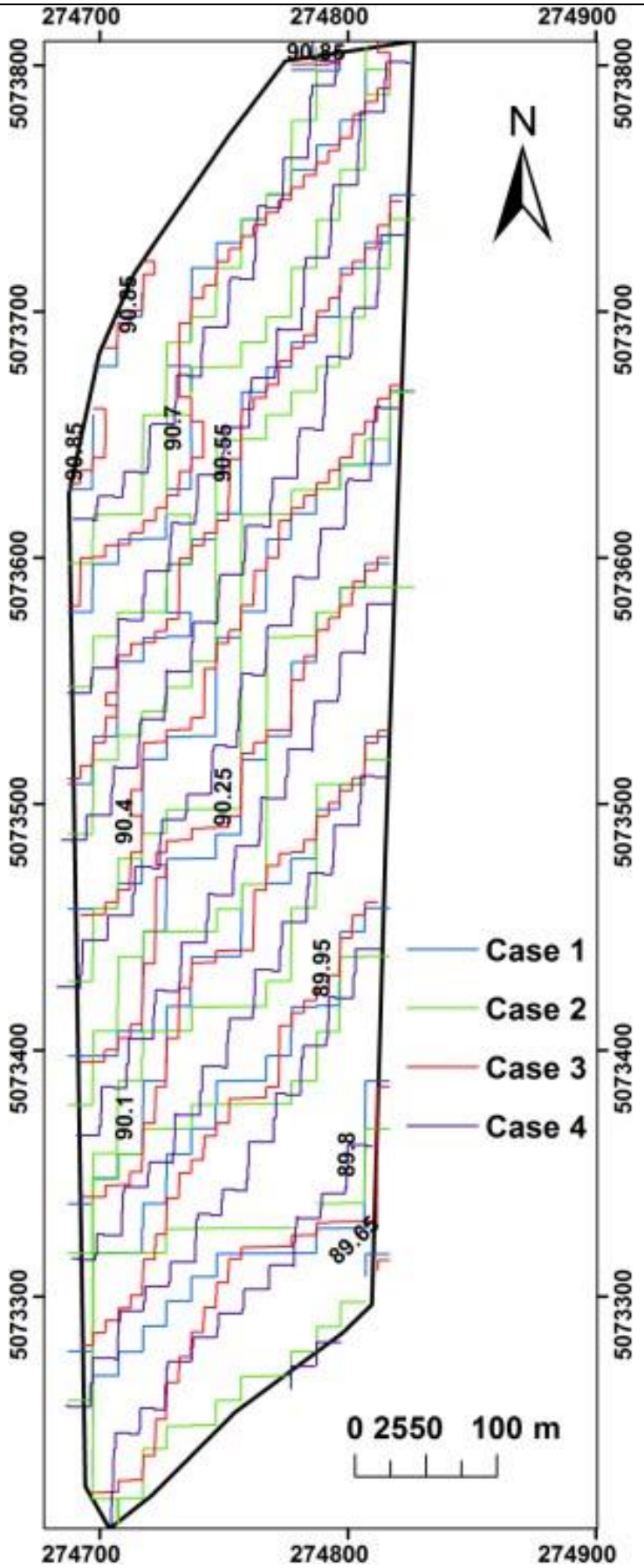
274700
274800
274900
5073800
5073700
5073600
5073500
5073400
5073300
N
90.85
90.85
90.85
90.7
90.55
90.25
90.4
90.1
89.95
89.8
89.65
Case 1
Case 2
Case 3
Case 4
0 2550 100 m

Figure 7-5: Contour lines of water table levels (m asl.) for model discretization scenarios compared with base case

7.4.5 Replenishment Scenarios

In the basic scenario (i.e., in absence of lake replenishment) in which lake stage is at 90.5 m. asl., the results show that leakage (outflow from the lake) is 895 m3 d^{-1} and the outflow from evapotranspiration is 18 m^3 d^{-1}. Discharge from aquifer to river is 721. m^3 d^{-1}, from which the recharge from lake to the aquifer is 174.95 m^3 d^{-1} and the average groundwater level is 89.68 m asl. as shown in Figure 7-6a. The results of the simulated scenarios are summarized in Table 7-4. In the first replenishment scenario, with increasing the lake water by 0.5 m (91 m asl.). The seepage from the lake is 1,298.8 m^3 d^{-1} and outflows through evapotranspiration rise by 161.20 m^3 d^{-1} with respect to the baseline situation. The average groundwater level rises by 0.28 m. In the second scenario, at the maximum lake stage of 91.5 m. asl., recharge rate from the lake to the aquifer increases by 745.59 m^3 d^{-1} compared to the baseline case. Consequently, the average water table rises by 0.77 m, and the amount of loss by evapotranspiration increases.

Table 7-4: Water budget components and changes in groundwater level compared to the baseline situation

Scenario	**Average lake level**	**Aquifer recharge from lake**	**Discharge from aquifer to river**	**Evapo-transpiration**	**Average change of groundwater level**
	(m asl.)	**(m^3d^{-1})**			**(m)**
Baseline case	**90.5**	**895.96**	**721.02**	**18**	**0**
1st replenishment	**91**	**1298.3**	**446.71**	**180.8**	**0.28**
2nd replenishment	**91.5**	**1409.7**	**488.46**	**685.66**	**0.77**

Simulated groundwater head contours for the second scenario with the head contours of the basic scenario are presented in (Figure 7-6b). All results point out that the planned replenishment scenarios of the lake will raise the groundwater level and augment, on the average, the groundwater system by over 65 % of the leakage from the lake.

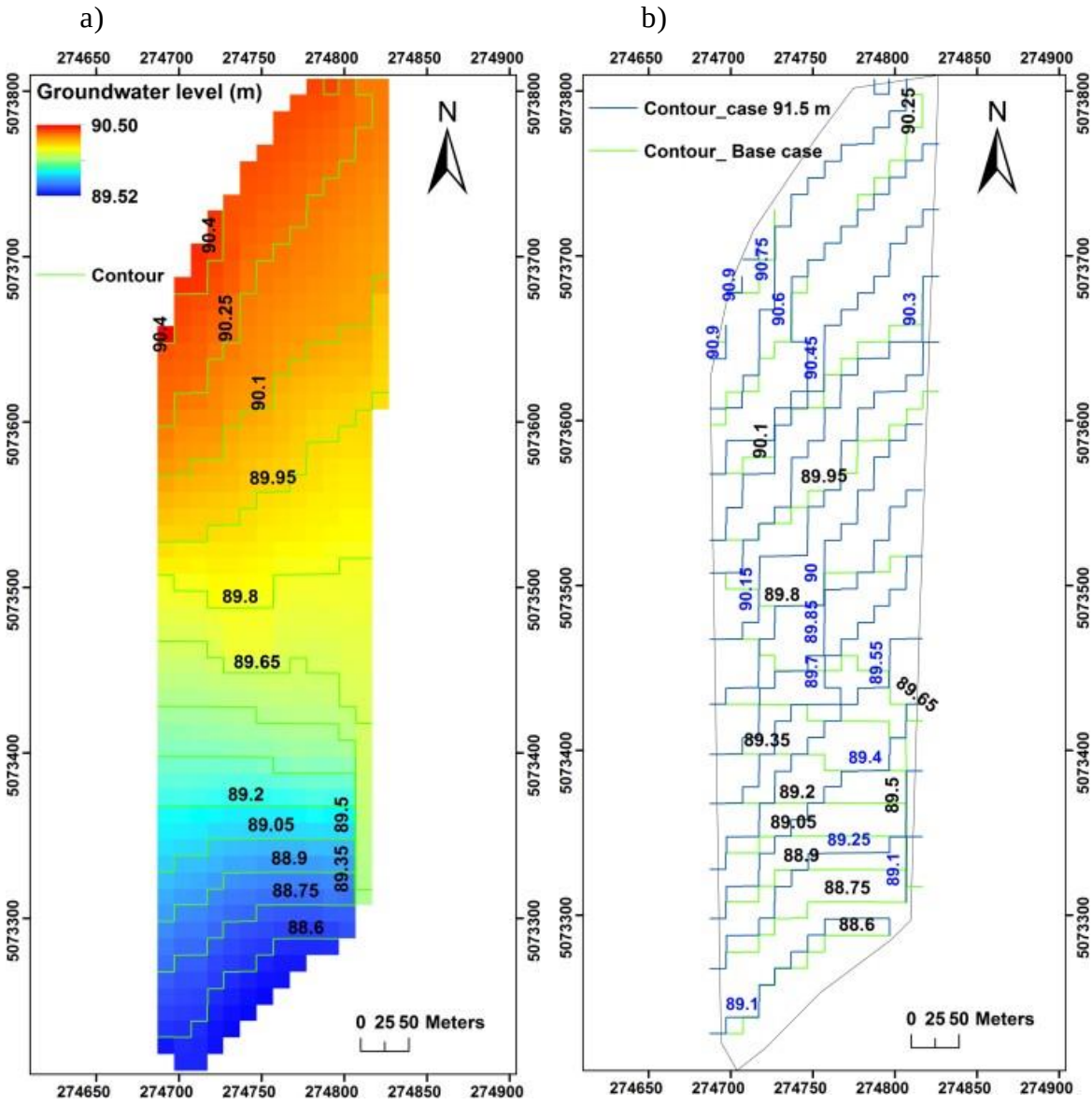

Figure 7-6: a) Simulated groundwater head contour map for basic scenario; b) Head contours for maximum replenishment lake stage 91.5 m.asl with head contours of basic scenario

7.5 Summary

The channelization of the Drava River changed the water budget of the Cún-Szaporca oxbow lakes in the floodplain. This chapter covers i) a holistic investigation of sediment sequences by satellite image processing (SIP), Ground Penetration Radar (GPR) record, particle size distribution (PSD) measuring from sediments in situ determining hydraulic conductivity from each augering; ii) reconstruction of layering, layer variability, alluvial sediment formations where the subsurface flow is crucial, iii) creating various modeling scenarios for different degree of the aquifer heterogeneity to assess losses from the lake and water retention in the system using a three-dimensional groundwater model using the finite difference code MODFLOW-2005 via ModelMuse as user graphical interface and iv) developing different water management scenarios through the lake replenishment to the Cún-Szaporca oxbow to gain a better understanding of the water budget of the whole system under the normal situation and for different lake replenishment scenarios. The results show that the application of a multilayered structure provided the most realistic result. Subsurface water monitoring and previous calculations also support that multilayered structures are characterized by considerable water retention capacity. The water budget for the simulated replenishment scenarios will maintain the water for close-to-natural ecosystems and agriculture in equilibrium. These outcomes will help the planners and all stakeholders better manage water resources in the oxbow area.

CHAPTER Eight

8. INTEGRATED WATER RESOURCES MANAGEMENT

Growing drought hazard and water demand for agriculture, ecosystem conservation, and tourism in the Hungarian Drava River floodplain call for novel approaches to maintain wetland habitats and enhance agricultural productivity. In this chapter, the calibrated coupled model of surface water (WetSpass-M) and groundwater model (MODFLOW-NWT) in chapter is applied to explore the hydrological feasibility of alternative water management, i.e., the restoration of natural reservoirs (abandoned paleochannels) to mitigate water shortage problems. Different management scenarios for two natural reservoirs are simulated with filling rates ranging from 0.5 m^3 s^{-1} to 1.5 m^3 s^{-1}. The findings of this study can be utilized in planning rehabilitation measures in lowlands with water shortage

8.1 Introduction

Incessant human interventions alter, at an increasing rate, the hydrological process and, consequently, reduce the availability of water in the floodplain. Currently, a competition between water users is seen as a serious problem in the Drava floodplain (Bonacci and Oskoruš, 2019) and it is predicted to radically aggravate in the next few years. In the Drava basin, alternative water resources have to be explored (Salem et al., 2020a). International examples show that the integrated (conjunctive) use of surface water and groundwater within a proper management system increases the efficiency of water utilization (Cheng et al., 2009; Salem et al., 2019), provides sufficient irrigation water for agriculture (El-Rawy et al., 2016; Seo et al., 2018; Singh et al., 2015), and improves the environmental conditions of irrigated lands (Liu et al., 2013).

Natural reservoirs are designed to store surface water, so their beds should have low seepage and permeability. However, they are influenced by natural and particularly strong artificial (due to lake regulation) driving forces, which imply large and fast-changing lake-water levels (lake-stages), implying a large impact on groundwater dynamics. That effect may result in flooding of the area adjacent to a reservoir also influencing contamination or agricultural productivity of that region. For all these reasons, the management reservoirs and their adjacent areas need appropriate models and methodologies adequately accounting for groundwater /surface-water interactions. The present study proposes an example of such methodology, based on modeled simulation of interactions between lake or reservoir and groundwater in the adjacent region. The consequences of applying a natural reservoir in augmenting surface water storage are investigated under variable management scenarios of recharging or feeding the reservoir. The assessment of such reservoir/groundwater interactions according to different scenarios of reservoir recharge is a precondition to establishing a new water governance in the region, which can, in turn, be the basis of exploiting economic opportunities. Sustainable ecotourism and related development would ensure a safe livelihood for the local population.

8.2 Material and methods

8.2.1 Study area

The same investigated area of Chapter Six

8.2.2 Methodology

Integrated Water Resources Management (IWRM) at the catchment scale depends heavily on the use of computer model simulations that capture surface water/groundwater allocations and the underlying hydrological processes. The coupling of traditionally surface hydrological models such as WetSpass, with a dedicated groundwater model such as MODFLOW has become a pivotal research area especially

when it comes to more complex IWRM scenarios. Therefore, in this study, calibrated integrated hydrological model WetSpass-M with groundwater flow model MODFLOW-NWT with ModelMuse as a graphical user interface in Chapter Six was applied to simulate different management scenarios for conjunctive use of surface water and groundwater.

8.3 Simulated Scenarios

The natural water reservoirs are the former oxbows, paleomeanders, and deeper-lying floodplain sections, which are under excess water effect. These areas may be suitable for the storage of surplus water provided by the adjacent watercourses. The model space covered two subareas: 1, the Korcsina oxbow system (Figure 8-1b); and 2, the Okor–Fekete-víz backswamps (Figure 8-1c). The exact location of the potential reservoir was selected from the analysis of the topography and hydraulic soil properties explored by auger samples. The selected subareas were simulated as natural reservoirs with filling and discharge conditions based on +2 m vertical water depth increasing theoretically with different stream discharges of 0.5, 0.75, 1, and 1.5 $m^3 s^{-1}$. (The excess water hazard on agricultural land excludes water level rise above +2 m.) Based on measurements of stream discharge, to obtain feeding with stream discharge larger than 1 $m^3 d^{-1}$, constructing a dam is required. Evaporation from the open water surface of the reservoir is the main challenge of the natural reservoir solution. The forested environs of the reservoir, however, reduce evaporation. This model is the first attempt to investigate whether water management through establishing a natural reservoir can be a major contribution to floodplain rehabilitation. Results of the management scenarios are discussed below.

.

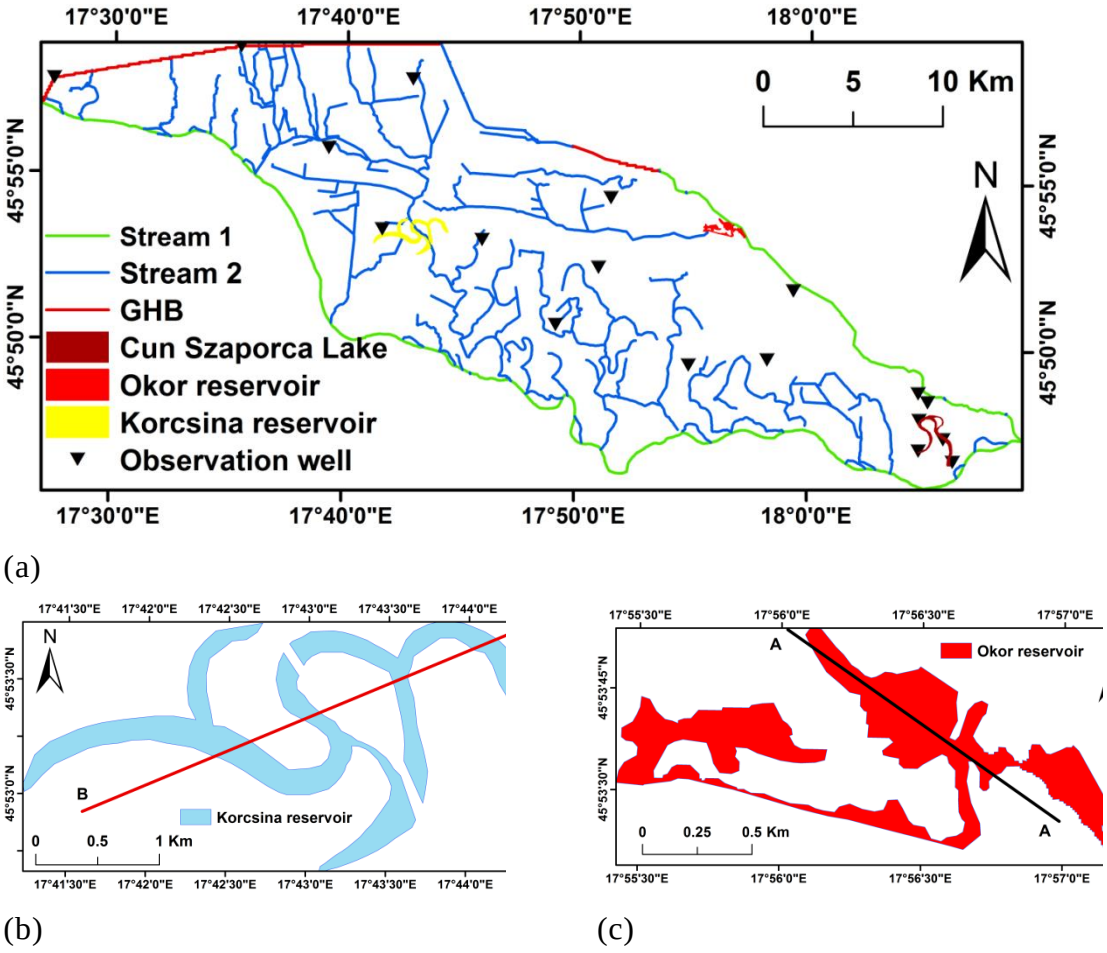

Figure 8-1: (a) Boundary conditions, observation wells, and planned reservoirs; (b) Korcsina reservoir; (c) Okor reservoir.

8.4 Results and Discussion

8.4.1 Korcsina Subarea

The Korcsina paleochannel system is a potential water reservoir in the western central part of the floodplain. With streams feeding 0.5 m^3 s^{-1}, the total upfilling (+2 m relative water level from 98 to 100 m) in the Korcsina reservoir would take 55 days, with 2,376,000 m^3 water demand. The discharge (seepage) period lasts 11 days from a level of 100 m to 98.75 m. By the end of the filling period, seepage from the reservoir to groundwater reaches 35,815 m^3. Recharge from groundwater to the reservoir in the filling period from the water level stage of 98 to 99 m and over this level becomes zero

Figure 8-2a). For filling at a rate of 0.75 m^3 s^{-1}, the reservoir reaches the stage 100 m after 27 days with reservoir seepage of 38,900 m^3, while the recharge from groundwater to the reservoir takes place in the first five days of the filling process at the level of 99 m (Figure 8-2b). In the filling with a discharge of 1 and 1.5 m^3 s^{-1}, 18 and 11 days are required to achieve +2 m relative water level rise in the reservoir (Figure 8-2c,d). For all scenarios with different discharges to the reservoir, the reservoir stage did not reach 98 m again because of the shallow groundwater table, which allows groundwater recharge larger than the seepage when reaching a level of 98.83 m (i.e., the inflow from groundwater to the reservoir, which is equal to the seepage from the reservoir at this stage) (Figure 8-2).

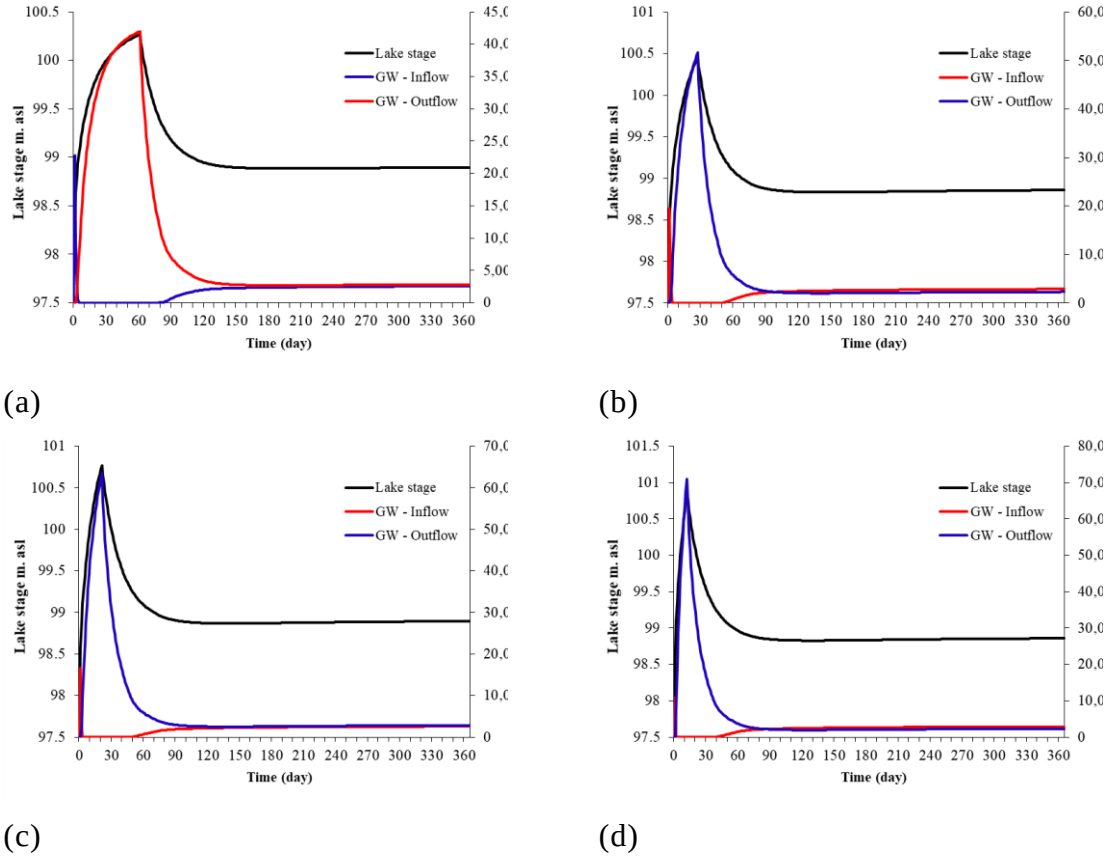

Figure 8-2: Daily variability of Lake Korcsina stage, groundwater seepage into the lake (GW-Inflow), seepage from the lake into groundwater (GW-Outflow), and net lake seepage (LAKnet) during the simulation period of one year. Note that the fluxes are referenced to the temporally variable lake with different feeding discharge from the stream. (a) Feeding at Q = 0.5 m^3 s^{-1}, (b) Q = 0.75 m^3 s^{-1}, (c) Q = 1.0 m^3 s^{-1}, (d) Q = 1.5 m^3 s^{-1}.

8.4.2 Simulation of the Water Storage Opportunities in the Okor–Fekete-víz Area

These randomly distributed and irregular-shaped paleochannels and backswamps are located at the confluence of the Okor and Fekete-víz streams. The main textural types in the west are medium to coarse sands, in the middle part fine sands, and the southeastern part loamy sands (Figure 3-6b). The bed level of the Okor natural reservoir is at 95.95 m. Feeding is from the two mentioned streams. With streams feeding at a rate of 0.5 m^3 s^{-1}, the reservoir stage does not reach +2 m relative water level (from 95.95 to 97.95 m), but it reaches 97.7 m within 61 days (Figure 8-3a), while with a stream discharge of 0.75 m^3 s^{-1} the reservoir stage is at 97.95 m after 22 days, with seepage of 49,733 m^3 (Figure 8-3b). Regarding the scenario of stream feeding at 1 m^3 s^{-1}, 13 days are needed to reach the stage of 97.95 m, while the discharge (seepage) period lasts for 180 days (the reservoir dries out) (Figure 8-3c). With a stream discharge of 1.5 m^3 s^{-1}, the reservoir achieves the stage of 97.95 within one week (62,215 m^3 seepage) Figure 8-3d). There is no recharge from groundwater to the Okor reservoir at the stage of 97.35 m during the filling and discharge period.

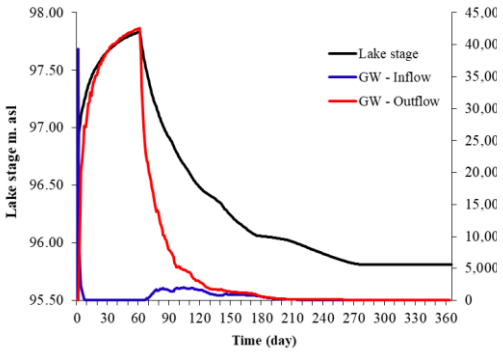

(a)

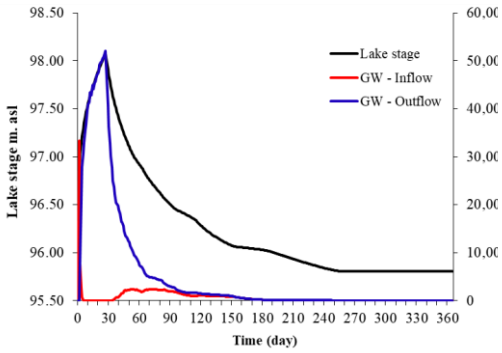

(b)

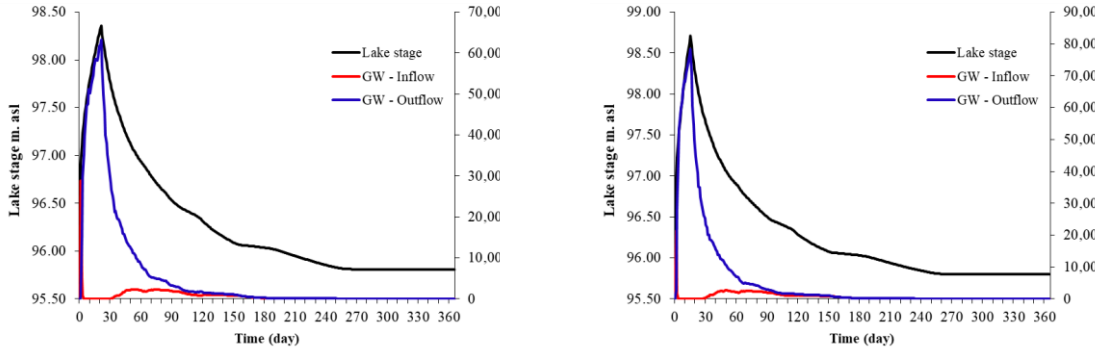

(c) (d)

Figure 8-3: Daily variability of Okor lake stage, groundwater seepage into the lake (GW-Inflow), seepage from the lake into groundwater (GW-Outflow), and net lake seepage (LLKnet) during simulation period of one year. Note that the fluxes are referenced to the temporally variable lake with different feeding discharges. (a) Feeding by Q = 0.5 m^3 s^{-1}, (b) Q = 0.75 m^3 s^{-1}, (c) Q = 1.0 m^3 s^{-1} and (d) Q = 1.5 m^3 $s^{-1.}$

For both reservoirs, and with a feeding discharge of 0.5 and 0.75 m^3 s^{-1}, the feeding stream capacity does not allow the recharge of the reservoirs in 60 days and 25 days, respectively, based on the observed discharge of the feeding stream. However, feeding the reservoir at a rate of 1.5 m^3 s^{-1}, a +2 m rise to be achieved in five days requires the construction of a dam on the feeding stream. Therefore, this scenario would not be economically feasible. Thus, the best scenario for both reservoirs is a feeding rate of 1.0 m^3 s^{-1}, as 18 and 13 days are needed for filling the Korcsina and Okor reservoirs, respectively, and water recharge to the reservoirs could be implemented by two filling periods per year, each providing water storage for six months. The drop in the water level in the reservoir after the filling period is attributed to the pressure differences between the reservoir water and the adjacent groundwater. The reservoir bed seepage analysis was a crucial step to understand the interactions between the reservoir and groundwater system. The seepage from the reservoir to the groundwater system, up to 25,000 m^3 d^{-1}, was dominant during stages higher than ~99 m, whereas the recharge from groundwater to the reservoir, up to 5000 m^3 d^{-1}, was dominant during stages below 99.00 m. Water levels in the reservoirs are primarily affected by the surrounding groundwater levels, regulated by the hyporheic flow of the streams. The first 1 m of filling increases the saturation of soil pores, which raises soil moisture content in the

root zone and the second meter creates an open water body, which is useful to create wetland habitats in the floodplain.

8.4.3 Spatio-Temporal Extent of Reservoir Impact

The assessment of the spatio-temporal impact of a lake (reservoir) on groundwater conditions is required to manage the groundwater systems adjacent to artificial lakes. The developed groundwater head of lakes Korcsina and Okor for a filling scenario with a discharge of 1 m^3 s^{-1} at different filling and discharge periods were plotted against distances at a cross-section which passes through the lakes (Figure 8-1b,c) for the selected stress periods (Figure 8-4 and Figure 8-5). The influence of the lake on groundwater levels decreases with distance (Figure 8-4 and Figure 8-5). However, there are differences between the trends of the two sections due to the variance in hydrogeological and hydraulic conditions for the two locations. The results clearly indicate that after 10 and 20 days of filling the Korcsina reservoir, the average groundwater head increased by 1 m and 1.6 m, respectively, with respect to the base case along the cross section. For the Okor reservoir, the average groundwater head increased by 0.7 m and 1.3 m after filling periods of 10 days and 20 days, respectively, with respect to the base case, while the average groundwater table decreased by 0.9 m and 1.0 m after discharge periods of 70 days and 170 days, respectively, compared to the base case (Figure 8-5). As depicted in the gradual rise in groundwater table after successive filling (Figure 8-4 and Figure 8-5), the natural reservoirs improve aquifer storage and hence maintain the level of ecosystem services and increase agricultural productivity in the Drava basin.

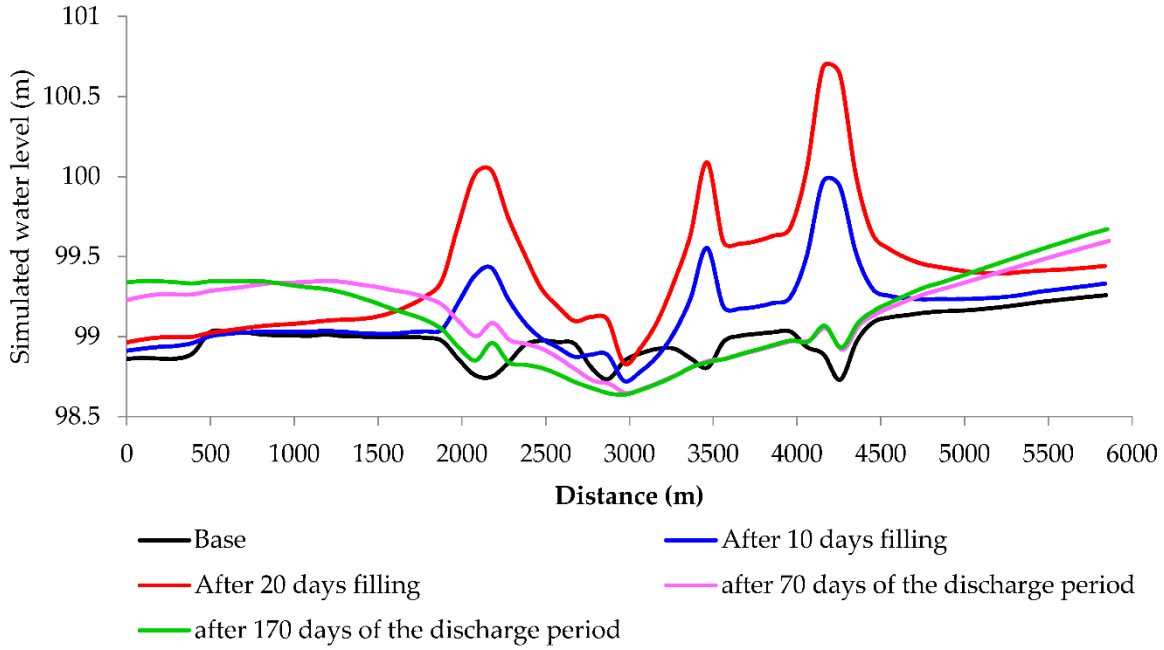

Figure 8-4: Simulated groundwater levels at a line crossing the Lake Korcsina at 10 and 20 days of filling and at 70 and 170 days of discharge period with respect to the base case.

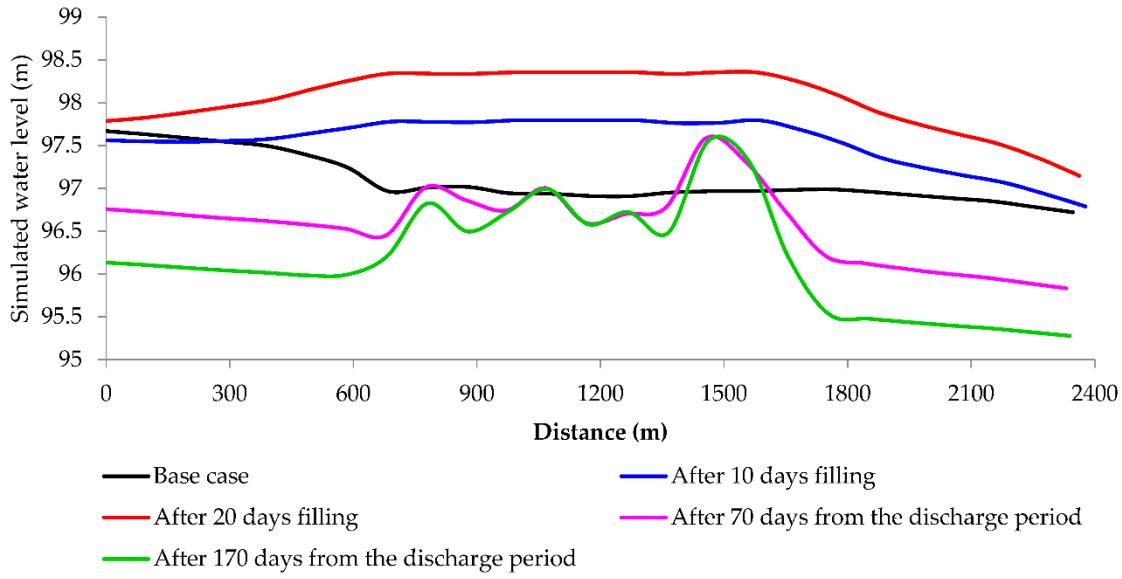

Figure 8-5: Simulated groundwater levels at a line crossing Lake Okor at 10 and 20 days of the filling period and 70 and 170 days of the discharge period with respect to the base case.

Lake–aquifer exchange fluxes in the Korcsina and Okor reservoirs are shown in Figure 8-6 and Figure 8-7: Lake–aquifer exchange fluxes of the Okor reservoir: (a) at the end of filling period of 10 days (+2 m reservoir stage), (b) for 40 days of the discharge period (+1 m) (positive represents upward reservoir seepage gain and negative represents downward reservoir seepage loss)., identifying the losing and gaining zones of the planned reservoirs with the help of the cell-to-cell flux terms in the model output files. Exchange fluxes between the reservoirs and the groundwater system for different periods of filling and discharge were analyzed. The sign on the graph indicates the direction of fluxes between the reservoirs and the aquifer. A positive sign represents upward reservoir seepage gain and negative represents downward reservoir seepage loss. For the Korcsina reservoir with 20 days of filling (+2 m), the seepage from reservoir to groundwater system ranged from 0 to 245 m^3 d^{-1} with an average value of 55 m^3 d^{-1}, with higher values in the northeast (Figure 8-6a). The average exchange between reservoir and aquifer was 1.4 m^3 d^{-1} after 40 days of discharge period, the majority of which the reservoir has gained from the aquifer (Figure 8-6b).

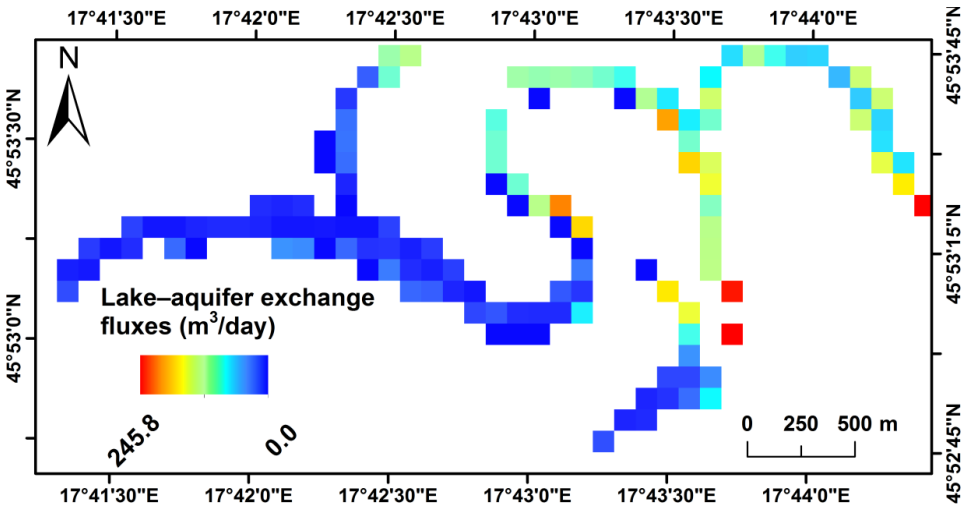

(a)

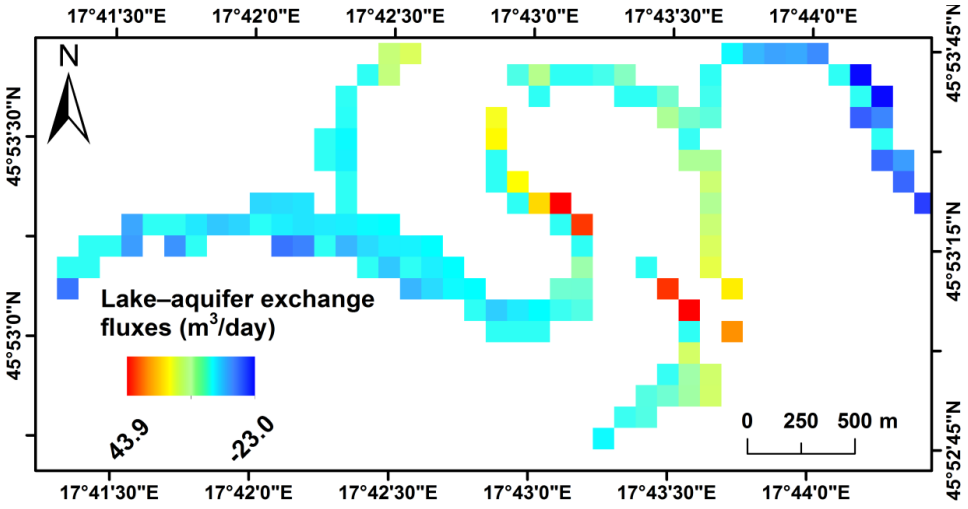

(b)

Figure 8-6: Lake–aquifer exchange fluxes for the Korcsina reservoir: (a) at the end of filling period of 14 days (+2 m reservoir stage), (b) for 40 days of discharge period (+1 m) (positive represents upward reservoir seepage gain and negative represents downward reservoir seepage loss).

Similar seepage patterns can be observed for the Okor reservoir (Figure 8-7a,b), with average values of seepage of 25.3 m^3 d^{-1} and 0.7 m^3 d^{-1} after 14 days of filling (+2 m) and 40 days of discharge (+1 m), respectively. The patterns of spatial seepage at various reservoir stages through filling and discharge periods are different, attributed to variations in reservoir-bed leakage and reservoir stages. The magnitude and direction of seepage between the reservoir and the underlying groundwater system rely on the reservoir-bed leakage and the difference between reservoir stage and hydraulic head of an underlying aquifer. In the Drava Plain, of highly variable alluvial deposits and soil textural types, the modeling of reservoir/groundwater interchanges is central to the planning of rehabilitation measures.

(a)

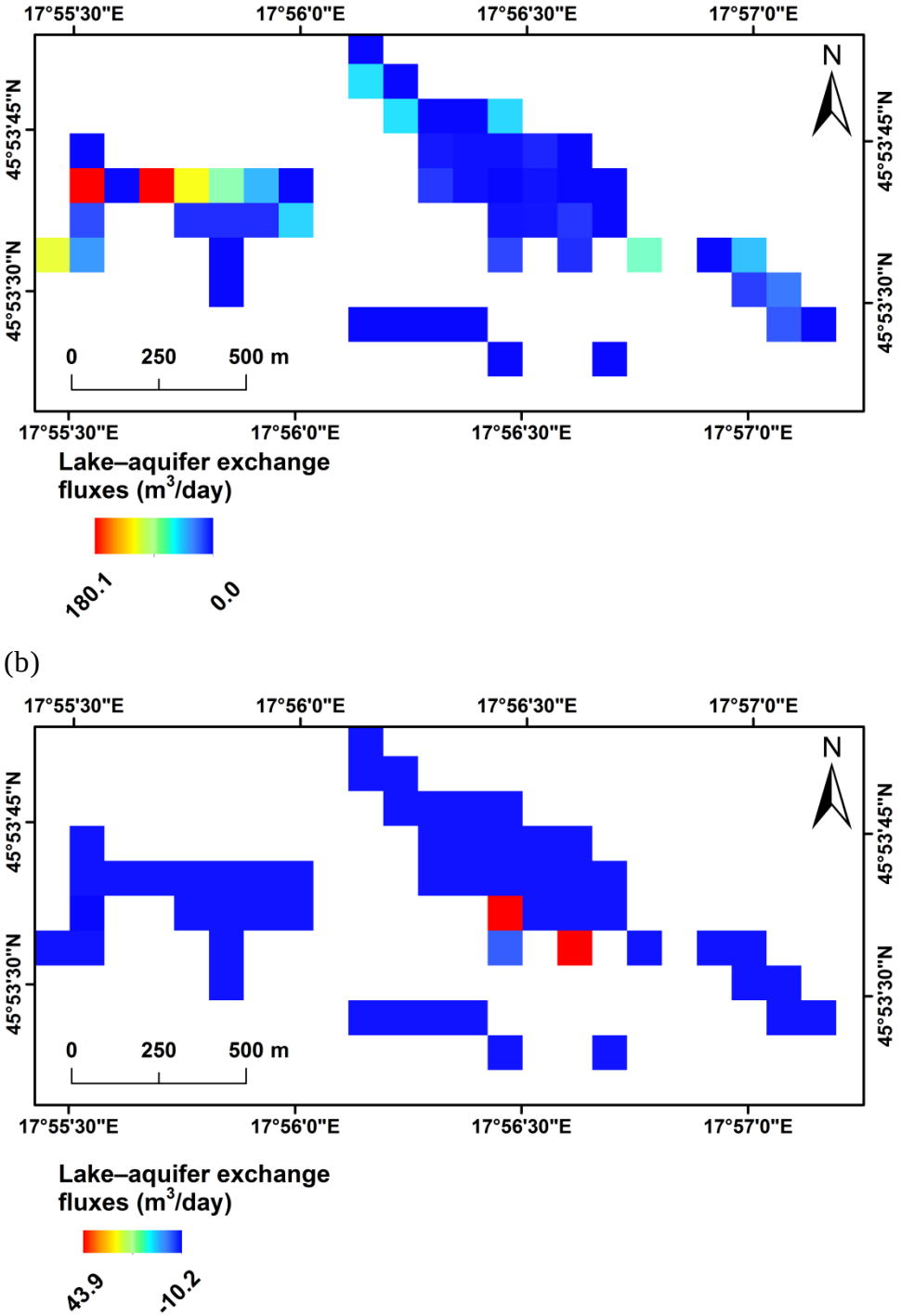

Figure 8-7: Lake–aquifer exchange fluxes of the Okor reservoir: (a) at the end of filling period of 10 days (+2 m reservoir stage), (b) for 40 days of the discharge period (+1 m) (positive represents upward reservoir seepage gain and negative represents downward reservoir seepage loss).

The findings point out that several factors influence the interactions of the reservoir with the groundwater system. The regulated recharge to the reservoir and the large

spatio-temporal variability of interactions indicate that sophisticated and complex modeling methods are required to depict such a complex hydrological system. Therefore, the integration of a spatially distributed water balance model (WetSpass-M), and a groundwater flow model (MODFLOW-NWT) to represent the volumetric exchanges between reservoir and groundwater was applied for case studies in the Drava floodplain.

8.5 Summary

This chapter assessed the feasibility of the natural reservoir in augmenting the water resources of the floodplain through surface water storage and to mitigate water shortage problems caused by drought and human interventions using MODFLOW-NWT with ModelMuse as a graphical interface. The two selected subareas were identified as potential natural reservoir sites. Simulated reservoirs had a filling and discharge conditions based on +2 m vertical water depth with different discharges from adjacent streams at 0.5, 0.75, 1, and 1.5 m^3 s^{-1} rates. The simulated water balance shows that reservoir-groundwater interactions are mainly governed by the inflow into and outflow from the reservoir. Overall, the study shows a promising direction for using a coupled surface-groundwater model in IWRM. Such an integrated management scheme is applicable for floodplain rehabilitation in other regions with similar hydromorphological conditions and hazards, too.

CHAPTER Nine

9. CONCLUSION AND FUTURE WORK

9.1 Introduction

The detailed conclusions have been recorded at the end of each chapter of the research. Conclusions based on the studies presented in the preceding chapters will be outlined. The recommendations for future works are given at the end of the chapter.

9.2 Main Conclusion

There were four main parts of this study: the first part is simulating long-term mean spatial patterns of actual evapotranspiration, surface runoff, and groundwater recharge of a highly regulated river system, the Drava River basin. A WetSpass-M model is utilized to estimate the spatial groundwater recharge on monthly, seasonal, and annual scales. The total components of water balance of the vegetated, bare soil, open-water, and impervious fraction per raster cell are calculated. The basic input data of WetSpass–M model include meteorological data (precipitation, air temperature, wind speed, and potential evapotranspiration), distributed groundwater depth, LAI, soil types, topography (DEM and slope), and land use/land cover of the investigated area. Such input data are prepared as grid maps using Geographic Information Systems (ArcGIS) collected for the period from 2000 to 2018. The cell size of the raster is 100 m × 100 m The spatial variability of groundwater recharge relies on climate conditions, groundwater depth, distributed land-cover, soil texture, topography, and slope. Land cover and soil textures are dominated by agricultural area and loam in the Drava basin. Water balance components under different land uses and soil textures were evaluated.

The water-table fluctuation method (WTF) is used to validate the performance of the WetSpass-M.

The second part is developing a 3-D steady-state and transient groundwater model using the finite difference code MODFLOW-2005 for the period from 1 January 2010 to 20 September 2018. The first three hydrological years from which data were available, i.e., from 1 January 2010 until 31 December 2012, were used as a warm-up period, after which the model was run (calibrated) throughout the following six hydrological years from 1 January 2013 to 20 September 2018 with a daily time step. The calibration process was carried out using measured lake stages and time series of daily groundwater levels from 18 observation wells. The sensitivity analysis was achieved using UCODE-2005 with the help of ModelMate. The interaction between the Cún-Szaporca oxbow lakes and groundwater is simulated using MODFLOW-NWT under ModelMuse environment, considering the interaction between surface water and groundwater by activating the Lake Package (LAK7), River Package (RIV), the Stream Flow Routing Package (SFR7), Recharge Package (RCH) and Evapotranspiration Package (ET). The sedimentological sequences were investigated using satellite images, GPR profiles, boreholes for revealing layering, and in situ studies of hydraulics of seepage. The origin and extension of layers were identified through geomorphological interpretation (distinguishing between point bar, dune, and other deposits). However, from the viewpoint of hydraulic modeling, a random spatial pattern of such deposits was reconstructed. Their hydrological properties show a wide range ($k = 10^{-4}$–10^{-7}). Different fluvial sediment structures scenarios were investigated to assess the interactions between groundwater and surface water at a critical part of this system: between a protected oxbow (which is fed by water according to the Old Drava Programme (ODP)) and the main river (Drava). Moreover, the model is applied to analyze two scenarios for the replenishment of the Cún-Szaporca oxbow lakes.

The third part is the coupling WetSpass model with MODFLOW to improve the simulation of impacts of long-term stressors, as this variable concerns the decision-makers for water resources. The integrated hydrologic modeling framework is applied to assess the impacts of LULC changes from 1990 to 2018 on the hydrology of the Drava floodplain, where human interference has led to a critical environmental situation. Five

different runs, for which, each run corresponds to one LULC map from the years 1990, 2000, 2006, 2012, and 2018, respectively, were conducted. To isolate, and yet capture, the effect of LULC changes, other input parameters such as meteorological data, topography (DEM and slope), distributed groundwater depth, and soil types were kept constant among all the five runs. Each run simulated the long-term average water balance components. Impacts of impervious cover changes on water balance components were assessed. Moreover, the integrated model is applied to evaluate the effects of LULC changes on water budget and groundwater level.

The fourth part covers the hydrological feasibility of alternative water management, i.e., the restoration of natural reservoirs (abandoned paleochannels) to mitigate water shortage problems was explored within the Drava Basin. A digital elevation model, GPR section, satellite images and hydraulic soil properties revealed by auger samples were used to identify possible allocations of a natural reservoir. The model space covered two subareas: 1, the Korcsina oxbow system; and 2, the Okor–Fekete-víz for two natural reservoirs were simulated using the integrated surface water-groundwater model with filling rates ranging from 0.5 m^3 s^{-1} to 1.5 m^3 s^{-1}. Different management scenarios for the selected subareas were simulated as natural reservoirs with filling and discharge conditions based on +2 m vertical water depth increasing theoretically with different stream discharges of 0.5, 0.75, 1, and 1.5 m^3 s^{-1}. The consequences of applying a natural reservoir in augmenting surface water storage are investigated under variable management scenarios of recharging or feeding the reservoir.

The primary findings of this thesis are as follows:

- For the surface water modeling of highly-regulated river basin:

The WetSpass-M model estimates the annually actual evapotranspiration of the basin, for the period from 2000 to 2018, to be 127 mm and 263 mm as minimum and maximum values respectively. This represents 27% of the annual average precipitation. 83% of total evapotranspiration occurs in the wet season, while the remaining 17% occurs during dry seasons. Around 29% (199 mm yr^{-1}) of the average annual rainfall feeds surface runoff with a minimum and maximum average values 77 mm yr^{-1} and 418 mm yr^{-1}, respectively. Annually simulated groundwater recharge ranges from 175 mm

yr^{-1} to 412 mm $yr^{-1}$with an average of 307 mm yr^{-1}, which correspond to 44% of mean annual rainfall. The analysis of simulation results shows that the WetSpass-M model works properly to simulate hydrological water budget components in the Drava basin..

- **For groundwater flow model:**

A regional steady and transient groundwater model was constructed for the Drava basin. Calibrated results of the transient groundwater flow model showed a good match between observed and simulated groundwater heads, with $R^2 = 0.98$. The mean error was −0.08 m, and the root mean square error was 0.4 m. Additionally, the calibration of lake stages showed a good agreement between simulated and observed stages with a correlation coefficient of 0.90, a mean error of −0.07 m, mean absolute error of 0.15 m, and root mean square error of 0.2 m. The parameters of the groundwater recharge (RCH), hydraulic conductivity (HKZ1), and evapotranspiration (EVT) had the highest composite scaled sensitivity values and were therefore the most sensitive parameters

- **For the impacts of Land-use/land-cover (LULC) change on the Drava basin hydrology:**

LULC change is considered to be a key human factor influencing groundwater recharge in floodplains. Without accurate estimations, the impact of LULC change on water balance components may be either understated or exaggerated. The expansion of artificial (sealed) surfaces between 2012 and 2018 was detected as the main contributor to the increase of surface runoff by 9 mm yr^{-1} in the Drava basin. The replacement of arable and meadow lands by forest, mudflat, with expanding willow shrub areas was identified as the strongest contributor to the major increase in evapotranspiration by 9 mm yr^{-1} and a decrease in groundwater recharge by 7 mm yr^{-1} between LULC in 2012 and 2018. These changes in LULC have resulted in a decline of groundwater recharge over an area of 5.3×10^7 m^3 amounting to a 0.1 m drop of groundwater level regarding the whole floodplain between 2012 and 2018. A decrease in groundwater recharge would directly reduce recharge for both deep and shallow aquifers and it increased the environmental threat in the floodplain. As a consequence, the conditions of agriculture that represent the primary source of subsistence for the local population became critical. The results also show that LULC changes have a direct effect on groundwater recharge

and the provision of floodplain ecosystem services. The coupled model proved to be a valuable assessment tool for the effective and sustainable implementation of floodplain rehabilitation plans. Finally, as a result of human intervention, available water resources in the Drava floodplain are rapidly diminishing, and effective integrated watershed management is required to address water availability. The approach tested in this study allows temporal and spatial estimation of hydrological components under the changes of LULC, providing quantitative information for decision-makers to implement sustainable management of water resources in the Drava floodplain.

- **For the water balance of the Cún-Szaporca oxbow lake:**

The theory for creating our modeling space is that the generated (sub) structures that are characterized by different hydraulic properties and formed during the sedimentation are analogous with fluvial features such as point bars, traces of lateral migration of river channel, and lateral accretion. The results of running of scenarios characterized by extended continuous layering in whole model space were shown to be unsuccessful. The application of a multilayered structure provided the most realistic result. The multilayered scenario result shows that the difference between input to groundwater (i.e. seepage from the oxbow lakes) and output to the main river channel amounts to 67% on the average. The replenishment scenario would result in raising the average groundwater level and, consequently, the recharge rate from the lake to aquifer will be increased. Water budget for the simulated scenarios will maintain the ecosystem and agriculture water in equilibrium.

- **For the feasibility of constructing natural reservoirs for two subareas: 1, the Korcsina oxbow system; and 2, the Okor–Fekete-víz back swamps as alternative water resource management within the Drava bain.**

For both reservoirs, around 60 days and 25 days of stream feeding of 0.5 and 0.75 $m^3\ s^{-1}$, respectively, are required to achieve the target water depth for the reservoir (+2 m), the optimal and economic scenario of filling the reservoirs is with a stream discharge of 1 $m^3\ s^{-1}$ for 14 days, based on the capacity of the feeding stream. Feeding at a rate of 1.5 $m^3\ s^{-1}$ would need around just six days, but this is not an economical scenario as it necessitates impoundment and dam construction. With feeding at 1 $m^3\ s^{-1}$, filling would

be repeated twice per year, as the reservoir lasts for 180 days. The effect of the reservoir on the groundwater table in the adjacent area depends on the reservoir stage, leakage, and the distribution of the groundwater head using the reservoir results in raising the groundwater table by 0.8 m at the end of the filling period. Natural reservoirs can be regarded as an economically feasible management practice of water retention and can help protect ecological values, the restoration of wetlands, and enhance agriculture productivity on the Hungarian section of the Drava floodplain. Moreover, the findings of this research can be utilized in planning rehabilitation measures in lowlands with water shortage. The simulated water balance shows that reservoir-groundwater interactions are mainly governed by the inflow into and outflow from the reservoir. Such an integrated management scheme is applicable for floodplain rehabilitation in other regions with similar hydromorphological conditions and hazards, too. The modeling workflows developed here can be used to apply new GW–SW interaction scenarios with a multitude of both natural and anthropogenic influences.

9.3 Recommendations for Future Works

Further research is needed to enhance the approach in light of the issues identified in this study, which include, but are not limited to:

- Since climate change has a substantial impact on the hydrologic features of soil and water management in a floodplain, the possible consequences of climate change on the hydrological response should be investigated.
- Land-use modeling should be improved further, incorporating different agricultural crops, and the influence of land-use change should be integrated with other global changes, such as climate change, to estimate the future of our groundwater systems.
- More soils data should be collected so that the subsurface, from the surface to the water table, can be better characterized. Moisture content measurements at various near-surface depths should also be made to better understand the dynamics of soil moisture and its relationship to cropping patterns and climate.
- This research may be expanded to investigate groundwater quality and groundwater pollution caused by surface water contamination.

REFERENCES

bdollahi, K., Bashir, I., Batelaan, O., 2012. WetSpass Graphical User Interface. Version 31-05-2012.Vrije University Brussel, Department of hydrologyand hydraulic engineering.

Abdollahi, K., Bashir, I., Verbeiren, B., Harouna, M.R., Van Griensven, A., Huysmans, M., Batelaan, O., 2017. A distributed monthly water balance model: formulation and application on Black Volta Basin. Environ Earth Sci 76, 198. https://doi.org/10.1007/s12665-017-6512-1

Abiye, T.A., Sulieman, H., Ayalew, M., 2009. Use of treated wastewater for managed aquifer recharge in highly populated urban centers: a case study in Addis Ababa, Ethiopia. Environ Geol 58, 55–59. https://doi.org/10.1007/s00254-008-1490-y

Abu-Saleem, A., 2010. Estimation of Water Balance Components in the Hasa Basin with GIS Based–WetSpass Model. (MSc. Thesis). Al Balqa Applied University, ,Jordan.

Abu-Saleem, A., Al-Zu`bi, Y., Rimawi, O., Al-Zu`bi, J., Alouran, N., 2010. Estimation of Water Balance Components in the Hasa Basin with GIS based WetSpass Model. J. of Agronomy 9, 119–125. https://doi.org/10.3923/ja.2010.119.125

Aish, A.M., 2014. Estimation of water balance components in the Gaza Strip with GIS based WetSpass model. Civil. Environ. Res 6.

Al Kuisi, M.A., El-Naqa, A., 2013. GIS based Spatial Groundwater Recharge estimation in the Jafr basin, Jordan – Application of WetSpass models for arid regions. Revista Mexicana de Ciencias Geológicas 30, 96–109.

Ala-aho, P., Rossi, P.M., Kløve, B., 2015. Estimation of temporal and spatial variations in groundwater recharge in unconfined sand aquifers using Scots pine inventories. Hydrol. Earth Syst. Sci. 19, 1961–1976. https://doi.org/10.5194/hess-19-1961-2015

Alemaw, B.F., Chaoka, T.R., 2003. A continental scale water balance model: a GIS-approach for Southern Africa. Physics and Chemistry of the Earth, Parts A/B/C 28, 957–966. https://doi.org/10.1016/j.pce.2003.08.040

Allam, M.N., Allam, G.I., 2007. Water Resources In Egypt: Future Challeges and Opportunities. Water International 32, 205–218. https://doi.org/10.1080/02508060708692201

Allen, R.G., Pereira, L.S., Raes, D., Smith, M., 1998. Crop evapotranspiration - Guidelines for computing crop water requirements - FAO Irrigation and drainage paper 56. FAO, Rome.

Alley, W.M., 2002. Flow and Storage in Groundwater Systems. Science 296, 1985–1990. https://doi.org/10.1126/science.1067123

Alley, W.M., Reilly, T., Franke, O.L., 1999. Sustainability of Ground-Water Resources; Volume 1186, p. 86.

Al-Maktoumi, A., El-Rawy, M., Zekri, S., 2016. Management options for a multipurpose coastal aquifer in Oman. Arab J Geosci 9, 636. https://doi.org/10.1007/s12517-016-2661-x

Amiri, M., Salem, A., Ghzal, M., 2022. Spatial-Temporal Water Balance Components Estimation Using Integrated GIS-Based Wetspass-M Model in Moulouya Basin, Morocco. IJGI 11, 139. https://doi.org/10.3390/ijgi11020139

Anderson, M.P., Hunt, R.J., Krohelski, J.T., Chung, K., 2002. Using High Hydraulic Conductivity Nodes to Simulate Seepage Lakes. Ground Water 40, 117–122. https://doi.org/10.1111/j.1745-6584.2002.tb02496.x

Anderson, M.P., Woessner, W.W., 1992. Applied groundwater modeling: simulation of flow and advective transport. Academic Press, San Diego.

Anderson, M.P., Woessner, W.W., Hunt, R.J., 2015. Applied groundwater modeling: simulation of flow and advective transport, Second edition. ed. Academic Press, London ; San Diego, CA.

Anibas, C., Fleckenstein, J.H., Volze, N., Buis, K., Verhoeven, R., Meire, P., Batelaan, O., 2009. Transient or steady-state? Using vertical temperature profiles to quantify groundwater-surface water exchange. Hydrol. Process. 23, 2165–2177. https://doi.org/10.1002/hyp.7289

Anuraga, T.S., Ruiz, L., Kumar, M.S.M., Sekhar, M., Leijnse, A., 2006. Estimating groundwater recharge using land use and soil data: A case study in South India. Agricultural Water Management 84, 65–76. https://doi.org/10.1016/j.agwat.2006.01.017

AQUAPROFIT, 2005. Az Ormánság komplex rehabilitációja és térségfejlesztése, Ős-Dráva Program (Complex rehabilitation and regional development in Ormánság. Old Drava Programme). AQUAPROFIT, Budapest, Hungary.

Arefaine, T., Nedaw, D., Gebreyohannes, T., 2012. Groundwater Recharge, Evapotranspiration and Surface Runoff Estimation Using WetSpass Modeling Method in Illala Catchment, Northern Ethiopia. Momona Ethiopian Journal of Science (MEJS) 4, 96–110.

Armanuos, A.M., Negm, A., Yoshimura, C., Valeriano, O.C.S., 2016. Application of WetSpass model to estimate groundwater recharge variability in the Nile Delta aquifer. Arab J Geosci 9, 553. https://doi.org/10.1007/s12517-016-2580-x

Arnold, T.R., 2013. Procedural knowledge for integrated modelling: Towards the Modelling Playground. Environmental Modelling & Software 39, 135–148. https://doi.org/10.1016/j.envsoft.2012.04.015

Asano, T., Cotruvo, J.A., 2004. Groundwater recharge with reclaimed municipal wastewater: health and regulatory considerations. Water Research 38, 1941–1951. https://doi.org/10.1016/j.watres.2004.01.023

Aslam, M., Salem, A., Singh, V.P., Arshad, M., 2021. Estimation of Spatial and Temporal Groundwater Balance Components in Khadir Canal Sub-Division, Chaj Doab, Pakistan. Hydrology 8, 178. https://doi.org/10.3390/hydrology8040178

Baalousha, H., 2009. Fundamentals of groundwater modelling, in: Groundwater: Modelling, Management and Contamination. Konig, L.F., Weiss, J.L., Eds. Nova Science Publishers, New York, NY, USA, pp. 149–166.

Bakker, P., Stone, E.J., Charbit, S., Gröger, M., Krebs-Kanzow, U., Ritz, S.P., Varma, V., Khon, V., Lunt, D.J., Mikolajewicz, U., Prange, M., Renssen, H., Schneider, B.,

Schulz, M., 2013. Last interglacial temperature evolution – a model inter-comparison. Clim. Past 9, 605–619. https://doi.org/10.5194/cp-9-605-2013

Bakundukize, C., Van Camp, M., Walraevens, K., 2011. Estimation of Groundwater Recharge in Bugesera Region (Burundi) using Soil Moisture Budget Approach. Geologica Belgica 14, 85–102.

Banta, E.R., 2011. ModelMate - A graphical user interface for model analysis (Techniques and Methods No. 6-E4). U.S. Geological Survey.

Batelaan, O., De Smedt, F., 2007. GIS-based recharge estimation by coupling surface–subsurface water balances. Journal of Hydrology 337, 337–355. https://doi.org/10.1016/j.jhydrol.2007.02.001

Batelaan, O., De Smedt, F., Triest, L., 2003. Regional groundwater discharge: phreatophyte mapping, groundwater modelling and impact analysis of land-use change. Journal of Hydrology 275, 86–108. https://doi.org/10.1016/S0022-1694(03)00018-0

Batelaan, O., Smedt, F.D., 2001. WetSpass: a flexible, GIS based, distributed recharge methodology for regional groundwater modelling. In Impact of Human Activity on Groundwater Dynamics, Gehrels, H., Peters, J., Leibundgut, C., Eds.; International Association of Hydrological Sciences: Wallingford, UK 11–17.

Batelaan, O., Woldeamlak, S.T., 2007. Arcview Interface for WetSpass, Version 13-06-2007;

Bear, J., 1979. Hydraulics of groundwater. McGraw-Hill, New York.

Bear, J., Verruijt, A., 1987. Modeling Groundwater Flow and Pollution. Springer Netherlands, Dordrecht. https://doi.org/10.1007/978-94-009-3379-8

Berendrecht, W., 2004. State space modelling of groundwater fluctuations (PhD). Delft university.

Berhanu, B., Melesse, A.M., Seleshi, Y., 2013. GIS-based hydrological zones and soil geo-database of Ethiopia. CATENA 104, 21–31. https://doi.org/10.1016/j.catena.2012.12.007

Beven, K.J., 2012. Rainfall-runoff modelling: the primer, 2nd ed. ed. Wiley-Blackwell, Chichester, West Sussex ; Hoboken, NJ.

Bhaduri, B., Harbor, J., Engel, B., Grove, M., 2000. Assessing Watershed-Scale, Long-Term Hydrologic Impacts of Land-Use Change Using a GIS-NPS Model. Environmental Management 26, 643–658. https://doi.org/10.1007/s002670010122

Bonacci, O., Oskoruš, D., 2019. Human Impacts on Water Regime, in: The Drava River: Environmental Problems and Solutions. Springer Science + Media: Cham, Switzerland, pp. 125–137.

Bowden, G.J., Dandy, G.C., Maier, H.R., 2005. Input determination for neural network models in water resources applications. Part 1—background and methodology. Journal of Hydrology 301, 75–92. https://doi.org/10.1016/j.jhydrol.2004.06.021

Brauman, K.A., Freyberg, D.L., Daily, G.C., 2012. Land cover effects on groundwater recharge in the tropics: ecohydrologic mechanisms. Ecohydrol. 5, 435–444. https://doi.org/10.1002/eco.236

Brindha, K., Neena Vaman, K.V., Srinivasan, K., Sathis Babu, M., Elango, L., 2014. Identification of surface water-groundwater interaction by hydrogeochemical indicators and assessing its suitability for drinking and irrigational purposes in Chennai, Southern India. Appl Water Sci 4, 159–174. https://doi.org/10.1007/s13201-013-0138-6

Bronstert, A., 2004. Rainfall-runoff modelling for assessing impacts of climate and land-use change. Hydrol. Process. 18, 567–570. https://doi.org/10.1002/hyp.5500

Buchberger, P., 1975. A Dráva-völgy árvédelmének története (History of flood control in the Drava Valley). Vízügyi közlemények 75, 103–113.

Burián, A., Horváth, G., Márk, L., 2019. Channel Incision Along the Lower Drava, in: The Drava River: Environmental Problems and Solutions. Springer Science + Media, Cham, Switzerland, pp. 139-157.

Büttner, G., 2014. CORINE Land Cover and Land Cover Change Products, in: Manakos, I., Braun, M. (Eds.), Land Use and Land Cover Mapping in Europe, Remote Sensing

and Digital Image Processing. Springer Netherlands, Dordrecht, pp. 55–74. https://doi.org/10.1007/978-94-007-7969-3_5

Calder, I.R., 1993. Hydrologic effects of landuse change, in: Handbook of Hydrology. McGraw-Hill, New York, USA, p. 13.1-13.50.

Calow, R.C., Robins, N.S., Macdonald, A.M., Macdonald, D.M.J., Gibbs, B.R., Orpen, W.R.G., Mtembezeka, P., Andrews, A.J., Appiah, S.O., 1997. Groundwater Management in Drought-prone Areas of Africa. International Journal of Water Resources Development 13, 241–262. https://doi.org/10.1080/07900629749863

Carrera-Hernández, J.J., Gaskin, S.J., 2008. Spatio-temporal analysis of potential aquifer recharge: Application to the Basin of Mexico. Journal of Hydrology 353, 228–246. https://doi.org/10.1016/j.jhydrol.2008.02.012

Čermák, J., Prax, A., 2001. Water balance of a Southern Moravian floodplain forest under natural and modified soil water regimes and its ecological consequences. Ann. For. Sci. 58, 15–29. https://doi.org/10.1051/forest:2001100

Chapman, D. (Ed.), 1996. Water quality assessments: a guide to the use of biota, sediments and water environmental monitoring, 2. ed. ed. E & FN Spon, London.

Chen, J.-F., Lee, C.-H., Yeh, T.-C.J., Yu, J.-L., 2005. A Water Budget Model for the Yun-Lin Plain, Taiwan. Water Resour Manage 19, 483–504. https://doi.org/10.1007/s11269-005-6809-9

Chen, S.M., Wang, Y.M., Tsou, I., 2013. Using artificial neural network approach for modelling rainfall–runoff due to typhoon. J Earth Syst Sci 122, 399–405. https://doi.org/10.1007/s12040-013-0289-8

Cheng, X., Anderson, M.P., 1993. Numerical Simulation of Ground-Water Interaction with Lakes Allowing for Fluctuating Lake Levels. Groundwater 31, 929–933. https://doi.org/10.1111/j.1745-6584.1993.tb00866.x

Cheng, Y., Lee, C.-H., Tan, Y.-C., Yeh, H.-F., 2009. An optimal water allocation for an irrigation district in Pingtung County, Taiwan. Irrig. and Drain. 58, 287–306. https://doi.org/10.1002/ird.411

Chhuon, K., Herrera, E., Nadaoka, K., 2016. Application of Integrated Hydrologic and River Basin Management Modeling for the Optimal Development of a Multi-Purpose Reservoir Project. Water Resour Manage 30, 3143–3157. https://doi.org/10.1007/s11269-016-1336-4

Chui, T.F.M., Freyberg, D.L., 2008. Simulating a Lake as a High-Conductivity Variably Saturated Porous Medium. Ground Water 46, 688–694. https://doi.org/10.1111/j.1745-6584.2008.00463.x

CLC, 2018. CORINE Land Cover Raster Data, 100 m. URL: https://land.copernicus.eu/pan-european/corine-land-cover/clc2018. Copernicus Europes eyes on earth. (15-03-2019).

CLC, 2012. CORINE Land Cover Raster Data, 100 mURL: http://www.eea.europa. eu/data-and-maps/data/clc-2012-vector-data-version. Europe Environment Agency.(15-01-2018).

CLC, 2006. CORINE Land Cover Raster Data, 100 m. URL: http://www.eea.europa. eu/data-and-maps/data/clc-2006-vector-data-version. Europe Environment Agency. (15-01-2018).

CLC, 2000. CORINE Land Cover Raster Data, 100 m. URL: http://www.eea.europa. eu/data-and-maps/data/corine-land-cover-2000-clc2000-seamless-vectordatabase. Europe Environment Agency. (2018-01-15).

CLC, 1990. CORINE Land Cover Raster Data, 100 m. http://www.eea.europa.eu/data-andmaps/ data/corine-land-cover-1990-raster. Europe Environment Agency. (15-01-2018).

Coplen, T.B., 2011. Guidelines and recommended terms for expression of stable-isotope-ratio and gas-ratio measurement results: Guidelines and recommended terms for expressing stable isotope results. Rapid Commun. Mass Spectrom. 25, 2538–2560. https://doi.org/10.1002/rcm.5129

Cunderlik, J., 2003. Hydrologic model selection for the CFCAS project: Assessment Of Water Resource Risk And Vulnerability To Changing Climate Conditions. (CFCAS project Report).

Dams, J., Dujardin, J., Reggers, R., Bashir, I., Canters, F., Batelaan, O., 2013. Mapping impervious surface change from remote sensing for hydrological modeling. Journal of Hydrology 485, 84–95. https://doi.org/10.1016/j.jhydrol.2012.09.045

Dams, J., Woldeamlak, S.T., Batelaan, O., 2008. Predicting land-use change and its impact on the groundwater system of the Kleine Nete catchment, Belgium. Hydrol. Earth Syst. Sci. 12, 1369–1385. https://doi.org/10.5194/hess-12-1369-2008

DDKÖVÍZIG, 2012. Revitalization of the Cún-Szaporca oxbow system.Final Master Plan. South-Transdanubian Environment and Water Directorate, Pécs, Hungary.

de Paulo, V.R. da S., Silva, M.T., Singh, V.P., de Souza, E.P., Braga, C.C., de Holanda, R.M., Almeida, R.S.R., de Assis Salviano de Sousa, F., Braga, A.C.R., 2018. Simulation of stream flow and hydrological response to land-cover changes in a tropical river basin. CATENA 162, 166–176. https://doi.org/10.1016/j.catena.2017.11.024

De Vries, A. (Ed.), 2013. Summary of master plans of wetland sub-group partners for water project (Masterplanning Europe's Wetlands). University of Debrecen, Centre for Environmental Management and Policy, Debrecen, Hungary.

Deng, X., Shi, Q., Zhang, Q., Shi, C., Yin, F., 2015. Impacts of land use and land cover changes on surface energy and water balance in the Heihe River Basin of China, 2000–2010. Physics and Chemistry of the Earth, Parts A/B/C 79–82, 2–10. https://doi.org/10.1016/j.pce.2015.01.002

Dezső, Halász, A., Czigány, S., Tóth, G., Lóczy, D., 2017. Estimating seepage loss during water replenishment to a floodplain oxbow: a case study from the Drava Plain. Geografia Fisica e Dinamica Quaternaria 61–75. https://doi.org/10.4461/GFDQ.2017.40.6

Dezső, J., Halász, A., Tóth, G., Mičijovský, J., Lóczy, D., 2015. Potential changes in the landscape due to ox-bow revitalization (case study from drava-basin, Hungary, role of fieldwork in geomorphology. pp. 22–23.

Dezső, J., Lóczy, D., Salem, A., Gábor, N., 2019. Floodplain connectivity, in: The Drava River: Environmental Problems and Solutions. Springer Science + Media: Cham, Switzerland, pp. 215–230.

Dezső, J., Salem, A., Lóczy, D., Slowik, M., Dávid, P., 2017. Randomly layered fluvial sediments influenced groundwater-surface water interaction. :, in: 17th International Multidisciplinary Scientific GeoConference SGEM 2017. Vienna, Austria, pp. 331–338. https://doi.org/10.5593/sgem2017H/33/S12.041

Dinçer, T., 1968. The Use of Oxygen 18 and Deuterium Concentrations in the Water Balance of Lakes. Water Resour. Res. 4, 1289–1306. https://doi.org/10.1029/WR004i006p01289

Doherty, J., Hunt, R., 2010. Approaches to Highly Parameterized Inversion: A Guide to Using PEST for Groundwater-Model Calibration; U.S. Geological Survey: Reston, VA, USA.

Doody, T.M., Benyon, G., Theiveyanathan, T., 2006. Quantifying water savings from willow removal in creeks in south-central NSW, in: 9th International River Symposium, Brisbane.

Dost, R., Obando, E.B., Bastiaanssen, W., Hoogeveen, J., 2013. Background Report: Water Accountingc In The Awash River Basin. Wageningen, The Netherlands, Eleaf.

Dujardin, J., Batelaan, O., Canters, F., Boel, S., Anibas, C., Bronders, J., 2011. Improving surface–subsurface water budgeting using high resolution satellite imagery applied on a brownfield. Science of The Total Environment 409, 800–809. https://doi.org/10.1016/j.scitotenv.2010.10.055

EC, 2000. Directive 2000/60/EEC: Establishing a framework for community action in the field of water policy, Official Journal of the European Communities,.

Ella, V.B., Melvin, S.W., Kanwar, R.S., Jones, L.C., Horton, R., 2002. Inverse three–dimensional groundwater modeling using the finite–difference method for recharge estimation in a glacial till aquitard. TRANSACTIONS OF THE ASAE 45, 703–715.

El-Rawy, M., Batelaan, O., Buis, K., Anibas, C., Mohammed, G., Zijl, W., Salem, A., 2020. Analytical and Numerical Groundwater Flow Solutions for the FEMME-Modeling Environment. Hydrology 7, 27. https://doi.org/10.3390/hydrology7020027

El-Rawy, M., Zlotnik, V.A., Al-Raggad, M., Al-Maktoumi, A., Kacimov, A., Abdalla, O., 2016. Conjunctive use of groundwater and surface water resources with aquifer recharge by treated wastewater: evaluation of management scenarios in the Zarqa River Basin, Jordan. Environ Earth Sci 75, 1146. https://doi.org/10.1007/s12665-016-5946-1

El-Zehairy, A.A., Lubczynski, M.W., Gurwin, J., 2018. Interactions of artificial lakes with groundwater applying an integrated MODFLOW solution. Hydrogeol J 26, 109–132. https://doi.org/10.1007/s10040-017-1641-x

European Commission, Statistical Office of the European Union, 2003. The Lucas survey: European statisticians monitor territory. Publications Office, Luxembourg.

Falťan, V., Petrovič, F., Oťaheľ, J., Feranec, J., Druga, M., Hruška, M., Nováček, J., Solár, V., Mechurová, V., 2020. Comparison of CORINE Land Cover Data with National Statistics and the Possibility to Record This Data on a Local Scale—Case Studies from Slovakia. Remote Sensing 12, 2484. https://doi.org/10.3390/rs12152484

Fenske, J.P., Leake, S.A., Prudic, D.E., 1996. Documentation of a computer program (RES1) to simulate leakage from reservoirs using the modular finite-difference ground-water flow model (MODFLOW) (Open-File Report No. 96–364). U.S. Geological Survey ; Branch of Information Services.

Feranec, J., Hazeu, G., Christensen, S., Jaffrain, G., 2007. Corine land cover change detection in Europe (case studies of the Netherlands and Slovakia). Land Use Policy 24, 234–247. https://doi.org/10.1016/j.landusepol.2006.02.002

Fetter, C.W., 2001. Applied hydrogeology, 4th ed. ed. Prentice Hall, Upper Saddle River, N.J.

Fohrer, N., Haverkamp, S., Eckhardt, K., Frede, H.-G., 2001. Hydrologic Response to land use changes on the catchment scale. Physics and Chemistry of the Earth, Part B: Hydrology, Oceans and Atmosphere 26, 577–582. https://doi.org/10.1016/S1464-1909(01)00052-1

Foster, S.S.D., 2001. The interdependence of groundwater and urbanisation in rapidly developing cities. Urban Water 3, 185–192. https://doi.org/10.1016/S1462-0758(01)00043-7

Fowe, T., Nouiri, I., Ibrahim, B., Karambiri, H., Paturel, J.E., 2015. OPTIWAM: An Intelligent Tool for Optimizing Irrigation Water Management in Coupled Reservoir–Groundwater Systems. Water Resour Manage 29, 3841–3861. https://doi.org/10.1007/s11269-015-1032-9

Freeze, R.A., 1969. The Mechanism of Natural Ground-Water Recharge and Discharge: 1. One-dimensional, Vertical, Unsteady, Unsaturated Flow above a Recharging or Discharging Ground-Water Flow System. Water Resour. Res. 5, 153–171. https://doi.org/10.1029/WR005i001p00153

Freeze, R.A., Cherry, J.A., 1979. Groundwater. Prentice-Hall, Englewood Cliffs, N.J.

Furman, A., 2008. Modeling Coupled Surface-Subsurface Flow Processes: A Review. Vadose Zone Journal 7, 741–756. https://doi.org/10.2136/vzj2007.0065

Gain, A.K., Giupponi, C., Renaud, F.G., 2012. Climate Change Adaptation and Vulnerability Assessment of Water Resources Systems in Developing Countries: A Generalized Framework and a Feasibility Study in Bangladesh. Water 4, 345–366. https://doi.org/10.3390/w4020345

Gale, I., 2005. Strategies for Managed Aquifer Recharge (MAR) in semi-arid areas. UNESCO IHP, Paris, France.

Gao, H., Hrachowitz, M., Fenicia, F., Gharari, S., Savenije, H.H.G., 2014. Testing the realism of a topography-driven model (FLEX-Topo) in the nested catchments of the

Upper Heihe, China. Hydrol. Earth Syst. Sci. 18, 1895–1915. https://doi.org/10.5194/hess-18-1895-2014

Gat, J.R., 2004. Planning and Management of a Sustainable and Equitable Water Supply under Stress of Water Scarcity and Quality Deterioration and the Constraints of Societal and Political Divisions: The Case for a Regional Holistic Approach,". Department of Environmental Science and Energy Research, the Weizmann Institute of Science, Rehovot, Israel,.

Gebremeskel, G., Kebede, A., 2018. Estimating the effect of climate change on water resources: Integrated use of climate and hydrological models in the Werii watershed of the Tekeze river basin, Northern Ethiopia. Agriculture and Natural Resources 52, 195–207. https://doi.org/10.1016/j.anres.2018.06.010

Gebremeskel, G., Kebede, A., 2017. Spatial estimation of long-term seasonal and annual groundwater resources: application of WetSpass model in the Werii watershed of the Tekeze River Basin, Ethiopia. Physical Geography 38, 338–359. https://doi.org/10.1080/02723646.2017.1302791

Gebreryfael, H., 2008. Groundwater resource assessment through distributed steady-state flow modeling, Aynalem well field. Mekelle, Ethiopia (MSc Thesis). International Institute for Geo-Information Science and Earth observation enschede, The Netherlands (unpubl).

Gebreyohannes, T., De Smedt, F., Walraevens, K., Gebresilassie, S., Hussien, A., Hagos, M., Amare, K., Deckers, J., Gebrehiwot, K., 2013. Application of a spatially distributed water balance model for assessing surface water and groundwater resources in the Geba basin, Tigray, Ethiopia. Journal of Hydrology 499, 110–123. https://doi.org/10.1016/j.jhydrol.2013.06.026

Gebru, T.A., Tesfahunegn, G.B., 2020. GIS based water balance components estimation in northern Ethiopia catchment. Soil and Tillage Research 197, 104514. https://doi.org/10.1016/j.still.2019.104514

Gehrels, H., Peter, N.E., Hoehn, E., Jensen, K., Leibundgut, C., Griffioen, J., Webb, B., Zaadnoordijk, W.J. (Eds.), 2001. Impact of human activity on groundwater

dynamics: proceedings of an international symposium (Symposium S3) held during the Sixth Scientific Assembly of the International Association of Hydrological Sciences (IAHS) at Maastricht, The Netherlands, from 18 to 27 July 2001, IAHS publication. IAHS, Wallingford, Oxfordshire.

Gharari, S., Hrachowitz, M., Fenicia, F., Gao, H., Savenije, H.H.G., 2014. Using expert knowledge to increase realism in environmental system models can dramatically reduce the need for calibration. Hydrol. Earth Syst. Sci. 18, 4839–4859. https://doi.org/10.5194/hess-18-4839-2014

Ghazavi, R., Ebrahimi, H., 2016. Impacts of land-use change on groundwater resources using remote sensing and numerical modeling. Journal of Biodiversity and Environmental Sciences (JBES) 9, 149–157.

Ghiglieri, G., Carletti, A., Pittalis, D., 2014. Runoff coefficient and average yearly natural aquifer recharge assessment by physiography-based indirect methods for the island of Sardinia (Italy) and its NW area (Nurra). Journal of Hydrology 519, 1779–1791. https://doi.org/10.1016/j.jhydrol.2014.09.054

Ghimire, C.P., Bruijnzeel, L.A., Lubczynski, M.W., Bonell, M., 2014. Negative trade-off between changes in vegetation water use and infiltration recovery after reforesting degraded pasture land in the Nepalese Lesser Himalaya. Hydrol. Earth Syst. Sci. 18, 4933–4949. https://doi.org/10.5194/hess-18-4933-2014

Ghosh, N.C., Kumar, S., Grützmacher, G., Ahmed, S., Singh, S., Sprenger, C., Singh, R.P., Das, B., Arora, T., 2015. Semi-Analytical Model for Estimation of Unsteady Seepage from a Large Water Body Influenced by Variable Flows. Water Resour Manage 29, 3111–3129. https://doi.org/10.1007/s11269-015-0985-z

Ghouili, N., Horriche, F.J., Zammouri, M., Benabdallah, S., Farhat, B., 2017. Coupling WetSpass and MODFLOW for groundwater recharge assessment: case study of the Takelsa multilayer aquifer, northeastern Tunisia. Geosci J 21, 791–805. https://doi.org/10.1007/s12303-016-0070-5

González del Tánago, M., Gurnell, A.M., Belletti, B., García de Jalón, D., 2016. Indicators of river system hydromorphological character and dynamics: understanding current

conditions and guiding sustainable river management. Aquat Sci 78, 35–55. https://doi.org/10.1007/s00027-015-0429-0

Govaerts, Y., 2013. Albedo influence on the climate.

Graf, R., Przybyłek, J., 2014. Estimation of Shallow Groundwater Recharge Using a Gis-Based Distributed Water Balance Model. Quaestiones Geographicae 33, 27–37. https://doi.org/10.2478/quageo-2014-0027

Guimerà, J., Vives, L., Carrera, J., 1995. A discussion of scale effects on hydraulic conductivity at a granitic site (El Berrocal, Spain). Geophys. Res. Lett. 22, 1449–1452. https://doi.org/10.1029/95GL01493

Gumiero, B., Mant, J., Hein, T., Elso, J., Boz, B., 2013. Linking the restoration of rivers and riparian zones/wetlands in Europe: Sharing knowledge through case studies. Ecological Engineering 56, 36–50. https://doi.org/10.1016/j.ecoleng.2012.12.103

Gumindoga, W., Rientjes, T.H.M., Haile, A.T., Dube, T., 2014. Predicting streamflow for land cover changes in the Upper Gilgel Abay River Basin, Ethiopia: A TOPMODEL based approach. Physics and Chemistry of the Earth, Parts A/B/C 76–78, 3–15. https://doi.org/10.1016/j.pce.2014.11.012

Gurwin, J., 2008. Numerical model of groundwater–surface water interaction in vicinity of the Turawa Lake, SW Poland. Unpublished research paper.

Han, D., Currell, M.J., Cao, G., Hall, B., 2017. Alterations to groundwater recharge due to anthropogenic landscape change. Journal of Hydrology 554, 545–557. https://doi.org/10.1016/j.jhydrol.2017.09.018

Harbaugh, A.W., 2005. MODFLOW-2005, the U.S. Geological Survey Modular Ground-water Model - the Ground-water Flow Process. US Geological Survey Reston, Virginia.

Harbaugh, A.W., 1990. A computer program for calculating subregional water budgets using results from the U.S. Geological Survey modular three-dimensional ground-water flow model (Open-File Report No. 90–392). US Geological Survey.

Harbaugh, A.W., Banta, E.R., Hill, M.C., McDonald, M.G., 2000. MODFLOW- 2000, the U.S. Geological Survey Modular Ground-Water Model—User Guide to Modularization Concepts and the Ground-Water Flow Process (Open-File Report No. 00–92). US Geological Survey.

Healy, R.W., Cook, P.G., 2002. Using groundwater levels to estimate recharge. Hydrogeology Journal 10, 91–109. https://doi.org/10.1007/s10040-001-0178-0

Healy, R.W., Scanlon, B.R., 2010. Estimating Groundwater Recharge. Cambridge University Press, Cambridge. https://doi.org/10.1017/CBO9780511780745

Hemmings, B., Whitaker, F., Gottsmann, J., Hughes, A., 2015. Hydrogeology of Montserrat review and new insights. Journal of Hydrology: Regional Studies 3, 1–30. https://doi.org/10.1016/j.ejrh.2014.08.008

Hendrickx, J.M.H., 1992. Groundwater Recharge. A Guide to Understanding and Estimating Natural Recharge (Volume 8, International Contributions to Hydrogeology): David N. Lerner, Arie S. Issar, and Ian Simmers. Verlag Heinz Heise, P.O.B. 610407, D-3000 Hannover 61, Germany. 1990. 345 p. ISBN 3-922705-91-X. J. environ. qual. 21, 512–512. https://doi.org/10.2134/jeq1992.00472425002100030036x

Heo, J., Yu, J., Giardino, J.R., Cho, H., 2015. Water Resources Response to Climate and Land-Cover Changes in a Semi-Arid Watershed, New Mexico, USA. Terr. Atmos. Ocean. Sci. 26, 463. https://doi.org/10.3319/TAO.2015.03.24.01(Hy)

Heymann, Y., Steenmans, C., Croissille, G., Bossard, M., 2014. CORINE Land Cover. Technical Guide. EUR12585 Luxembourg, Office for Official Publications of the EC.

Hill, M.C., Banta, E.R., Harbaugh, A.W., Anderman, E.R., 2000. MODFLOW- 2000, the U.S. Geological Survey Modular Ground-Water Model—User Guide to the Observation, Sensitivity, and Parameter-Estimation Processes and Three Post-Processing Programs (Open-File Report No. 00–184). US Geological Survey.

Hill, M.C., Tiedeman, C.R., 2007. Effective groundwater model calibration: with analysis of data, sensitivities, predictions, and uncertainty. Wiley-Interscience, Hoboken, N.J.

Hoff, H., 2002. The water challenge: Joint Water Project. Global Change Newsletter 46–48.

Hu, R., Fan, Z., Wang, Y., 2002. Groundwater resources and their characteristics in arid lands of Northwestern China. Journal Natural Resources 17, 321-326.

Hulisz, P., Michalski, A., Dąbrowski, M., Kusza, G., Łéczyński, L., 2015. Human-induced changes in the soil cover at the mouth of the Vistula River Cross-Cut (northern Poland). Soil Science Annual 66, 67–74. https://doi.org/10.1515/ssa-2015-0021

Hunt, R., 2003. Ground Water-Lake Interaction Modeling Using the LAK3 Package for MODFLOW 2000. Ground Water 41, 114–118. https://doi.org/10.1111/j.1745-6584.2003.tb02575.x

Hutjes, R.W.A., Kabat, P., Running, S.W., Shuttleworth, W.J., Field, C., Bass, B., da Silva Dias, M.F., Avissar, R., Becker, A., Claussen, M., Dolman, A.J., Feddes, R.A., Fosberg, M., Fukushima, Y., Gash, J.H.C., Guenni, L., Hoff, H., Jarvis, P.G., Kayane, I., Krenke, A.N., Liu, C., Meybeck, M., Nobre, C.A., Oyebande, L., Pitman, A., Pielke Sr., R.A., Raupach, M., Saugier, B., Schulze, E.D., Sellers, P.J., Tenhunen, J.D., Valentini, R., Victoria, R.L., Vörösmarty, C.J., 1998. Biospheric Aspects of the Hydrological Cycle. Journal of Hydrology 212–213, 1–21. https://doi.org/10.1016/S0022-1694(98)00255-8

IHMS, 2006. Integrated Hydrological Modelling System Manual.

IPCC, 2001. climate change 2001: the scientific basis. Contribution of Working Group 1 to the Third Assessment Report of the Intergovernmental Panel on Climate Change, edited by J. T. Houghton, Y. Ding, D. J. Griggs, M. Noguer, P. J. van der Linden, X. Da: BOOK REVIEWS. Cambridge Press, CambrUniversity idge, United Kingdom and New York, NY, USA 881.

Jason, A., Arblaster, K., Bartley, J., et al., 2008. Climate change-induced water stress and its impacts on natural and managed ecosystems. European Parlament.

Jat, M.K., Khare, D., Garg, P.K., 2009. Urbanization and its impact on groundwater: a remote sensing and GIS-based assessment approach. Environmentalist 29, 17–32. https://doi.org/10.1007/s10669-008-9176-2

Jha, M.K., Chowdhury, A., Chowdary, V.M., Peiffer, S., 2007. Groundwater management and development by integrated remote sensing and geographic information systems: prospects and constraints. Water Resour Manage 21, 427–467. https://doi.org/10.1007/s11269-006-9024-4

Jinno, K., Tsutsumi, A., Alkaeed, O., Saita, S., Berndtsson, R., 2009. Effects of land-use change on groundwater recharge model parameters. Hydrological Sciences Journal 54, 300–315. https://doi.org/10.1623/hysj.54.2.300

Jodar-Abellan, A., Valdes-Abellan, J., Pla, C., Gomariz-Castillo, F., 2019. Impact of land use changes on flash flood prediction using a sub-daily SWAT model in five Mediterranean ungauged watersheds (SE Spain). Science of The Total Environment 657, 1578–1591. https://doi.org/10.1016/j.scitotenv.2018.12.034

Juhász, J., 2002. Hidrogeológia (Hydrogeology). Akadémiai Kiadó, Budapest.

Jyrkama, M.I., Sykes, J.F., 2007. The impact of climate change on spatially varying groundwater recharge in the grand river watershed (Ontario). Journal of Hydrology 338, 237–250. https://doi.org/10.1016/j.jhydrol.2007.02.036

Kahsay, G.H., Gebreyohannes, T., Gebremedhin, M.A., Gebrekirstos, A., Birhane, E., Gebrewahid, H., Welegebriel, L., 2019. Spatial groundwater recharge estimation in Raya basin, Northern Ethiopia: an approach using GIS based water balance model. Sustain. Water Resour. Manag. 5, 961–975. https://doi.org/10.1007/s40899-018-0272-2

Kallimanis, A.S., Koutsias, N., 2013. Geographical patterns of Corine land cover diversity across Europe: The effect of grain size and thematic resolution. Progress in Physical Geography: Earth and Environment 37, 161–177. https://doi.org/10.1177/0309133312465303

Kanduč, T., Grassa, F., McIntosh, J., Stibilj, V., Ulrich-Supovec, M., Supovec, I., Jamnikar, S., 2014. A geochemical and stable isotope investigation of groundwater/surface-water interactions in the Velenje Basin, Slovenia. Hydrogeol J 22, 971–984. https://doi.org/10.1007/s10040-014-1103-7

Karimi, P., Bastiaanssen, W.G.M., Sood, A., Hoogeveen, J., Peiser, L., Bastidas-Obando, E., Dost, R.J., 2015. Spatial evapotranspiration, rainfall and land use data in water accounting – Part 2: Reliability of water acounting results for policy decisions in the Awash Basin. Hydrol. Earth Syst. Sci. 19, 533–550. https://doi.org/10.5194/hess-19-533-2015

Kendy, E., er, P., Todd Walter, M., Zhang, Y., Liu, C., Steenhuis, T.S., 2003. A soil-water-balance approach to quantify groundwater recharge from irrigated cropland in the North China Plain: QUANTIFYING RECHARGE IN THE NORTH CHINA PLAIN. Hydrol. Process. 17, 2011–2031. https://doi.org/10.1002/hyp.1240

Khan, S., Mushtaq, S., Hanjra, M.A., Schaeffer, J., 2008. Estimating potential costs and gains from an aquifer storage and recovery program in Australia. Agricultural Water Management 95, 477–488. https://doi.org/10.1016/j.agwat.2007.12.002

Kidmose, J., Engesgaard, P., Nilsson, B., Laier, T., Looms, M.C., 2011. Spatial Distribution of Seepage at a Flow-Through Lake: Lake Hampen, Western Denmark. Vadose Zone Journal 10, 110. https://doi.org/10.2136/vzj2010.0017

Kim, N.W., Chung, I.M., Won, Y.S., Arnold, J.G., 2008. Development and application of the integrated SWAT–MODFLOW model. Journal of Hydrology 356, 1–16. https://doi.org/10.1016/j.jhydrol.2008.02.024

Klemeš, V., 1983. Conceptualization and scale in hydrology. Journal of Hydrology 65, 1–23. https://doi.org/10.1016/0022-1694(83)90208-1

Krabbenhoft, D.P., Bowser, C.J., Anderson, M.P., Valley, J.W., 1990. Estimating groundwater exchange with lakes: 1. The stable isotope mass balance method. Water Resour. Res. 26, 2445–2453. https://doi.org/10.1029/WR026i010p02445

Krešić, N., 2009. Groundwater resources: sustainability, management, and restoration. McGraw-Hill, New York.

Kubicz, J., Kajewski, I., Kajewska-Szkudlarek, J., Dąbek, P.B., 2019. Groundwater recharge assessment in dry years. Environ Earth Sci 78, 555. https://doi.org/10.1007/s12665-019-8565-9

LaBaugh, J.W., Winter, T.C., Rosenberry, D.O., Schuster, P.F., Reddy, M.M., Aiken, G.R., 1997. Hydrological and chemical estimates of the water balance of a closed-basin lake in north central Minnesota. Water Resour. Res. 33, 2799–2812. https://doi.org/10.1029/97WR02427

Lambin, E.F., Baulies, X., Bockstael, N.E., et al., 2002. Land-use and land-cover change implementation strategy (IHDP Report No. 10).

Landon, M.K., Rus, D.L., Harvey, F.E., 2001. Comparison of Instream Methods for Measuring Hydraulic Conductivity in Sandy Streambeds. Groundwater 39, 870–885. https://doi.org/10.1111/j.1745-6584.2001.tb02475.x

Leavesley, G.H., Hutjes, R.W.A., Troutman, B.M., Saindon, L.G., 1983. Precipitation-Runoff Modeling System: User's Manual. U.S. Geological Survey (WaterResources Investigation report No. 83–4238). US Geological Survey.

Leblanc, M., Favreau, G., Tweed, S., Leduc, C., Razack, M., Mofor, L., 2007. Remote sensing for groundwater modelling in large semiarid areas: Lake Chad Basin, Africa. Hydrogeol J 15, 97–100. https://doi.org/10.1007/s10040-006-0126-0

Lee, D.R., 1977. A device for measuring seepage flux in lakes and estuaries1. Limnol. Oceanogr. 22, 140–147. https://doi.org/10.4319/lo.1977.22.1.0140

Lee, K.S., Chung, E.-S., 2007. Hydrological effects of climate change, groundwater withdrawal, and land use in a small Korean watershed. Hydrol. Process. 21, 3046–3056. https://doi.org/10.1002/hyp.6513

Lee, T.M., 1996. Hydrogeologic Controls on the Groundwater Interactions with an Acidic Lake in Karst Terrain, Lake Barco, Florida. Water Resour. Res. 32, 831–844. https://doi.org/10.1029/96WR00162

Lin, Y.-P., Hong, N.-M., Wu, P.-J., Lin, C.-J., 2007. Modeling and assessing land-use and hydrological processes to future land-use and climate change scenarios in watershed land-use planning. Environ Geol 53, 623–634. https://doi.org/10.1007/s00254-007-0677-y

Liu, L., Cui, Y., Luo, Y., 2013. Integrated Modeling of Conjunctive Water Use in a Canal-Well Irrigation District in the Lower Yellow River Basin, China. J. Irrig. Drain Eng. 139, 775–784. https://doi.org/10.1061/(ASCE)IR.1943-4774.0000620

Liuzzo, L., Noto, L.V., Arnone, E., Caracciolo, D., La Loggia, G., 2015. Modifications in Water Resources Availability Under Climate Changes: A Case Study in a Sicilian Basin. Water Resour Manage 29, 1117–1135. https://doi.org/10.1007/s11269-014-0864-z

Lóczy, D. (Ed.), 2019. The Drava River: Environmental Problems and Solutions, Springer Geography. Springer International Publishing, Cham. https://doi.org/10.1007/978-3-319-92816-6

Lóczy, D., 2018. Geological and Geomorphological Setting, in: The Drava River: Environmental Problems and Solutions. Springer Science + Media: Cham, Switzerland., pp. 5–21.

Lóczy, D., 2013. Hydromorphological-geoecological foundations of floodplain management Case study from Hungary.

Lóczy, D., Dezső, J., Czigány, S., Gyenizse, P., Pirkhoffer, E., Amadé Halász, 2014. Rehabilitation potential of the Drava river floodplain in Hungary, in: Water Resources and Wetlands. Tulcea (Romania), pp. 21–29. https://doi.org/10.13140/2.1.4324.4802

Lóczy, D., Dezső, J., Czigány, S., Prokos, H., Tóth, G., 2017. An environmental assessment of water replenishment to a floodplain lake. Journal of Environmental Management 202, 337–347. https://doi.org/10.1016/j.jenvman.2017.01.020

Lóczy, D., Tóth, G., Hermann, T., Rezsek, M., Nagy, G., Dezső, J., Salem, A., Gyenizse, P., Gobin, A., Vacca, A., 2020. Perspectives of land evaluation of floodplains under conditions of aridification based on the assessment of ecosystem services. HunGeoBull 69, 227–243. https://doi.org/10.15201/hungeobull.69.3.1

Lovász, G.., 1972. A Dráva-Mura vízrendszer vízjárási és lefolyási viszonyai (River regime and runoff in the Drava-Mura water system). Akadémiai Kiadó, Budapest, Hungary.

Lu, J., Sun, G., McNulty, S.G., Amatya, D.M., 2005. A comparison of six potential evapotranspiration methods for regional use in the southeastern united states. J Am Water Resources Assoc 41, 621–633. https://doi.org/10.1111/j.1752-1688.2005.tb03759.x

Manfreda, S., Fiorentino, M., Iacobellis, V., 2005. DREAM: a distributed model for runoff, evapotranspiration, and antecedent soil moisture simulation. Adv. Geosci. 2, 31–39. https://doi.org/10.5194/adgeo-2-31-2005

Manghi, F., Mortazavi, B., Crother, C., Hamdi, M.R., 2009. Estimating Regional Groundwater Recharge Using a Hydrological Budget Method. Water Resour Manage 23, 2475–2489. https://doi.org/10.1007/s11269-008-9391-0

Markstrom, S.L., Niswonger, R.G., Regan, R.S., Prudic, D.E., 2008. GSFLOW—Coupled Ground-Water and Surface-Water Flow Model Based on the Integration of the Precipitation-Runoff Modeling System (PRMS) and the Modular Ground-Water Flow Model (MODFLOW-2005), in: U.S. Geological Survey Techniques and Methods 6-D1,. U.S. Geological Survey, Reston, Virginia, p. 240P.

Martin, N., 2005. Development of a Water Balance for the Atankwidi Catchment, West Africa—A Case Study of Groundwater Recharge in a Semi-Arid Climate (Ph.D. Thesis). University of Göttingen, Göttingen, Germany.

Marttila, H., Dudley, B.D., Graham, S., Srinivasan, M.S., 2018. Does transpiration from invasive stream side willows dominate low-flow conditions? An investigation using hydrometric and isotopic methods in a headwater catchment. Ecohydrology 11, e1930. https://doi.org/10.1002/eco.1930

Mayer, W.B., Turner, B.L., 1994. Changes in land use and land cover: A global perspective, Cabridge university press, Cambridge, 1994. ISBN 0 521 47085 4,. Land Degrad. Dev. 6, 573 pp. https://doi.org/10.1002/ldr.3400060308

McColl, C., Aggett, G., 2007. Land-use forecasting and hydrologic model integration for improved land-use decision support. Journal of Environmental Management 84, 494–512. https://doi.org/10.1016/j.jenvman.2006.06.023

McDonald, M.G., Harbaugh, A.W., 1988. A Modular Three-Dimensional Finite-Difference Ground-Water Flow Model, Book 6, Chapter A1. U.S. Geological Survey, Techniques of Water-Resources Investigations, Reston.

McMahon, T.A., Peel, M.C., Lowe, L., Srikanthan, R., McVicar, T.R., 2013. Estimating actual, potential, reference crop and pan evaporation using standard meteorological data: a pragmatic synthesis. Hydrol. Earth Syst. Sci. 17, 1331–1363. https://doi.org/10.5194/hess-17-1331-2013

Meinzer, O., Stearns, N., 1929. A study of ground water in the Pomperaug Basin, Connecticut : with special reference to intake and discharge. US Geol. Surv. Water Suppl. Pap 597, 73–146. https://doi.org/10.3133/wsp597B

Meresa, E., Taye, G., 2018. Estimation of groundwater recharge using GIS-based WetSpass model for Birki watershed, the eastern zone of Tigray, Northern Ethiopia. Sustain. Water Resour. Manag. https://doi.org/10.1007/s40899-018-0282-0

Merritt, M.L., Konikow, L.F., 2000. Documentation of a computer program to simulate lake-aquifer interaction using the MODFLOW ground water flow model and the MOC3D solute-transport model, Water-Resources Investigations Report 2000-4167. https://doi.org/10.3133/wri004167

Miall, A.D., 2006. The Geology of Fluvial Deposits. Springer Berlin Heidelberg, Berlin, Heidelberg. https://doi.org/10.1007/978-3-662-03237-4

Montanari, L., Sivapalan, M., Montanari, A., 2006. Investigation of dominant hydrological processes in a tropical catchment in a monsoonal climate via the downward approach. Hydrol. Earth Syst. Sci. 10, 769–782. https://doi.org/10.5194/hess-10-769-2006

Moon, S.-K., Woo, N.C., Lee, K.S., 2004. Statistical analysis of hydrographs and water-table fluctuation to estimate groundwater recharge. Journal of Hydrology 292, 198–209. https://doi.org/10.1016/j.jhydrol.2003.12.030

Moore, R.J., 2007. The PDM rainfall-runoff model. Hydrol. Earth Syst. Sci. 11, 483–499. https://doi.org/10.5194/hess-11-483-2007

MTA ATK TAKI, 2013. http://mta-taki.hu/osztalyok/gis-labor/agrotopo.

Mustafa, S.T., Shamsudduha, M., Huysmans, M., 2016. Effect of irrigation return flow on groundwater recharge in an overexploited aquifer in Bangladesh, in: Geophysical Research Abstracts. p. 1.

Mylopoulos, N., Mylopoulos, Y., Tolikas, D., Veranis, N., 2007. Groundwater modeling and management in a complex lake-aquifer system. Water Resour Manage 21, 469–494. https://doi.org/10.1007/s11269-006-9025-3

Nakayama, T., Watanabe, M., 2008. Missing role of groundwater in water and nutrient cycles in the shallow eutrophic lake Kasumigaura, Japan. Hydrol. Process. 22, 1150–1172. https://doi.org/10.1002/hyp.6684

National Research Council, 2008. Water Implications of Biofuels Production in the United States. Washington, D.C.: National Academies Press.

Nie, W., Yuan, Y., Kepner, W., Nash, M.S., Jackson, M., Erickson, C., 2011. Assessing impacts of Landuse and Landcover changes on hydrology for the upper San Pedro watershed. Journal of Hydrology 407, 105–114. https://doi.org/10.1016/j.jhydrol.2011.07.012

Niehoff, D., Fritsch, U., Bronstert, A., 2002. Land-use impacts on storm-runoff generation: scenarios of land-use change and simulation of hydrological response in a meso-scale catchment in SW-Germany. Journal of Hydrology 267, 80–93. https://doi.org/10.1016/S0022-1694(02)00142-7

Niswonger, R.G., Panday, S., Ibaraki, M., 2011. MODFLOW-NWT, A Newton formulation for MODFLOW-2005 (Techniques and Methods No. 6-A37). U.S. Geological Survey.

Obuobie, E., 2008. Estimation of groundwater recharge in the context of future climate change in the White Volta River basin, West Africa. University of Bonn, Germany.

Ong, J.B., Zlotnik, V.A., 2011. Assessing Lakebed Hydraulic Conductivity and Seepage Flux by Potentiomanometer. Ground Water 49, 270–274. https://doi.org/10.1111/j.1745-6584.2010.00717.x

Ortmann-Ajkai, A., Czirok, A., Dénes, A., Oldal, I., Fehér, G., Gots, Zs., Kamarás-Buchberger, E., Szabó, E., Vörös, Zs., Wágner, L., 2003. Dráva holtágak komplex állapotértékelése (Complex baseline survey of the Drava oxbows). In: Hanyus E (ed) Az EU Víz Keretirányelvének bevezetése a Dráva vízgyűjtőjén (Introduction of the EU Water Framework Directive). WWF, Budapest, Hungary.

Otz, M.H., Otz, H.K., Otz, I., Siegel, D.I., 2003. Surface water/groundwater interaction in the Piora Aquifer, Switzerland: evidence from dye tracing tests. Hydrogeology Journal 11, 228–239. https://doi.org/10.1007/s10040-002-0237-1

Owor, M., Taylor, R., Mukwaya, C., Tindimugaya, C., 2011. Groundwater/surface-water interactions on deeply weathered surfaces of low relief: evidence from Lakes Victoria and Kyoga, Uganda. Hydrogeol J 19, 1403–1420. https://doi.org/10.1007/s10040-011-0779-1

Pálfai, I., 2001. Magyarország holtágai (Oxbows in Hungary). Hungarian Ministry of Transport and Water Management, Budapest.

Pan, Y., Gong, H., ZHou, D., Li, X., Nakagoshi, N., 2011. Impact of land use change on groundwater recharge in Guishui River Basin, China. Chin. Geogr. Sci. 21, 734–743. https://doi.org/10.1007/s11769-011-0508-7

Pechlivanidis, I.G., Jackson, B.M., McIntyre, N.R., Wheater, H.S., 2013. Catchment scale hydrological modelling: A review of model types, calibration approaches and uncertainty analysis methods in the context of recent developments in technology and applications. Global NEST Journal 13, 193–214. https://doi.org/10.30955/gnj.000778

Penman, H.L., 1948. Natural evaporation from open water, bare soil and grass. Proc. R. Soc. Lond. A 193, 120–145. https://doi.org/10.1098/rspa.1948.0037

Pinto, I.S., Overall, S.S. (Lead, CIIMAR, Araújo (CIIMAR, R., Klaus-Peter Zulka (EEA, Santamaría (CSCIS, L., Euller, K., Kropik, M., Pullin (Bangor, T.W. (UNIVIE) W.S.F.A., Vandewalle, M., Neßhöver (UFZ, C., 2013. Final knowledge assessment reports of the 3 case studies and lessons learned. Deliverable 3.1 of the EU-FP7-project KNEU, contract No. 265299. https://doi.org/10.13140/RG.2.1.1481.4801

Poelmans, L., Van Rompaey, A., Batelaan, O., 2010. Coupling urban expansion models and hydrological models: How important are spatial patterns? Land Use Policy 27, 965–975. https://doi.org/10.1016/j.landusepol.2009.12.010

Poeter, E.E., Hill, M.C., Banta, E.R., Mehl, S., Christensen, S., 2006. UCODE_2005 and Six Other Computer Codes for Universal Sensitivity Analysis, Calibration, and Uncertainty Evaluation (Techniques and Methods 6-A11). U.S. Geological Survey.

Prudic, D.E., Konikow, L.F., Banta, E.R., 2004. A new stream-flow routing (SFR1) package to simulate stream-aquifer interaction with MODFLOW-2000 (Open-File Report No. 2004–1042). US Geological Survey.

Rasmussen, W.C., Andreasen, G.E., 1959. Hydrologic budget of the Beaverdam Creek basin, Maryland. US Geol Surv Water-Supply Pap 1472:106. https://doi.org/10.3133/wsp1472

Rasoulzadeh, A., Moosavi, A.A., 2008. Study of uncertainty to estimate parameters of WTF groundwater model using inverse method (in Persian), in: 7th Hydraulic Symp. Tehran, Iran.

Rawal, D., Vyas, A., Rao, S.S., 2016. APPLICATION OF GIS AND GROUNDWATER MODELLING TECHNIQUES TO IDENTIFY THE PERCHED AQUIFERS TO DEMARKATE WATER LOGGING CONDITIONS IN PARTS OF MEHSANA. ISPRS Ann. Photogramm. Remote Sens. Spatial Inf. Sci. III–8, 173–180. https://doi.org/10.5194/isprsannals-III-8-173-2016

Rodriguez-Lloveras, X., Bussi, G., Francés, F., Rodriguez-Caballero, E., Solé-Benet, A., Calle, M., Benito, G., 2015. Patterns of runoff and sediment production in response to land-use changes in an ungauged Mediterranean catchment. Journal of Hydrology 531, 1054–1066. https://doi.org/10.1016/j.jhydrol.2015.11.014

Rorabaugh, M.I., 1964. Estimating changes in bank storage and ground-water contribution to streamflow: International Association of Scientific Hydrology, Publication 63.

Rorabaugh, M.I., Simons, W.D., 1966. Exploration of methods relating ground water to surface water, Columbia River basin – second phase (Open-File Report). US Geological Survey.

Rudnick, S., Lewandowski, J., Nützmann, G., 2015. Investigating Groundwater-Lake Interactions by Hydraulic Heads and a Water Balance. Groundwater 53, 227–237. https://doi.org/10.1111/gwat.12208

Rwanga, S.S., Ndambuki, J.M., 2017. Approach to Quantify Groundwater Recharge Using GIS Based Water Balance Model: A Review. Int'l Journal of Research in Chemical, Metallurgical and Civil Engg. (IJRCMCE) 4.

Sacks, L.A., 2002. Estimating ground-water inflow to lakes in central Florida using the isotope mass-balance approach (No. 2002–4192), Water-Resources Investigations Report. https://doi.org/10.3133/wri024192

Sacks, L.A., Lee, T.M., Swancar, A., 2014. The suitability of a simplified isotope-balance approach to quantify transient groundwater–lake interactions over a decade with climatic extremes. Journal of Hydrology 519, 3042–3053. https://doi.org/10.1016/j.jhydrol.2013.12.012

Sacks, L.A., Swancar, A., Lee, T.M., 1998. Estimating ground-water exchange with lakes using water-budget and chemical mass-balance approaches for ten lakes in ridge areas of Polk and Highlands counties, Florida (Water-Resources Investigations Report No. 98–4133). U.S. Geological Survey.

Salem, A., Dezső, J., El-Rawy, M., 2019a. Assessment of Groundwater Recharge, Evaporation, and Runoff in the Drava Basin in Hungary with the WetSpass Model. Hydrology 6, 23. https://doi.org/10.3390/hydrology6010023

Salem, A., Dezső, J., El-Rawy, M., 2018a. Hydrological modelling for the interaction between grondwater and surface water along the Drava floodplain, Hungary, in: 14th Miklos Iványi International PhD & DLA Sumposium. Pécs, Hungary.

Salem, A., Dezső, J., El-Rawy, M., Lóczy, D., 2020a. Hydrological Modeling to Assess the Efficiency of Groundwater Replenishment through Natural Reservoirs in the

Hungarian Drava River Floodplain. Water 12, 250. https://doi.org/10.3390/w12010250

Salem, A., Dezső, J., Elrawy, M., loczy, D., 2019b. Water management and retention opportunities along the Hungarian section of the Drava River, in: 2nd Euro-Mediterranean Conference for Environmental Integration (EMCEI). Sousse, Tunisia.

Salem, A., Dezső, J., El-Rawy, M., Lóczy, D., 2019c. Statistical analysis of precipitation trend for Drava flood plain region in Hungary, in: GSRD International Conferenc, 579th International Conferences on Engineering and Natural Science (ICENS). Istanbul, Turkey, pp. 43–47.

Salem, A., Dezső, J., Elrawy, M., loczy, D., Halmai, Á., 2019d. Estimation of groundwater recharge distribution using Gis based WetSpass model in the Cun-Szaporca oxbow, Hungary, in: 19th International Multidisciplinary Scientific GeoConference SGEM 2019. Albena, Bulgaria, pp. 169–176. https://doi.org/10.5593/sgem2019/3.1/S12.022

Salem, A., Dezső, J., loczy, D., 2021. Integrated hydrolgocial modelling for integrated water resources management in Drava River floodplain, in: International Conference on the Status and Future of the World's Large Rivers.

Salem, A.; Dezső, J.; Lóczy, D. Integrated assessment of the impact of land use changes on groundwater recharge and groundwater level in the Drava floodplain, Hungary. Scientific Reports 2022, under review.

Salem, A., Dezső, J., Lóczy, D., El-Rawy, M., Slowik, M., 2018b. Modeling Surface Water-Groundwater Interaction in an Oxbow of the Drava Floodplain. Palermo, Italy, pp. 1832–1822. https://doi.org/10.29007/hb5d

Salem, A., Dezso, J., Mustafa El-Rawy, 2019e. Conjunctive Management of Groundwater and Surface Water Resources Using MODFLOW in Drava Basin, Hungary, in: Chapman Conference on the Quest for Sustainability of Heavily Stressed Aquifers at Regional to Global Scales. AGU.

Salem, A., Mihoub, M., loczy, D., 2020b. Comparison of water balance of North Algeria and South-Western Hungary, in: 16th Miklos Iványi International PhD & DLA Sumposium. Pécs, Hungary.

Sanford, W., 2002. Recharge and groundwater models: an overview. Hydrogeology Journal 10, 110–120. https://doi.org/10.1007/s10040-001-0173-5

Savenije, H.H.G., 2001. Equifinality, a blessing in disguise? Hydrol. Process. 15, 2835–2838. https://doi.org/10.1002/hyp.494

Scanlon, B.R., Healy, R.W., Cook, P.G., 2002. Choosing appropriate techniques for quantifying groundwater recharge. Hydrogeology Journal 10, 18–39. https://doi.org/10.1007/s10040-001-0176-2

Scanlon, B.R., Keese, K.E., Flint, A.L., Flint, L.E., Gaye, C.B., Edmunds, W.M., Simmers, I., 2006. Global synthesis of groundwater recharge in semiarid and arid regions. Hydrol. Process. 20, 3335–3370. https://doi.org/10.1002/hyp.6335

Schwartz, F.W., Gallup, D.N., 1978. Some factors controlling the major ion chemistry of small lakes: Examples from the prairie parkland of Canada. Hydrobiologia 58, 65–81. https://doi.org/10.1007/BF00018896

Seo, S.B., Mahinthakumar, G., Sankarasubramanian, A., Kumar, M., 2018. Conjunctive Management of Surface Water and Groundwater Resources under Drought Conditions Using a Fully Coupled Hydrological Model. J. Water Resour. Plann. Manage. 144, 04018060. https://doi.org/10.1061/(ASCE)WR.1943-5452.0000978

Shakya, D.R., 2001. Spatial and temporal groundwater modeling integrated with remote sensing and GIS : hard rock experimental catchment, Sardon, Spain. (MSc. Thesis). University of Twente, Enschede, Netherlands.

Shao, Q., Traylen, A., Zhang, L., 2012. Nonparametric method for estimating the effects of climatic and catchment characteristics on mean annual evapotranspiration: Nonparametric method for mean annual evapotranspiration. Water Resour. Res. 48. https://doi.org/10.1029/2010WR009610

Sheer, D.P., 1981. Assuring Water Supply for the Washington Metropolitan Area-25 Years of Progress. Pp. 39–66 in a 1980s View of Water Management in the Potomac River Basin. Report of the Committee on Governmental Affairs, U.S. Congress, Senate, 97th Congress, 2d Session, November 12. Washington, D.C.: U.S. Government Printing Office.

Singh, G., Saraswat, D., 2016. Development and evaluation of targeted marginal land mapping approach in SWAT model for simulating water quality impacts of selected second generation biofeedstock. Environmental Modelling & Software 81, 26–39. https://doi.org/10.1016/j.envsoft.2015.12.001

Singh, H., Sinha, T., Sankarasubramanian, A., 2015. Impacts of Near-Term Climate Change and Population Growth on Within-Year Reservoir Systems. J. Water Resour. Plann. Manage. 141, 04014078. https://doi.org/10.1061/(ASCE)WR.1943-5452.0000474

Singh, R., Senay, G., Velpuri, N., Bohms, S., Scott, R., Verdin, J., 2013. Actual Evapotranspiration (Water Use) Assessment of the Colorado River Basin at the Landsat Resolution Using the Operational Simplified Surface Energy Balance Model. Remote Sensing 6, 233–256. https://doi.org/10.3390/rs6010233

Singhal, B.B.S., Gupta, R.P., 2010. Applied Hydrogeology of Fractured Rocks. Springer Netherlands, Dordrecht. https://doi.org/10.1007/978-90-481-8799-7

Sivapalan, M., 2003. Prediction in ungauged basins: a grand challenge for theoretical hydrology. Hydrol. Process. 17, 3163–3170. https://doi.org/10.1002/hyp.5155

Słowik, M., Dezső, J., Marciniak, A., Tóth, G., Kovács, J., 2018. Evolution of river planforms downstream of dams: Effect of dam construction or earlier human-induced changes?: Evolution of river planforms downstream of dams. Earth Surf. Process. Landforms 43, 2045–2063. https://doi.org/10.1002/esp.4371

SMEC, 2007. Hydrological Study Of Tana Beles Sub-Basins, Part I.

Soleimani-Motlagh, M., Ghasemieh, H., Talebi, A., Abdollahi, K., Dragoni, W., 2020. Groundwater budget deficit caused by drought and overexploitation. Water Supply 20, 621–632. https://doi.org/10.2166/ws.2019.193

Solomatine, D.P., Wagener, T., 2011. Hydrological Modeling, in: Treatise on Water Science. Elsevier, pp. 435–457. https://doi.org/10.1016/B978-0-444-53199-5.00044-0

Sommerwerk, N., Hein, T., Schneider-Jacoby, M., Baumgartner, C., Ostojić, A., Siber, R., Bloesch, J., Paunović, M., Tockner, K., 2009. The Danube River Basin, in: Rivers of Europe. Elsevier, pp. 59–112. https://doi.org/10.1016/B978-0-12-369449-2.00003-5

Sophocleous, M., 2005. Groundwater recharge and sustainability in the High Plains aquifer in Kansas, USA. Hydrogeol J 13, 351–365. https://doi.org/10.1007/s10040-004-0385-6

Sophocleous, M., 2002. Interactions between groundwater and surface water: the state of the science. Hydrogeology Journal 10, 52–67. https://doi.org/10.1007/s10040-001-0170-8

Sophocleous, M.A., 1991. Combining the soilwater balance and water-level fluctuation methods to estimate natural groundwater recharge: Practical aspects. Journal of Hydrology 124, 229–241. https://doi.org/10.1016/0022-1694(91)90016-B

Stauffer, R.E., 1985. Use of solute tracers released by weathering to estimate groundwater inflow to seepage lakes. Environ. Sci. Technol. 19, 405–411. https://doi.org/10.1021/es00135a003

Stauffer, RobertE., 1991. Effects of citrus agriculture on ridge lakes in Central Florida. Water Air Soil Pollut 59. https://doi.org/10.1007/BF00283176

Su, X., Cui, G., Du, S., Yuan, W., Wang, H., 2016. Using multiple environmental methods to estimate groundwater discharge into an arid lake (Dakebo Lake, Inner Mongolia, China). Hydrogeol J 24, 1707–1722. https://doi.org/10.1007/s10040-016-1439-2

Suzanne, S., 2001. Priority questions for land use/cover change research in the next couple of years. LUCC Newsletter 1–9.

Szalay, M., 2014. Joint Drava River Corridor Analysis. ational Institute for Environment Department of Water Resources Management, Budapest, Hungary.

Tam, V.T., Batelaan, O., Beyen, I., 2016. Impact assessment of climate change on a coastal groundwater system, Central Vietnam. Environ Earth Sci 75, 908. https://doi.org/10.1007/s12665-016-5718-y

Tang, Z., Engel, B.A., Pijanowski, B.C., Lim, K.J., 2005. Forecasting land use change and its environmental impact at a watershed scale. Journal of Environmental Management 76, 35–45. https://doi.org/10.1016/j.jenvman.2005.01.006

Theis, C.V., 1937. Amount of ground-water recharge in the southern High Plains. Trans. AGU 18, 564. https://doi.org/10.1029/TR018i002p00564

Tilahun, K., Merkel, B.J., 2009. Estimation of groundwater recharge using a GIS-based distributed water balance model in Dire Dawa, Ethiopia. Hydrogeol J 17, 1443–1457. https://doi.org/10.1007/s10040-009-0455-x

Tong, S.T.Y., Liu, A.J., 2006. Modelling the hydrologic effects of land-use and climate changes. IJRAM 6, 344. https://doi.org/10.1504/IJRAM.2006.009543

Trescott, P.C., Larson, S.P., 1977. Solution of three-dimensional groundwater flow equations using the strongly implicit procedure. Journal of Hydrology 35, 49–60. https://doi.org/10.1016/0022-1694(77)90076-2

Turner, J.V., Allison, G.B., Holmes, J.W., 1984. The water balance of a small lake using stable isotopes and tritium. Journal of Hydrology 70, 199–220. https://doi.org/10.1016/0022-1694(84)90122-7

UN/WWAP, 2006. The United Nations World Water Development Report 3: Water in a Changing World. France and Earth Scan, Paris, London.

Ursu, A., Stoleriu, C.C., Ion, C., Jitariu, V., Enea, A., 2020. Romanian Natura 2000 Network: Evaluation of the Threats and Pressures through the Corine Land Cover Dataset. Remote Sensing 12, 2075. https://doi.org/10.3390/rs12132075

Været, L., Kelbe, B., Haldorsen, S., Taylor, R.H., 2009. A modelling study of the effects of land management and climatic variations on groundwater inflow to Lake St Lucia, South Africa. Hydrogeol J 17, 1949–1967. https://doi.org/10.1007/s10040-009-0476-5

Van Landtschoote, A., 2017. Hydrogeological investigation and recharge estimation of Gumera river catchment in Lake Tana basin, northern Ethiopia (Master). Ghent University, Ghent, Belgium.

VKKI, 2010. Vízgyűjtő-gazdálkodási terv. Dráva részvízgyűjtő (Water Basin Management Plan: Drava Partial Water Basin). Central Directorate for Water Management and Environmental Protection, Budapest.

Waikar, M.L., Somwanshi, M.A., 2014. Data Preparation For Assessing Impact Of Climate Change On Groundwater Recharge. International Journal Of Innovative Research In Advanced Engineering (Ijirae) 1.

Walker, G.R., Zhang, L., Ellis, T.W., Hatton, T.J., Petheram, C., 2002. Estimating impacts of changed land use on recharge: review of modelling and other approaches appropriate for management of dryland salinity. Hydrogeology Journal 10, 68–90. https://doi.org/10.1007/s10040-001-0181-5

Wang, B., Jin, M., Nimmo, J.R., Yang, L., Wang, W., 2008. Estimating groundwater recharge in Hebei Plain, China under varying land use practices using tritium and bromide tracers. Journal of Hydrology 356, 209–222. https://doi.org/10.1016/j.jhydrol.2008.04.011

Wang, D., Gong, J., Chen, L., Zhang, L., Song, Y., Yue, Y., 2013. Comparative analysis of land use/cover change trajectories and their driving forces in two small watersheds in the western Loess Plateau of China. International Journal of Applied Earth Observation and Geoinformation 21, 241–252. https://doi.org/10.1016/j.jag.2012.08.009

Wang, G., Zhang, Y., Liu, G., Chen, L., 2006. Impact of land-use change on hydrological processes in the Maying River basin, China. SCI CHINA SER D 49, 1098–1110. https://doi.org/10.1007/s11430-006-1098-6

Wang, H., Gao, J., Zhang, S., Zhang, M., Li, X., 2013. Modeling the Impact of Soil and Water Conservation on Surface and Ground Water Based on the SCS and Visual Modflow. PLoS ONE 8, e79103. https://doi.org/10.1371/journal.pone.0079103

Wang, Y., Lei, X., Liao, W., Jiang, Y., Huang, X., Liu, J., Song, X., Wang, H., 2012. Monthly spatial distributed water resources assessment: a case study. Computers & Geosciences 45, 319–330. https://doi.org/10.1016/j.cageo.2011.11.028

Wang, Z.-M., Batelaan, O., De Smedt, F., 1996. A distributed model for water and energy transfer between soil, plants and atmosphere (WetSpa). Physics and Chemistry of the Earth 21, 189–193. https://doi.org/10.1016/S0079-1946(97)85583-8

Wijesekara, G.N., Gupta, A., Valeo, C., Hasbani, J.-G., Qiao, Y., Delaney, P., Marceau, D.J., 2012. Assessing the impact of future land-use changes on hydrological processes in the Elbow River watershed in southern Alberta, Canada. Journal of Hydrology 412–413, 220–232. https://doi.org/10.1016/j.jhydrol.2011.04.018

Winston, R.B., 2009. ModelMuse-A graphical user interface for MODFLOW-2005 and PHAST: US Geological Survey techniques and methods 6-A29. US Geological Survey. Available online at http://pubs. usgs. gov/tm/tm6A29.

Winter, T.C., Harvey, J.W., Franke, O.L., Alley, W.M., 1999. Ground Water and Surface Water: A Single Resource. U.S. Geological Survey Circular 1139, USA.

Winter, T.C., LaBaugh, J.W., Rosenberry, D.O., 1988. The design and use of a hydraulic potentiomanometer for direct measurement of differences in hydraulic head between groundwater and surface water. Limnol. Oceanogr. 33, 1209–1214. https://doi.org/10.4319/lo.1988.33.5.1209

Winter, T.C., Mallory, S.E., Allen, T.R., Rosenberry, D.O., 2000. The Use of Principal Component Analysis for Interpreting Ground Water Hydrographs. Ground Water 38, 234–246. https://doi.org/10.1111/j.1745-6584.2000.tb00335.x

Woessner, W.W., 2000. Stream and Fluvial Plain Ground Water Interactions: Rescaling Hydrogeologic Thought. Ground Water 38, 423–429. https://doi.org/10.1111/j.1745-6584.2000.tb00228.x

Wren, D.G., Davidson, G.R., Walker, W.G., Galicki, S.J., 2008. The evolution of an oxbow lake in the Mississippi alluvial floodplain. Journal of Soil and Water Conservation 63, 129–135. https://doi.org/10.2489/jswc.63.3.129

WWAP, 2015. United Nations World Water Assessment Programme. The United Nations World Water Development Report 2015: Water for a Sustainable World. Paris, UNESCO.

Xu, C.Y., 2002. Modelling in Hydrology. In: Textbook of Hydrologic Models. Uppsala University Department of Earth Sciences Hydrology, Unppsala.168 pp.

Yang, L., Feng, Q., Yin, Z., Wen, X., Deo, R.C., Si, J., Li, C., 2019. Application of multivariate recursive nesting bias correction, multiscale wavelet entropy and AI-based models to improve future precipitation projection in upstream of the Heihe River, Northwest China. Theor Appl Climatol 137, 323–339. https://doi.org/10.1007/s00704-018-2598-y

Yihdego, Y., 2005. Three dimensional groundwater model of the aquifer around Lake Naivasha area, Kenya. (MSc. Thesis). ITC, University of Twente, Enschede, The Netherlands.

Yihdego, Y., Becht, R., 2013. Simulation of lake–aquifer interaction at Lake Naivasha, Kenya using a three-dimensional flow model with the high conductivity technique and a DEM with bathymetry. Journal of Hydrology 503, 111–122. https://doi.org/10.1016/j.jhydrol.2013.08.034

Yin, L., Zhou, Y., Huang, J., Wenninger, J., Hou, G., Zhang, E., Wang, X., Dong, J., Zhang, J., Uhlenbrook, S., 2014. Dynamics of willow tree (Salix matsudana) water use and its response to environmental factors in the semi-arid Hailiutu River catchment, Northwest China. Environ Earth Sci 71, 4997–5006. https://doi.org/10.1007/s12665-013-2891-0

Yin, Z., Feng, Q., Yang, L., Wen, X., Si, J., Zou, S., 2017. Long Term Quantification of Climate and Land Cover Change Impacts on Streamflow in an Alpine River Catchment, Northwestern China. Sustainability 9, 1278. https://doi.org/10.3390/su9071278

Zarei, M., Ghazavi, R., 2016. Estimating Groundwater Recharge, Evapotranspiration and Surface Runoff using Land-use data: A Case Study in Northeast Iran. Biological Forum – An International Journal 8, 196–202.

Zektser, I.S., Everett, L.G., 2004. Groundwater resources of the world and their use. National Groundwater Association Press, Westerville, Ohio.

Zhang, D., Madsen, H., Ridler, M.E., Refsgaard, J.C., Jensen, K.H., 2015. Impact of uncertainty description on assimilating hydraulic head in the MIKE SHE distributed hydrological model. Advances in Water Resources 86, 400–413. https://doi.org/10.1016/j.advwatres.2015.07.018

Zhang, L., Dawes, W.R., Walker, G.R., 2001. Response of mean annual evapotranspiration to vegetation changes at catchment scale. Water Resour. Res. 37, 701–708. https://doi.org/10.1029/2000WR900325

Zhang, Y., Gable, C.W., Person, M., 2006. Equivalent hydraulic conductivity of an experimental stratigraphy: Implications for basin-scale flow simulations: EQUIVALENT CONDUCTIVITY OF EXPERIMENTAL STRATIGRAPHY. Water Resour. Res. 42. https://doi.org/10.1029/2005WR004720

Zhang, Y., Liu, S., Cheng, F., Shen, Z., 2017. WetSpass-Based Study of the Effects of Urbanization on the Water Balance Components at Regional and Quadrat Scales in Beijing, China. Water 10, 5. https://doi.org/10.3390/w10010005

Zhang, Y., Person, M., Gable, C.W., 2007. Representative hydraulic conductivity of hydrogeologic units: Insights from an experimental stratigraphy. Journal of Hydrology 339, 65–78. https://doi.org/10.1016/j.jhydrol.2007.03.007

Zomlot, Z., Verbeiren, B., Huysmans, M., Batelaan, O., 2017. Trajectory analysis of land use and land cover maps to improve spatial–temporal patterns, and impact assessment on groundwater recharge. Journal of Hydrology 554, 558–569. https://doi.org/10.1016/j.jhydrol.2017.09.032

Zomlot, Z., Verbeiren, B., Huysmans, M., Batelaan, O., 2015. Spatial distribution of groundwater recharge and base flow: Assessment of controlling factors. Journal of Hydrology: Regional Studies 4, 349–368. https://doi.org/10.1016/j.ejrh.2015.07.005

APPENDICES

Appendix A:

Assessment of monthly water balance components using WetSpass-M model

The monthly water balance per a grid cell can be represented by:

$$P_m = SR_m + ET_m + R_m, \quad \text{(A-1)}$$

where P_m is monthly precipitation, SR_m is monthly surface runoff, ET_m is monthly evapotranspiration, and R_m is monthly groundwater recharge. The surface runoff (SR) calculation relies on the relationship between the land-use, soil, slope, precipitation intensity, interception, and soil infiltration capacity. SR_m is calculated on the monthly scale using:

$$SR_m = C_{sr}\, C_h\, (P_m - I_m), \quad \text{(0-2)}$$

where I_m is monthly interception, C_{sr} is actual surface runoff coefficient (-) that represents the monthly precipitation part, which contributes, directly, to runoff, and C_h is a coefficient that describes the moisture condition of soil (Zarei and Ghazavi, 2016). Monthly interception (I_m) is determined by:

$$I_m = P_m\, I_R, \quad \text{(0-3)}$$

where I_m is interception [mm/month], P_m is monthly precipitation [mm/month] and I_R is interception ratio. In WetSpass-M, total monthly evapotranspiration per grid cell (ETm; mm/month) is determined by:

$$ET_m = a_v ET_v + a_s ET_s + a_o ET_o + a_i ET_i, \quad \text{(A-4)}$$

where the area fraction and evapotranspiration for vegetated cover area, bare soil, open water and impervious surface are denoted by a_v, ET_v, a_s, ET_s, a_o, ET_o, a_i, and ET_i, respectively. Vegetated area evapotranspiration (ET_v) is a sum of actual transpiration and interception for the vegetated cover area (Batelaan et al., 2003). Monthly groundwater recharge R_m (mm/month) in WetSpass-M is determined as a residual parameter of water balance:

$$R_m = P_m - SR_m - ET_m, \quad (0\text{-}5)$$

where P_m is monthly precipitation, SR_m is monthly surface runoff, and ET_m is monthly evapotranspiration (Abdollahi et al., 2017). A more detailed description of complete mathematical formulation for the WetSpass–M can be found in Abdolaahi et al. (2017).

Appendix B

a)

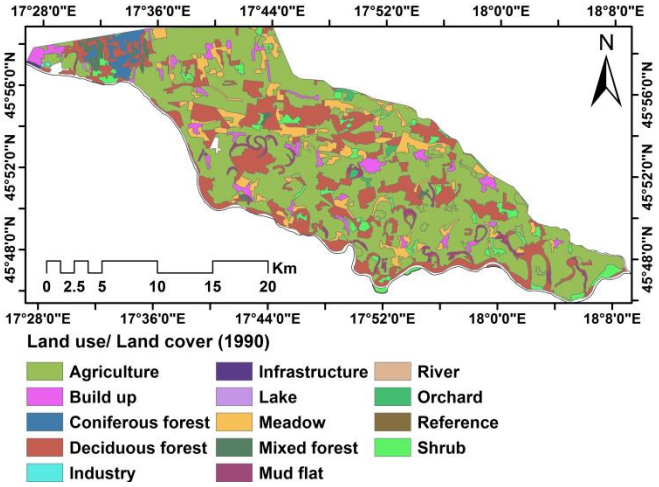

b)

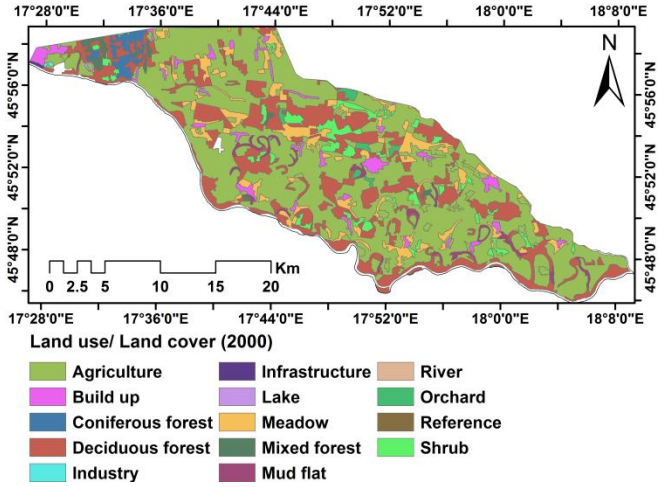

c)

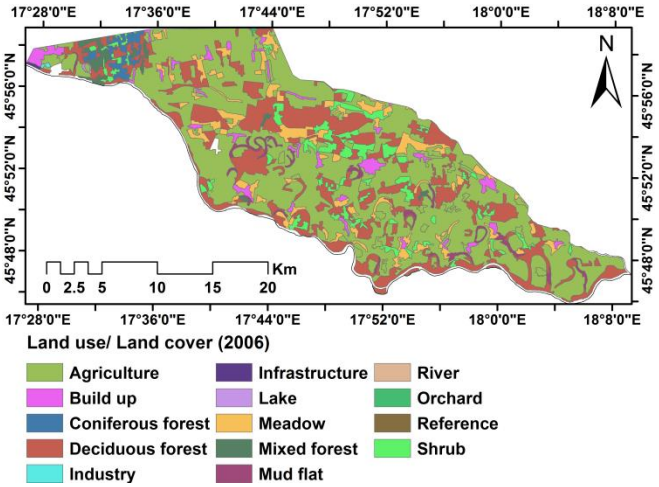

d)

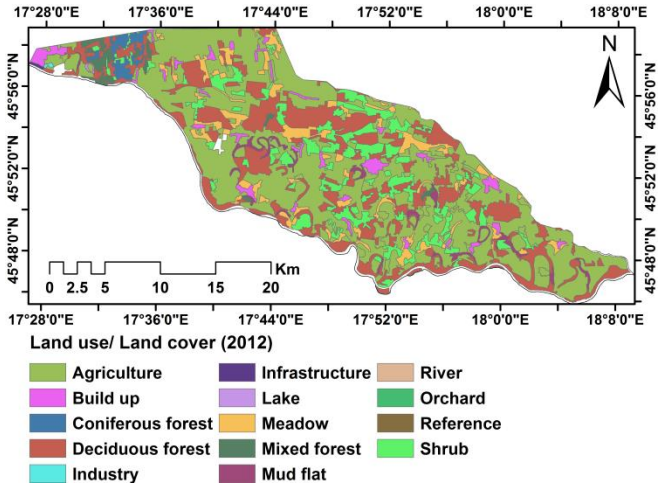

e)

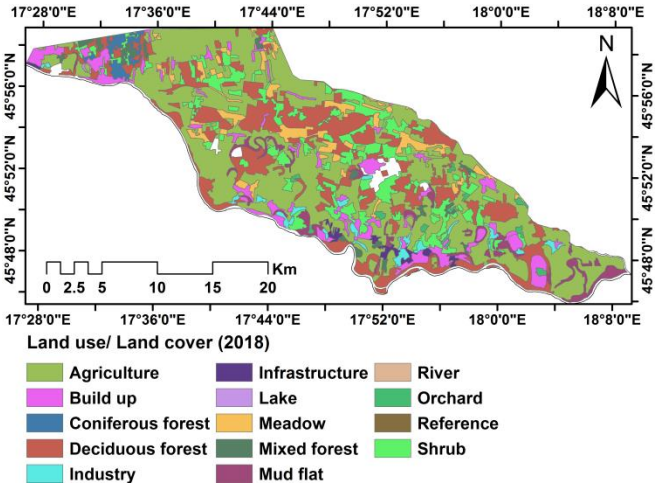

Figure B1: Land use/ Land cover of the study area at: (a) 1990; (b) 2000; (c) 2006; (d) 2012; and (e) 2018.

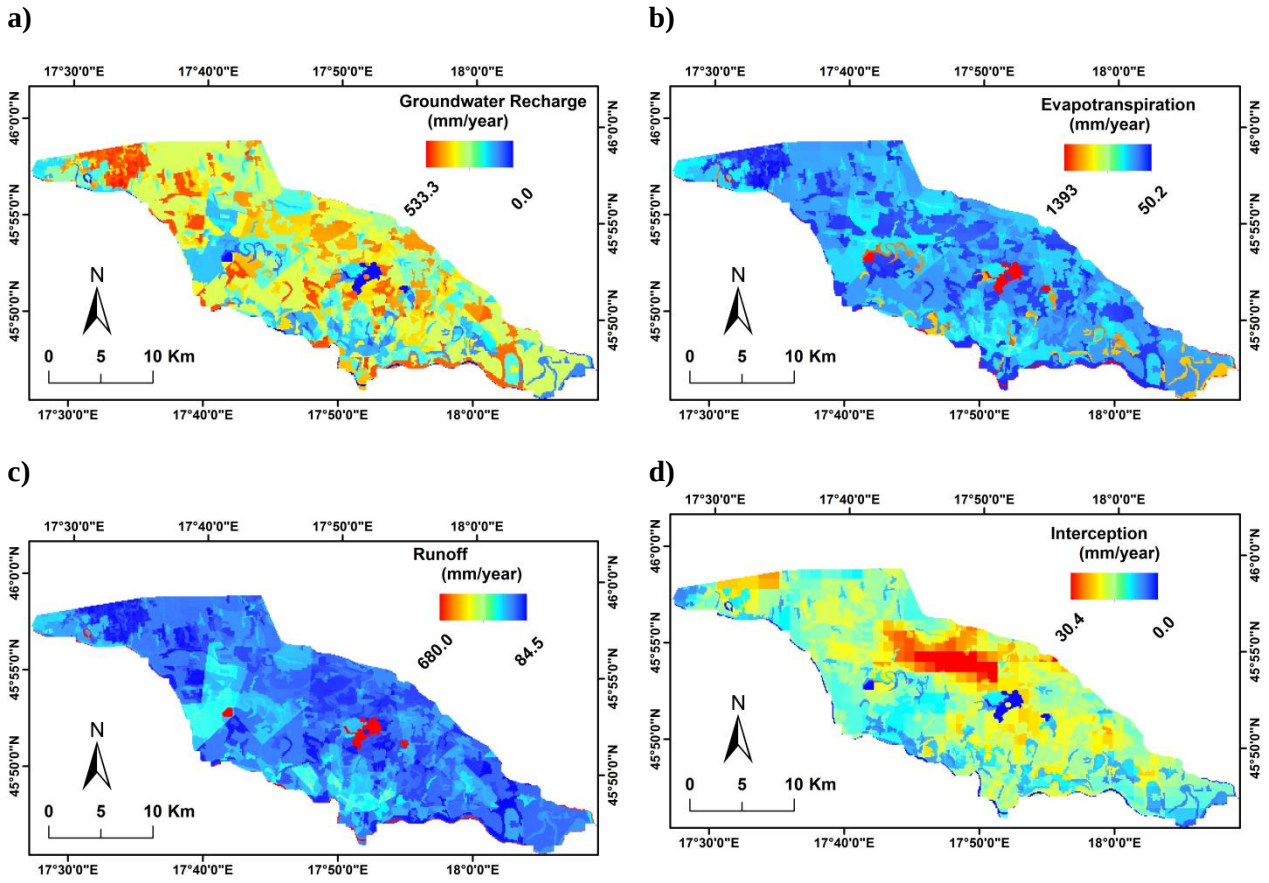

e)

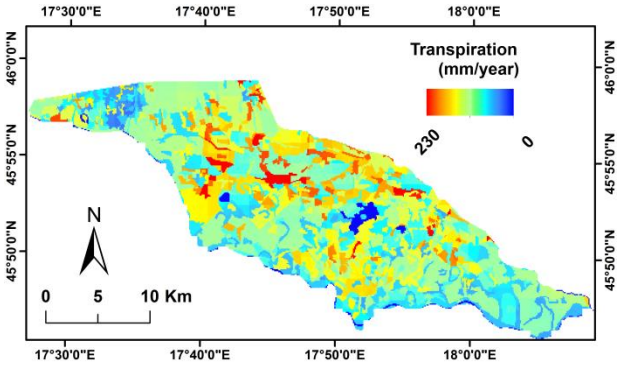

Figure B2: Spatial distribution of annual average water balance components for LULC in 2018: (a) groundwater recharge; (b) actual evapotranspiration; (c) surface runoff; and (d) interception; and (e) transpiration

a)

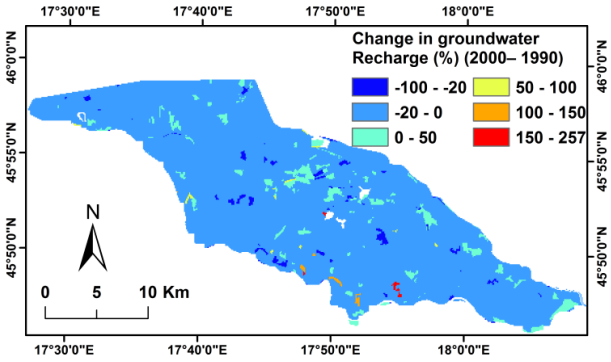

b)

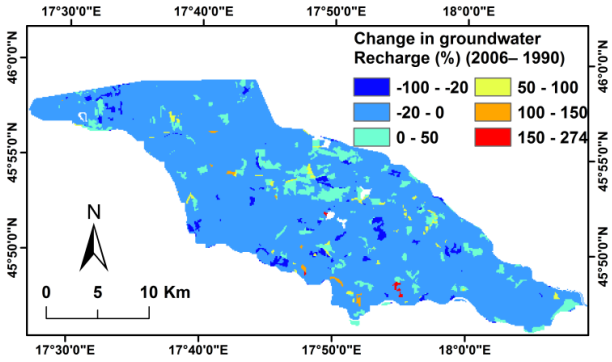

c)

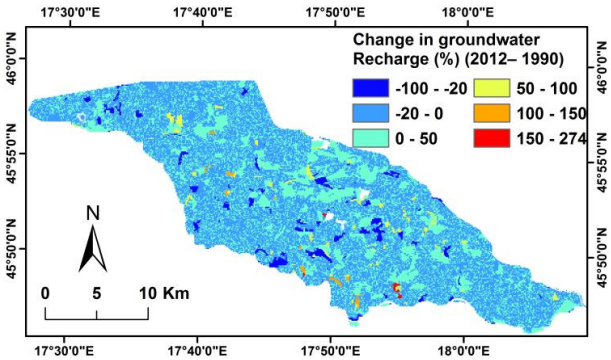

d)

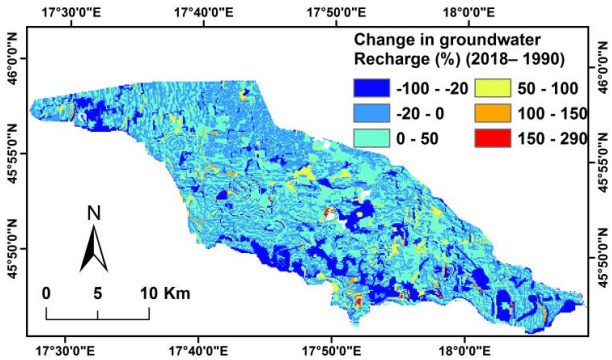

Figure B3: Change in groundwater recharge of the simulated LULC scenarios with respect to the base year 1990: (a) 2000 – 1990; (b) 2006 – 1990; (c) 2012 – 1990; and (d) 2018 – 1990

Table B1: The location, average annual groundwater depth, and average annual change in groundwater

Station	Longitude and latitude	Average annual groundwater depth (m)	Average annual change in groundwater (m)
Drávafok	$17^0$45′50″E, $45^0$53′50″N	3	1.35
Sellye	$17^0$50′52″E, $45^0$52′52″N	3.11	1.05
Kemse	$17^0$54′48″E, $45^0$49′48″N	2.2	1.18
Vajszló	$17^0$59′16″E, $45^0$51′16″N	3.25	0.77
Kákics	$17^0$51′22″E, $45^0$54′22″N	1.4	1.7
Lakócsa	$17^0$41′32″E, $45^0$53′32″N	1.63	1.45
Dráva-iványi NY	$17^0$49′3″E, $45^0$50′3″N	1.5	1.6
Vejti NY	$17^0$58′10″E, $45^0$49′10″N	3.15	1.8
Potony	$17^0$39′10″E, $45^0$55′10″N	2.34	1.64
Ketujfalu	$17^0$42′46″E, $45^0$57′46″N	2.6	1.1
CUN_2	$18^0$5′6″E, $45^0$48′6″N	3.59	1
CUN_3	$18^0$4′41″E, $45^0$48′41″N	1.66	1.18
CUN_5	$18^0$4′43″E, $45^0$46′43″N	2.3	1.22
CUN_1	$18^0$4′44″E, $45^0$47′44″N	1.69	1.7
CUN_4	$18^0$5′46″E, $45^0$47′46″N	3.19	1.8
Szaporca K-8	$18^0$6′12″E, $45^0$46′12″N	2.78	0.6
Darány	$17^0$35′20″E, $45^0$58′20″N	1.69	1.53
Barcs	$17^0$27′17″E, $45^0$57′17″N	4.82	0.8

Table B2: Average annual actual evapotranspiration across different combinations of soil texture and LULC in 2018

	Soil texture						
LULC classes	**Sand**	**Sandy Loam**	**Loam**	**Clay Loam**	**Clay**	**Average**	**St.dev**
Build up	218	227	237	248	258	238	14
Industry	219	221	234	242	254	234	13

Infrastructure	217	-	241	254	267	245	18
Agriculture	168	196	204	215	220	201	18
Meadow	165	190	202	235	236	206	27
Orchard	153	-	186	195	189	181	16
Deciduous forest	257	311	344	346	392	330	45
Coniferous forest	362	-	411	-	-	386	25
Mixed forest	269	331	359	371	406	347	46
Shrub	395	347	335	296	239	322	52
Reference	-	-	190	-	219	205	15
Mud flat	477	511	526	543	573	526	32
River	1345	1330	1356	1357	1358	1349	11
Lake	-	-	1371	-		1371	0
Average	354	407	443	391	384		
St.dev	314	340	388	320	312		

1.

-, (no value) as there is no such LULC for a given soil texture

Table B3: Average annual surface runoff across different combinations of soil texture and LULC in 2018

	Soil texture						
LULC classes	**Sand**	**Sandy Loam**	**Loam**	**Clay Loam**	**Clay**	**Average**	**St.dev**
Build up	225	233	252	260	297	253	25
Industry	280	271	297	307	337	298	23
Infrastructure	180	-	218	238	279	229	36
Agriculture	174	196	209	235	293	222	41

Meadow	118	142	155	177	242	167	42
Orchard	143	-	178	211	258	198	42
Deciduous forest	101	120	139	167	229	151	45
Coniferous forest	105	-	154	-	-	130	24
Mixed forest	103	132	145	175	239	159	46
Shrub	141	162	177	200	259	188	41
Reference	-	-	213	-	288	251	38
Mud flat	207	218	237	255	299	243	32
River	160	161	162	162	162	161	1
Lake	-	-	162	-	-	162	0
Average	161	182	193	217	265		
St.dev	53	48	45	44	43		

2.

-, (no value) as there is no such LULC for a given soil texture